

**MODELING OF HYDRATE PHASE TRANSITION USING
THE MEAN SPHERICAL APPROXIMATION (MSA)**

BY

Gaber Bark Al Jaberi

A Thesis Presented to the
DEANSHIP OF GRADUATE STUDIES

KING FAHD UNIVERSITY OF PETROLEUM & MINERALS

DHAHRAN, SAUDI ARABIA

In Partial Fulfillment of the
Requirements for the Degree of

MASTER OF SCIENCE

In

PETROLEUM ENGINEERING

APRIL, 2019

KING FAHD UNIVERSITY OF PETROLEUM & MINERALS
DHAHRAN- 31261, SAUDI ARABIA
DEANSHIP OF GRADUATE STUDIES

This thesis, written by **Gaber Bark Al-Jaberi** under the direction of his thesis advisor and approved by his thesis committee, has been presented and accepted by the Dean of Graduate Studies, in partial fulfillment of the requirements for the degree of **MASTER OF SCIENCE IN PETROLEUM ENGINEERING.**



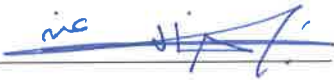
Dr. Abdullah Sultan
(Advisor)



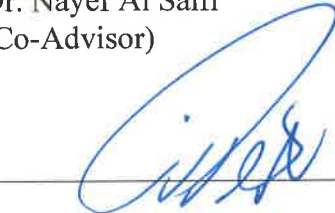
Dr. Dhafer Al Shehri
Department Chairman



Dr. Nayef Al Saifi
(Co-Advisor)



Dr. Salam A. Zummo
Dean of Graduate Studies



Dr. Hassan Alasiri
(Member)

17/6/2019

Date



Dr. Shirish Patil
(Member)



Dr. Sidqi Abu-Khamsin
(Member)

© Gaber Al Jaber

2019

To my dear parents and sibling

ACKNOWLEDGMENTS

I would like to start by acknowledging and thanking Almighty Allah for everything that gave me and will give me through my entire life. Allah says in the Quran “If you counted up the favors of Allah, you never would be able to count them” and I would never be able even to give thanks for them. I praise Allah for the blessing that without it the achievement of this work would not be possible.

Our Prophet (ﷺ) said: He who does not thank Allah does not thank people. Acknowledging individuals is not only words that are written and forgotten, its prayer for these individuals who helped us in our journey. I will try to do my best in acknowledging them!

I would like to start with my advisor Dr. Abdullah Sultan who was a mentor, an inspiration and an older brother with his supervision through my journey in KFUPM. He showed me all the support at all levels and provide the guidance and suggestions that made for this work specifically and research generally. Simply, Thank you.

Sincere thanks for my co-advisor Dr. Nayef Al Saifi for all his support and comment through this work. His office door was always open to me for answering my questions. Simply, Thank you.

I am grateful for my committee members Dr. Hassen Alasiri, Dr. Shirish Patil, and Dr. Sidqi Abu-Khamsin for their comments and effort in assessing my thesis work and their observation to improve this research. Simply, Thank you.

An appreciation sent to the King Fahad University of Petroleum & Minerals for providing me a scholarship to peruse my Bachelor and Master studies. Also, I extend my sincere

thanks and appreciation to the College of Petroleum Engineering and Geosciences and the Department of Petroleum Engineering for making our life as a student easy by ensuring that all the need facilities are available. Special admiration for all the faculty of my department for all the knowledge that I acquire through my journey in the Bachelor and Master studies. Simply, Thank you all.

My appreciation will not be complete without evident gratitude and admiration to my family. My parents who raised me and help me through my entire life. I wish that I make you happy through my whole remaining life! My siblings that made me smile through my life and I'm proud to be a brother for them. Simply, Thank you.

Thanks to my friends, I won't specify their names because I want to thank them for all the times that I spent with them. The bad ones that made me a better person or the good ones which became a good memory. Thank you.

TABLE OF CONTENTS

ACKNOWLEDGMENTS	V
TABLE OF CONTENTS	VII
LIST OF TABLES	IX
LIST OF FIGURES	X
LIST OF ABBREVIATIONS	XIV
ABSTRACT	XVII
ملخص الرسالة.....	XIX
CHAPTER 1 INTRODUCTION	1
1.1 Motivation	1
1.2 Thesis Objectives	7
1.3 Thesis Organization	7
CHAPTER 2 THEROTICAL BACKGROUND	8
2.1 Basic and Electrolyte Thermodynamic	8
2.1.1 Phase Equilibrium	8
2.1.2 Equation of State	11
2.1.3 Electrolyte Thermodynamics.....	38
2.2 Electrolyte Modeling	47
2.2.1 Electrolyte Solution Theories	48
2.2.2 Dielectric Models.....	65
2.2.3 Solvation Model.....	68
2.3 Hydrate Modeling	69
CHAPTER 3 LITERATURE REVIEW	79
3.1 Modeling the Electrolyte	79

3.1.1	Electrolyte Equation of State	79
3.1.2	Perturbation Theory for Electrolyte.....	93
3.2	Modeling the Gas Hydrate with Electrolyte	97
CHAPTER 4 ELECTROLYTE PROPERTIES USING SAFT-VR MIE COUPLED WITH PRIMITIVE MSA.....		104
4.1	Introduction	104
4.2	Methodology.....	104
4.3	Results and Discussion	109
CHAPTER 5 GAS SOLUBILITY IN THE PRESENCE OF ELECTROLYTE		128
5.1	Introduction	128
5.2	Methodology.....	129
5.3	Results and Discussion	130
CHAPTER 6 GAS HYDRATE IN THE PRESENCE OF ELECTROLYTE.....		137
6.1	Introduction	137
6.2	Methodology.....	138
6.3	Results and Discussion	139
CHAPTER 7 CONCLUSION & RECOMMENDATIONS.....		149
7.1	Conclusion.....	149
7.2	Recommendations and Future Work.....	150
REFERENCES		152
VITAE.....		176

LIST OF TABLES

Table 1-1: Properties of the three common hydrate crystal structure	2
Table 2-1: Cubic Equations of State	15
Table 2-2: SAFT-VR Mie parameters for different compounds	36
Table 2-3: Numerical Constants of Uematsu and Franck Model	65
Table 2-4: Solvent parameters	67
Table 2-5: Kihara potential parameters for different hydrate formers	74
Table 2-6: Langmuir constant adjustable parameters by Parrish & Prausnitz, 1972.....	75
Table 2-7: Literature values of reference thermodynamic properties	77
Table 3-1: Summary of the literature for electrolyte modeling	95
Table 4-1: SAFT-VR Mie parameters for different ions	107
Table 4-2: Dispersion attractive energies between the unlike ions	107
Table 4-3: Absolute Average Deviation Percentage for the Pressure, Mean Ionic Activity Coefficient, Osmotic Coefficient for different Electrolyte Solutions, Optimized parameters for each salt and Data used in the optimization process.....	126
Table 4-3: Absolute Average Deviation Percentage for the Pressure, Mean Ionic Activity Coefficient, Osmotic Coefficient for different Electrolyte Solutions, Optimized parameters for each salt and Data used in the optimization process (continue)	127
Table 5-1: The Component, Salt, Condition, Optimized Interaction Parameters used, the Average Absolute Deviation Percent of the Model and the Experimental Data used in the Optimization and Comparison Process	136
Table 6-1: The Gas Hydrate Former, Salt, Condition, Optimized Interaction Parameters used, the Average Absolute Deviation Percent of the Model and the Experimental Data used in the Optimization and Comparison Process	148

LIST OF FIGURES

Figure 1-1: The three common hydrate crystal structure.....	2
Figure 1-2: Hydrate related publications per decade in the 20th century.....	6
Figure 2-1: Representations of SAFT Theory	19
Figure 4-1: Comparison between the Experimental Results and SAFT-VR Mie EOS for the Vapor Pressure of Lithium Chloride as function of Salt Concentration at T = 303 K	112
Figure 4-2: Comparison between the Experimental Results and SAFT-VR Mie EOS for the Osmotic Coefficient and Mean Ionic Activity Coefficient (MIAC) of Lithium Chloride as function of Salt Concentration at T = 298 K	112
Figure 4-3: Comparison between the Experimental Results and SAFT-VR Mie EOS for the Vapor Pressure of Lithium Bromide as function of Salt Concentration at T = 298 K	113
Figure 4-4: Comparison between the Experimental Results and SAFT-VR Mie EOS for the Osmotic Coefficient and Mean Ionic Activity Coefficient (MIAC) of Lithium Bromide as function of Salt Concentration at T = 303 K	113
Figure 4-5: Comparison between the Experimental Results and SAFT-VR Mie EOS for the Vapor Pressure of Lithium Iodide as function of Salt Concentration at T = 298 K	114
Figure 4-6: Comparison between the Experimental Results and SAFT-VR Mie EOS for the Osmotic Coefficient and Mean Ionic Activity Coefficient (MIAC) of Lithium Iodide as function of Salt Concentration at T = 303 K	114
Figure 4-7: Comparison between the Experimental Results and SAFT-VR Mie EOS for the Osmotic Coefficient and Mean Ionic Activity Coefficient (MIAC) of Sodium Fluoride as function of Salt Concentration at T = 298 K	115
Figure 4-8: Comparison between the Experimental Results and SAFT-VR Mie EOS for the Vapor Pressure of Sodium Chloride as function of Salt Concentration at T = 298 K	115
Figure 4-9: Comparison between the Experimental Results and SAFT-VR Mie EOS for the Osmotic Coefficient and Mean Ionic Activity Coefficient (MIAC) of Sodium Chloride as function of Salt Concentration at T = 298 K	116
Figure 4-10: comparison between the Experimental Results and SAFT-VR Mie EOS for the Vapor Pressure of Sodium Bromide as function of Salt Concentration at T = 348 K	116
Figure 4-11: Comparison between the Experimental Results and SAFT-VR Mie EOS for the Osmotic Coefficient and Mean Ionic Activity Coefficient (MIAC) of Sodium Bromide as function of Salt Concentration at T = 298 K	117

Figure 4-12: Comparison between the Experimental Results and SAFT-VR Mie EOS for the Vapor Pressure of Sodium Iodide as function of Salt Concentration at T = 298 K	117
Figure 4-13: Comparison between the Experimental Results and SAFT-VR Mie EOS for the Osmotic Coefficient and Mean Ionic Activity Coefficient (MIAC) of Sodium Iodide as function of Salt Concentration at T = 298 K	118
Figure 4-14: Comparison between the Experimental Results and SAFT-VR Mie EOS for the Osmotic Coefficient and Mean Ionic Activity Coefficient (MIAC) of Potassium Fluoride as function of Salt Concentration at T = 298 K	118
Figure 4-15: Comparison between the Experimental Results and SAFT-VR Mie EOS for the Vapor Pressure of Potassium Chloride as function of Salt Concentration at T = 298 K	119
Figure 4-16: Comparison between the Experimental Results and SAFT-VR Mie EOS for the Osmotic Coefficient and Mean Ionic Activity Coefficient (MIAC) of Potassium Chloride as function of Salt Concentration at T = 298 K	119
Figure 4-17: Comparison between the Experimental Results and SAFT-VR Mie EOS for the Vapor Pressure of Potassium Bromide as function of Salt Concentration at T = 303 K	120
Figure 4-18: Comparison between the Experimental Results and SAFT-VR Mie EOS for the Osmotic Coefficient and Mean Ionic Activity Coefficient (MIAC) of Potassium Bromide as function of Salt Concentration at T = 298 K	120
Figure 4-19: Comparison between the Experimental Results and SAFT-VR Mie EOS for the Vapor Pressure of Potassium Iodide as function of Salt Concentration at T = 348 K	121
Figure 4-20: Comparison between the Experimental Results and SAFT-VR Mie EOS for the Osmotic Coefficient and Mean Ionic Activity Coefficient (MIAC) of Potassium Iodide as function of Salt Concentration at T = 298 K	121
Figure 4-21: Comparison between the Experimental Results and SAFT-VR Mie EOS for the Vapor Pressure of Calcium Bromide as function of Salt Concentration at T = 303 K	122
Figure 4-22: Comparison between the Experimental Results and SAFT-VR Mie EOS for the Mean Ionic Activity Coefficient (MIAC) of Calcium Bromide as function of Salt Concentration at T = 298 K	122
Figure 4-23: Comparison between the Experimental Results and SAFT-VR Mie EOS for the Vapor Pressure of Calcium Chloride as function of Salt Concentration at T = 303 K	123
Figure 4-24: Comparison between the Experimental Results and SAFT-VR Mie EOS for the Osmotic Coefficient and Mean Ionic Activity Coefficient (MIAC) of Calcium Chloride as function of Salt Concentration at T = 298 K	123

Figure 4-25: Comparison between the Experimental Results and SAFT-VR Mie EOS for the Vapor Pressure of Calcium Iodide as function of Salt Concentration at T = 303 K	124
Figure 4-26: Comparison between the Experimental Results and SAFT-VR Mie EOS for the Mean Ionic Activity Coefficient (MIAC) of Barium Bromide as function of Salt Concentration at T = 298 K	124
Figure 4-27: Comparison between the Experimental Results and SAFT-VR Mie EOS for the Vapor Pressure of Barium Bromide as function of Salt Concentration at T = 303 K	125
Figure 4-28: Comparison between the Experimental Results and SAFT-VR Mie EOS for the Vapor Pressure of Barium Chloride as function of Salt Concentration at T = 303 K	125
Figure 4-29: Comparison between the Experimental Results and SAFT-VR Mie EOS for the Mean Ionic Activity Coefficient (MIAC) of Lithium Chloride as function of Salt Concentration at T = 298 K	126
Figure 5-1: Comparison between the Experimental Results and SAFT-VR Mie EOS for the Solubility of Methane in NaCl Solution at concentrations of 1 M and 4 M @ 324.65 K	132
Figure 5-2: Comparison between the Experimental Results and SAFT-VR Mie EOS for Solubility of Methane in NaCl Solution at concentrations of 1 M @ 275.65 K	132
Figure 5-3: Comparison between the Experimental Results and SAFT-VR Mie EOS for the Solubility of Methane in NaCl Solution at concentrations of 1 M @ 398.15 K	133
Figure 5-4: Comparison between the Experimental Results and SAFT-VR Mie EOS for Solubility of Methane in KCl Solution at concentrations of 1 M, 2.5 and 4 M @ 313.15 K	133
Figure 5-5: Comparison between the Experimental Results and SAFT-VR Mie EOS for Solubility of Methane in KCl Solution at concentrations of 1 M, 2.5 and 4 M @ 353.29 K	134
Figure 5-6: Comparison between the Experimental Results and SAFT-VR Mie EOS for the Solubility of Methane in KCl Solution at concentrations of 1 M, 2.5 and 4 M @ 373.17 K	134
Figure 5-7: Comparison between the Experimental Results and SAFT-VR Mie EOS for the Solubility of Methane in CaCl ₂ Solution at concentration of 1 M @ 298.15 K, 344.15 K and 398 K	135
Figure 5-8: Comparison between the Experimental Results and SAFT-VR Mie EOS for the Solubility of Carbon Dioxide in NaCl Solution at concentration of 1 M @ 353.15.15 K and 398 K	135
Figure 5-9: Comparison between the Experimental Results and SAFT-VR Mie EOS for the Solubility of Carbon Dioxide in CaCl ₂ Solution at concentrations of 1 M, 2.28 M and 3.89 M @ 349 K	136
Figure 6-1: Comparison between the Experimental Results and SAFT-VR Mie EOS with MDH Model for the Methane Gas Hydrate in Pure Water and NaCl Solution at concentration of 1.328 M and 2.0795 M	142

Figure 6-2: Comparison between the Experimental Results and SAFT-VR Mie EOS with MDH Model for the Methane Gas Hydrate in Pure Water and NaCl Solution at concentration of 1.328 M and 2.0795 M	142
Figure 6-3: Comparison between the Experimental Results and SAFT-VR Mie EOS with MDH Model for the Methane Gas Hydrate in Pure Water and CaCl ₂ Solution at concentration of 0.474 M	143
Figure 6-4: Comparison between the Experimental Results and SAFT-VR Mie EOS with MDH Model for the Ethane Gas Hydrate in Pure Water and NaCl Solution at concentration of 0.906 M	143
Figure 6-5: Comparison between the Experimental Results and SAFT-VR Mie EOS with MDH Model for the Ethane Gas Hydrate in Pure Water and KCl Solution at concentration of 0.7 M and 1.4 M	144
Figure 6-6: Comparison between the Experimental Results and SAFT-VR Mie EOS with MDH Model for the Ethane Gas Hydrate in Pure Water and CaCl ₂ Solution at concentration of 0.474 M and 1.59 M	144
Figure 6-7: Comparison between the Experimental Results and SAFT-VR Mie EOS with MDH Model for the Carbon Dioxide Gas Hydrate in Pure Water and NaCl Solution at concentration of 0.529 M and 0.9 M	145
Figure 6-8: Comparison between the Experimental Results and SAFT-VR Mie EOS with MDH Model for the Carbon Dioxide Gas Hydrate in Pure Water and KCl Solution at concentration of 0.70746 M	145
Figure 6-9: Comparison between the Experimental Results and SAFT-VR Mie EOS with MDH Model for the Carbon Dioxide Gas Hydrate in Pure Water and CaCl ₂ Solution at concentration of 0.2816 M	146
Figure 6-10: Comparison between the Experimental Results and SAFT-VR Mie EOS with MDH Model for the Propane Gas Hydrate in Pure Water and NaCl Solution at concentration of 0.906 M	146
Figure 6-11: Comparison between the Experimental Results and SAFT-VR Mie EOS with MDH Model for the Propane Gas Hydrate in Pure Water and KCl Solution at concentration of 0.7059 M	147
Figure 6-12: Comparison between the Experimental Results and SAFT-VR Mie EOS with MDH Model for the Propane Gas Hydrate in Pure Water and CaCl ₂ Solution at concentration of 0.7059 M	147

LIST OF ABBREVIATIONS

%AAD	:	Percent Absolute Average Deviation.
ANN	:	Artificial Neural Network.
CGI	:	Crystal Growth Inhibition.
COSMO-RS	:	Conductor-like Screening Model for Realistic Solvation.
CPA	:	Cubic Plus Association.
DH	:	Debye-Huckel Theory.
eNRTL	:	Electrolyte Non-Random Two-Liquid.
EOS	:	Equation of State.
ePC-SAFT Theory	:	Electrolyte Perturbated Chain Statistical Associating Fluid
FREZCHEM	:	Freezing Chemistry Model.
GC-ePPC-SAFT	:	Group Contribution Polar Perturbed Chain Statistical
Association Fluid Theory.		
HNC	:	Hypernetted Chain Integral Equation.
HS-RDF	:	Hard-Sphere Radial Distribution Function.
KHI	:	Kinetic Hydrate Inhibitor.
LJ-RDF	:	Lennard-Jones Radial Distribution Function.
LJ-SAFT	:	Lennard-Jones Statistical Association Fluid Theory.
LR	:	Lewis-Randall framework.
MD	:	Molecular dynamic.
MDH	:	Modified Debye-Huckel
MEG	:	Mono-ethylene glycol.
MIAC	:	Mean Ionic Activity Coefficient.

Mie-RDF	:	Mie Radial Distribution Function.
MM	:	McMillan-Mayer framework.
MSA	:	Mean Spherical Approximation.
mSRK	:	Modified Soave-Redlich-Kwong EOS
NPMSA	:	Non-Primitive Mean Spherical Approximation.
NPT	:	Number of Particles-Pressure-Temperature ensemble.
NVE	:	Number of Particles-Volume-Energy ensemble.
NVT	:	Number of Particles-Volume-Temperature ensemble.
OZ	:	Ornstein-Zernicke Equation.
PACT	:	Perturbed Anisotropic Chain Theory.
PB	:	Poisson-Boltzmann Equation.
PC-SAFT	:	Perturbated Chain Statistical Associating Fluid Theory.
PHSC-EOS	:	Perturbed Hard Sphere Equation of State.
PMSA	:	Primitive Mean Spherical Approximation.
PPC-SAFT Theory.	:	Polar Perturbated Chain Statistical Associating Fluid Theory.
PR-EOS	:	Peng-Robinson Equation of State.
PT-EOS	:	Patel-Tega Equation of State.
PY	:	Percus-Yevick Equation.
RK-EOS	:	Redlich-Kwong Equation of State.
RPM	:	Restricted Primitive Model.
SAFT-HR	:	Statistical Associating Fluid Theory Huang-Radosz.
SAFT-VR Mie Potential.	:	Statistical Associating Fluid Theory Variable Range Mie Potential.
SAFT-VR	:	Statistical Associating Fluid Theory Variable Range.

SAFT-VR+DE Equation.	:	Statistical Associating Fluid Theory Variable Range Dipole
SAFT-VRE Electrolyte.	:	Statistical Associating Fluid Theory Variable Range for
SAFT	:	Statistical Associating Fluid Theory.
SRK-EOS	:	Soave-Redlich-Kwong Equation of State.
THI	:	Thermodynamics Inhibitor.
VdW-EOS	:	Van der Waals Equation of State.
vdWP	:	van der Waals & Plattuuew.
VLE	:	Vapor Liquid Equilibrium.
μ VT	:	Chemical Potential-Volume-Temperature ensemble.

ABSTRACT

Full Name : Gaber Bark Al -Jaberi
Thesis Title : Modeling of Hydrate Phase Transition using Mean Approximation (MSA) Mode
Major Field : Petroleum Engineering
Date of Degree : April, 2019

The purpose of this thesis work is to contribute to the development of modeling electrolytes in solution. The main objectives of the thesis are; to build a model that capable of predicting the electrolyte solution properties, the gas solubility in a different electrolyte solution and the impact of different electrolyte (salts) on the incipient formation conditions of gas hydrate.

The model consists of the SAFT-VR Mie to model the vapor-liquid mixtures which was coupled with the primitive version of the Mean Spherical Approximation (MSA) to model the electrolyte solutions properties (i.e., the mean the ionic activity coefficient, the osmotic coefficient, and the vapor pressure). The gas solubility of different gases is predicted using a modified version of Debye-Huckle (M-DH) coupled with SAFT-VR Mie. The van der Waals Plattuuew model (vdWP) is used to model the gas hydrate phase while the (M-DH) utilized to capture the electrolyte effect. All the modeled results were compared to experimental results.

Excellent results were obtained from the codes in modeling the electrolyte solutions properties, the gas solubility, and the gas hydrate incipient conditions in the presence of the electrolyte. Fifteen electrolyte systems were studied for their properties with the highest

average absolute deviation (AADP) of 22.51%. For the gas solubility, nineteen systems were analyzed for different conditions (i.e., concentrations, and composition), and the highest AADP was less than 5%. The gas hydrate modeling in the presence of an electrolyte was achieved with excellent matching for the twenty-one systems with the highest AADP less than 5%.

ملخص الرسالة

الاسم الكامل: جابر برك الجابري

عنوان الرسالة: نمذجة هيدرات الغاز باستخدام المتوسط التقريبي الكروي

التخصص: هندسة البترول

تاريخ الدرجة العلمية: ابريل – 2019

الهدف من هذه الرسالة هو المساهمة في تطوير نمذجة الاملاح في المحاليل من خلال بناء نموذج قادر على توقع خواص المحاليل الكهربائية، وبناء نموذج قادر على توقع ذوبان الغازات في مختلف المحاليل الكهربائية، وكذلك بناء نموذج قادر على توقع تأثير الاملاح على ظروف التكون الاولي لغاز الهيدرات. يتكون النموذج من SAFT-VR Mie لنمذجة مخاليط البخار-السائل ومقرونة بالنسخة البدائية من التقريب الكروي المتوسط لنمذجة خصائص المحاليل الكهربائية (الخصائص تشمل متوسط معامل النشاط الايوني، ومحامل التناضح، وضغط البخار). ذوبان مختلف الغازات تم توقعه باستخدام نسخة معدلة من نموذج Debye-Huckle مقرون بنموذج SAFT-VR Mie. تم استخدام نموذج van der Waals Plattuuew لنمذجة غاز الهيدرات بينما نموذج Debye-Huckle تم استخدامه لالتقاط تأثير الاملاح على غاز الهيدرات. جميع نتائج النماذج تمت مقارنتها مع نتائج التجارب المعملية. تم الحصول على تنبؤ ممتاز من النماذج في نمذجة خواص المحاليل الكهربائية، وذوبان الغازات، وظروف تكون غاز الهيدرات في وجود الاملاح. خمس عشرة نظام كهربائي تمت دراسته لخصاها، وكان اعلى معدل انحراف مطلق يساوي ٢٢,٥١٪. تسعة عشر نظاماً تم دراسة ذوبان الغاز فيها (تختلف في تركيز والتركيب)، وكان اعلى معدل انحرافي مطلق اقل من ٥٪. واحد عشرين نظام للغاز هيدرات في وجود الاملاح تمت دراستها، وكان اعلى معدل انحرافي مطلق اقل من ٥

CHAPTER 1

INTRODUCTION

1.1 Motivation

Natural gas hydrate (NGH) is a crystalline compound that forms (usually at high pressure and low temperature) when water molecules create a cage structure around smaller guest molecule. The gas hydrates are a clathrates material that has different cages made of water molecules trapping guest of nonpolar molecule. The first documented hydrate existence was made by Sir Humphrey Davy in 1810 when he found that mixture of chlorine with water freeze at a higher temperature than pure water (Englezos 1993). Three conditions must be satisfied to form the gas hydrate: first is the presence of hydrate formers for each hydrate structure such as methane, ethane and other gases. Second, suitable pressure and temperature condition to form the gas hydrate and third is the presence of water (Drive and Carroll 2009). Gas hydrate can exist in three different structures: structure I, structure II and structure H. The structure H is not common but S-I and S-II structures are abundant natural hydrates. The Structure I is formed when the water molecules and small gases (guest molecules) such as methane, ethane, carbon dioxide, and hydrogen sulphide are in thermodynamic equilibrium. This structure consists of eight cavities including two smalls with pentagonal faces (5^{12}) and six large cavities with pentagonal faces and hexagonal faces ($5^{12}6^2$). The unit cell (the smallest repeating unit of a crystal structure) of this structure

consists of 46 water molecules per eight cavities. For structure II, it is formed when the water is in thermodynamic equilibrium with larger guest molecules such as propane, or iso-butane. This structure contains 136 water molecules per 24 cavities consist of 16 small cavities with pentagonal faces (5^{12}) and eight cavities with pentagonal faces and hexagonal faces ($5^{12}6^4$). When large molecules such as neo-hexane are in thermodynamic equilibrium with water, the structure H is formed. It has three cavities type with different sizes; one cavity with large size ($5^{12}6^8$), two cavities of a medium size ($4^35^66^3$) and three cavities of the small size (5^{12}). It contains 34 water molecules per six cavities (Claussen 1951; Jeffrey and McMullen 1967). Figure 1-1 shows these three repeating hydrate unit crystals and their constitutive cages and Table 1-1 shows a summary of the three hydrate structures (Sloan et al. 2010; Sloan and Koh 2008). More hydrate structures have been discovered which rarely occur such as Tetragonal structure of bromine hydrate and hydrate structure containing choline hydroxide tetra-n-propylammonium fluoride and xenon hydrates (Loveday et al. 2001; Udachin and Ripmeester 1999)

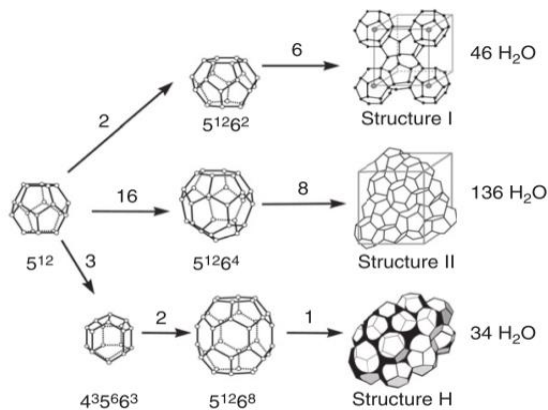


Figure 1-1: The three common hydrate crystal structure

Table 1-1: Properties of the three common hydrate crystal structure

Hydrate crystal structure	I		II		H		
	Small	Large	Small	Large	Small	Medium	Large
Description	5 ¹²	5 ¹² 6 ²	5 ¹²	5 ¹² 6 ⁴	5 ¹²	4 ³ 5 ⁶ 6 ³	5 ¹² 6 ⁸
Number of cavities/unit cell	2	6	16	8	3	2	1
Average cavity radius ^a (Å)	3.95	4.33	3.91	4.73	3.94 ^b	4.04 ^b	5.79 ^b
Variation in radius ^c (%)	3.4	14.4	5.5	1.73	4.0*	8.5*	15.1*
No. of water molecules/cavity ^d	20	24	20	28	20	20	36

The spotlight has been focused on the gas hydrate in recent years due to their importance. Gas hydrate has many applications; it can be considered as a potential energy source in the futures, a source for geological information (Sloan and Koh 2008) a way for natural gas transportation and can be used for natural gas storage (Veluswamy et al. 2016). The consideration of the gas hydrate as a future energy source is due to two main reasons: the vast amount of NGH that exist in the world which estimated to be double the fossil fuel and one cube of NGH equal to 180 of natural gas at stander condition (Li et al. 2016). The second reason is the gas hydrate deposits spreading over the globe in offshore and onshore location (Li et al. 2016). Hydrate presence can be interpolated to important information. It can be linked to some geologic hazards like submarine slope failure due to the movement of the earth in the deep ocean (Nixon and Grozic 2007). Gas hydrate can be used as a suitable way of transporting natural gas as well (Sloan and Koh 2008) According to Takaoki et al. (2002), gas hydrate can be used as a small pellet to transport natural gas (Takaoki et al. 2002). For storing natural gas, it can be stored as gas hydrate at low pressure and temperature. This will provide an effective way of storing natural gas. For example, only 1/156 of the volume in the free state is needed for natural gas with a volume of 4.42

m³ at 15 °C and atmospheric pressure. In that case, it only requires 0.028 m³ of volume to store it in the hydrate solid state (Parent and Bishnoi 1996).

With all the previous promising applications, however, gas hydrate can cause flow assurance problems like blocking the flow lines, wellhead and valves which will cause a loss of production and may even lead to blowout. In 1939, Hammerschmidt found that gas hydrate could form under normal operation conditions and block the transport lines which gave the researchers an opportunity on how to solve this problem (Anderson, Tester, Borghi, & Trout, 2005). When the blockage happened, one of the remedies options is injecting chemicals by using coiled tubing. If the plug is not accessible, reducing the pressure or increasing the temperature by thermal method could be the solution (Sloan et al., 2010).

However, these remedy methods are not always applicable or efficient and they could cause a loss of production. As a result, prevention (inhabitation) methods are more appealing. The prevention is done by using chemical inhibitors. There are two kinds of chemical inhibitors; thermodynamic inhibitor and kinetic inhibitor. For the thermodynamic inhibitor (THI), it changes the conditions where the hydrate become stable. This is done by shifting the equilibrium curve of the gas hydrate to higher pressure and lower temperature which will destabilize the gas hydrate phase. Methanol and Mono-ethylene glycol (MEG) are examples of thermodynamic inhibitors. More than 500 million dollars spent each year on hydrate prevention by methanol injection (Lederhos et al. 1996). For the kinetic inhibitor (KHI), it slows down the rate of hydrate formation. It delays the nucleation and growth of hydrate for a period of time (Chong et al. 2016; Tohidi et al. 2015). There are two main reasons that KHIs attract the petroleum industry attention; less environmental impact and

low operating cost comparing to THIs (Al-eisa et al. 2015). Two types of KHIs that have been used commercially; water-soluble polymeric material and non-polymeric material. The first tends to prevent the gas hydrate formation by forming a hydrogen bond with water while the second works as synergists (Kelland 2006).

All the previous discussion can justify the growing in the number of publication for natural gas hydrate subjects in the last few years as shown in Figure 1-2 (Chong et al. 2016). It shows the subject area distribution of publications (B), country-wise distribution of publications (C) and the histogram of research progress in the subject (A). Over the years, different models were developed to predict the gas hydrate transition phase due to its application and the difficulties with the experimental measurement. Examples of these difficulties are the experiment conditions (pressure and temperature), the high equipment cost, excessive time consumption, etc. On top of that, the presence of electrolyte in the system makes it more difficult to model it theoretically. Different researchers have attempted to model the gas hydrate gas in the presence of salts (Atik, Windmeier, and Oellrich 2010; Guo 1999; Haghghi 2009; Javanmardi, Moshfeghian, and Maddox 1998; H Jiang and Adidharma 2012b, 2012a; Kwaterski and Herri 2014; Maribo-mogensen, Kontogeorgis, and Thomsen 2014; Marion, Catling, and Kargel 2006; Mei et al. 1996; Mohammadi et al. 2014; Mohammadi and Richon 2007; Osfoury et al. 2015; Saito, Marshall, and Kobayashi 1964; Shahnazar and Hasan 2014).

Even though some of these models predict their systems with reasonable accuracy, many of them miss the physical meaning or need many fitting parameters. Therefore, this thesis work will utilize the Statistical Associating Fluid Theory Variable Range with Mie potential (SAFT-VR Mie) and couple it with the primitive mean spherical approximation

(PMSA) to model the different electrolyte solution properties. Also, SAFT-VR Mie will be coupled with a Modified version of Debye-Huckle (M-DH) to model the solubility of different gases in electrolyte solutions. Finally, the gas hydrate with the salt presence will be modeled using SAFT-VR Mie, M-DH and van der Waals-Plattuuew model (vdWP). These models will be discussed more thoroughly in Chapter 2. Using the mentioned models will give a predictive ability of the model to predict the behavior with the least fitting parameters due to their theoretical background.

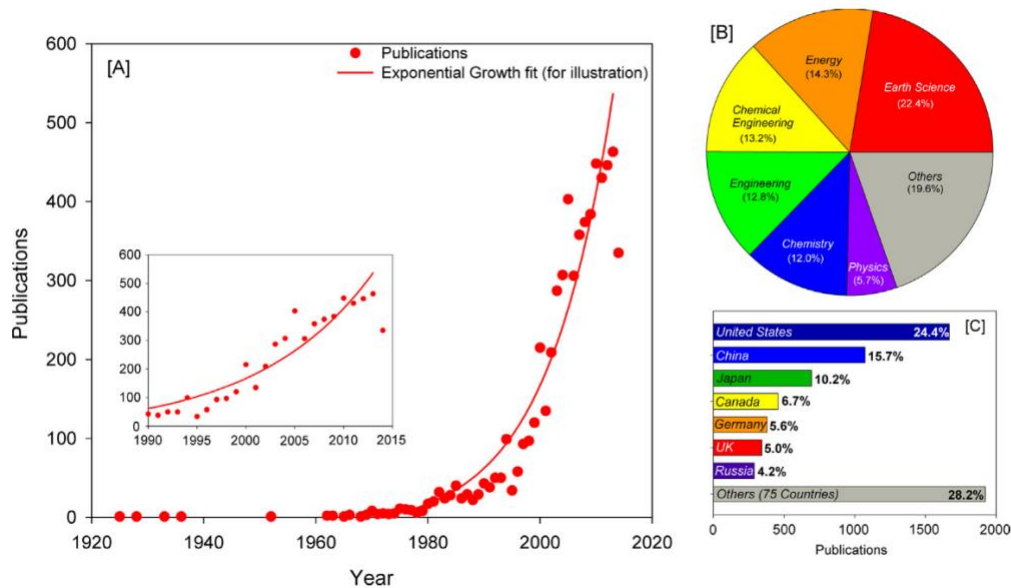


Figure 1-2: Hydrate related publications per decade in the 20th century.

1.2 Thesis Objectives

There are three main objectives of this work:

- Modeling the electrolyte solution properties using SAFT-VR Mie with electrolyte term represented by PMSA.
- Modeling the effect of electrolyte solution on the gas solubility using SAFT-VR Mie coupled with M-DH to describe the electrolyte effect.
- Modeling gas hydrate mixtures in the presence of salts where the vdWP model is utilized for the hydrate phase while the SAFT-VR Mie is used for the vapor and liquid phases. The electrolyte effect is represented by M-DH model.

1.3 Thesis Organization

Theoretical background for basic thermodynamic, electrolyte thermodynamics, hydrate modeling will be presented in Chapter 2. Chapter 3 will highlight the literature works related to the electrolyte modeling and molecular dynamics related to the electrolyte effect on the gas hydrate. In Chapter 4, the electrolyte properties using the mean spherical approximation will be presented. Chapter 5 and 6 will use the SAFT-VR Mie model, the Modified DH and the vdWP to model gas solubility and hydrate gas system with different electrolyte. The conclusion of this work with future recommendation will be presented in Chapter 7.

CHAPTER 2

THEROTICAL BACKGROUND

In this chapter, a theoretical background that relative to this thesis work will be presented which includes three sections: basic and electrolyte thermodynamics, electrolyte modeling and hydrate modeling.

2.1. Basic and Electrolyte Thermodynamic

This section will focus on the phase equilibrium, equations of state (EOS) and electrolyte thermodynamics.

2.1.1 Phase Equilibrium

Any system is in thermodynamic equilibrium when all the drive forces are equal for all its components in every phase in the system. That means that the system is at thermal, mechanical and chemical equilibrium (Malanowski and Anderko 1992). This can be expressed mathematically for all the phases π as the following:

$$T' = T'' = \dots = T^\pi \quad (2.1-1)$$

$$p' = p'' = \dots = p^\pi \quad (2.1-2)$$

$$\mu_i' = \mu_i'' = \dots = \mu_i^\pi \quad (2.1-3)$$

where T , p and μ are system temperature, system pressure and chemical potential for component i in each phase; respectively.

Due to the difficulty in calculating the chemical potential, Gilbert N. Lewis introduced the concept of the fugacity (Lewis & Randall, 1923). The chemical potential can be calculated by the following equation:

$$\mu_i = \Gamma_i(T) + RT \ln(y_i P) \quad (2.1-4)$$

where $\Gamma_i(T)$ and R are an integration constant and gas constant; respectively.

In the ideal gases, the Gibbs free energy can be calculated by the following equation:

$$dG_i^{ig} = RT \ln(P) \quad (2.1-5)$$

where G_i^{ig} is the ideal gas Gibbs free energy.

Equation (2.1-5) is limited to the ideal gas, for a real gas, the previous equation will become:

$$dG_i = RT \ln(f) \quad (2.1-6)$$

where f is the fugacity.

Since the chemical potential is the Gibbs free energy for the pure component, equation (2.1-6) will become as the following after the integration:

$$\mu - \mu^* = RT \ln(f) \quad (2.1-7)$$

Modeling the phase equilibrium can be done by two main approaches based on the fugacity; γ - ϕ approach and ϕ - ϕ approach (Malanowski and Anderko 1992). The γ - ϕ approach is utilized by using the activity coefficient (γ) and the fugacity coefficient (ϕ). For vapor-liquid equilibrium (VLE), the fugacity of the vapor equal to the fugacity of the liquid as the following expression:

$$\widehat{f}_i^L(P, T) = \widehat{f}_i^v(P, T) \quad (2.1-8)$$

$$\widehat{f}_i^L = \gamma_i x_i f_i^L \quad (2.1-9)$$

$$\widehat{f}_i^v = \widehat{\Phi}_i^v y_i P \quad (2.1-10)$$

where \widehat{f}_i^v , \widehat{f}_i^L , γ_i , $\widehat{\Phi}_i^v$, x_i and y_i are fugacity of component i in the vapor phase in the mixture, fugacity of component i in the liquid phase in the mixture, activity of component i , fugacity coefficient of vapor phase for the i component in the mixture, mole fraction of

the liquid phase for the i component and mole fraction of the vapor phase for the i component; respectively.

The activity can be calculated from different models where the fugacity coefficient can be calculated from the equation of state. The ϕ - ϕ approach uses the equation of state for each phase as the following:

$$y_i \Phi_i^v = x_i \Phi_i^L \quad (2.1-11)$$

where Φ_i^L and Φ_i^v are fugacity coefficient of liquid phase and vapor phase for the i component; respectively.

From the previous discussion, the equation of state is essential in the phase equilibrium calculation. There are different types of equations of state which will be shown in the next section.

2.1.2 Equation of State

The equation of state is an analytical description that relates different parameters together, these parameters are the pressure, temperature and volume (Ahmed, 2007). The description of this relationship is critical in getting the phase behavior and the require properties of the system. There are many equations of state, the starting point was with the ideal gas equation in 1834 by Clapeyron. It is expressed as the following:

$$PV = RT \quad (2.1-12)$$

where V and R are volume and gas constant; respectively.

The assumptions that were assumed for this law created some extreme limitations for its applications (Ahmed, 2007). These assumptions include: molecule occupied no volume, no intermolecular forces exist, no attractive and repulsion forces between the molecules and gas molecules are insignificant in volume compared to the system and the distance between the molecules (Ahmed, 2007). Therefore, many scientists have tried to address these limitations by developing a new equation of state. These developments will be discussed in the following subsections.

2.1.2.1 Cubic Equation of State

This category of the equation of state is the most popular due to simplicity and the acceptable accuracy for simple systems. The reason behind the name is because it becomes a cubic equation when it is rearranged with respect to the volume (Pedersen and Christensen 2007). Also, there are many cubic equations of state available in the literature, the most important will be highlighted.

- Van der Waals Equation of State (VdW EOS)

Van der Waals in (1873) developed an equation of state that eliminates two assumptions in the ideal gas law which are: insignificant gas molecules volume compared to the system and the absence of the attractive and repulsion forces (Van der Waals, 1873). He introduced a parameter (b) to account for the gas molecules especially at high pressure. This parameter

will be subtracted from the volume of the system as the equation (2.1-13) in Table (2-1). For the second assumption, he introduced a correction term to account for the attractive forces and the repulsion forces were implemented in the co-volume parameter. The equation became as equation (2.1-14) in Table (2-1). The a and b are constants that depend on the critical properties of the compounds and the defined as equation (2.1-15) and equation (2.1-16) in Table (2-1).

- Redlich-Kwong Equation of State (RK EOS)

Redlich and Kwongin (1948) observed that VdW EOS did not consider the temperature's effect on the attraction term (Redlich and Kwong 1948). They modified the attraction term in VdW EOS ($-\frac{a}{v^2}$) to become equation (2.1-17) in Table (2-1). The a and b are constants which also depend on the critical properties of the compounds as shown in equation (2.1-18) and equation (2.1-19) in Table (2-1).

- Soave-Redlich-Kwong Equation of State (SRK EOS)

Soave in (1972) proposed a modification to RK-EOS in the attraction term (Soave 1972). He introduced a temperature dependent term which represented by equation (2.1-21) and the equation of state will become as equation (2.1-20) in Table (2-1).

- Peng-Robinson Equation of State (PR-EOS)

Peng and Robinson in (1974) investigated SRK-EOS and found there some problems in predicting the liquid density especially in near the critical region (Peng and Robinson 1976). They proposed a modification to RK-EOS by modifying the attraction term as equation (2.1-25) in Table (2-1).

- Schmidt-Wenzel Equation of State

In 1980, Schmidt and Wenzel noticed that that SRK-EOS give a good result for molecules with small acentric factor where PR-EOS is best for substance with acentric factor value around one third (Corbett 2000; Schmidt and Wenzel 1980). Therefore, they introduced a correction factor that depends on acentric factor in the attraction term and their EOS has the form which is shown as equation (2.1-31) in Table (2-1) while the definition of the parameters are listed in Table (2-1) as well.

Patel-Teja Equation of State (PT-EOS)

Patel and Teja in (1982) modified the attraction term by including an additional term to improve the volumetric properties in the liquid region (Patel and Teja 1982). Their equation of state is shown in equation (2.1-38) in Table (2-1) with the definition of its parameters. PT-EOS considered as a general form to PR-EOS and SRK-EOS since it reduced to them by substituting η by 0.307 and 0.333, respectively (Corbett 2000).

However, the limitation of the cubic equation of state in predicting the properties of systems that contain hydrogen bonding compound was the reason for a new project such as the cubic plus association equation of state (Kontogeorgis et al. 2006a).

Table 2-1: Cubic Equations of State

Name	Year	Equation	Parameters
VdW-EOS	1873	$P(V - b) = RT$ (2.1-13)	$a = \Omega_a \frac{R^2 T_c^2}{P_c}$ (2.1-15)
		$P = \frac{RT}{V - b} - \frac{a}{V^2}$ (2.1-14)	$b = \Omega_b \frac{RT_c}{P_c}$ (2.1-16)
RK-EOS	1948	$P = \frac{RT}{V - b} - \frac{a}{V(V + b)\sqrt{T}}$ (2.1-17)	$a = \Omega_a \frac{R^2 T_c^{2.5}}{P_c}$ (2.1-18)
			$b = \Omega_b \frac{RT_c}{P_c}$ (2.1-19)
SRK-EOS	1972		$\alpha(T) = \left[1 + m \left(1 - \sqrt{\frac{T}{T_c}} \right) \right]^2$ (2.1-21)
		$P = \frac{RT}{V - b} - \frac{a \alpha(T)}{V(V + b)}$ (2.1-20)	$m = 0.48 + 1.74\omega - 0.176\omega^2$ (2.1-22)
			$a = \Omega_a \frac{R^2 T_c^2}{P_c}$ (2.1-23)
			$b = \Omega_b \frac{RT_c}{P_c}$ (2.1-24)
PR-EOS	1974		$\alpha(T) = \left[1 + m \left(1 - \sqrt{\frac{T}{T_c}} \right) \right]^2$ (2.1-26)
		$P = \frac{RT}{V - b} - \frac{a \alpha(T)}{V(V + b) + b(V - b)}$ (2.1-25)	If $\omega \leq 0.49$ $m = 0.3796 + 1.5422\omega - 0.2699\omega^2$ (2.1-27)
			If $\omega > 0.49$ $m = 0.3796 + 1.4850\omega - 0.1644\omega^2 + 0.0167\omega^3$ (2.1-28)
			$a = \Omega_a \frac{R^2 T_c^2}{P_c}$ (2.1-29)
			$b = \Omega_b \frac{RT_c}{P_c}$ (2.1-30)
SW-EOS	1980		$a = \Omega_a \frac{R^2 T_c^2}{P_c}$ (2.1-32)
		$P = \frac{RT}{V - b} - \frac{a \alpha(T)}{V^2 + (1 + 3\omega)bV - 3\omega b^2}$ (2.1-31)	$b = \Omega_b \frac{RT_c}{P_c}$ (2.1-33)
			$\Omega_a = [1 - \eta(1 - q)]^3$ (2.1-34)
			$\Omega_b = \eta q$ (2.1-35)
			$\eta = 1/[3 \cdot (1 + q\omega)]$ (2.1-36)
			$q = 0.25989 - 0.017\omega + 0.00375\omega^2$ (2.1-37)
PT-EOS	1982		$a = \Omega_a \frac{R^2 T_c^2}{P_c}$ (2.1-39)
		$P = \frac{RT}{V - b} - \frac{a \alpha(T)}{V(V + b) + c(V - b)}$ (2.1-38)	$b = \Omega_b \frac{RT_c}{P_c}$ (2.1-40)
			$c = \Omega_c \frac{RT_c}{P_c}$ (2.1-41)
			$\Omega_a = 3\eta^2 + 3(1 - 2\eta)\Omega_b + \Omega_b^2 + (1 - 3\eta)$ (2.1-42)
			$\Omega_b = 0.3249\eta - 0.022005$ (2.1-43)
			$\Omega_c = 1 - 3\eta$ (2.1-44)
		$\eta = 0.329032 - 0.076799\omega + 0.0211947\omega^2$ (2.1-45)	

where a , b , c , P_c , T_c , ω , Ω_a and Ω_b are attraction parameter, gas molecules volume parameter (co-volume), adjustable parameter for the attraction term, critical pressure, critical temperature, acentric factor, constants; respectively. Ω_a and Ω_b are equal to 0.4219 (VdW), 0.4274 (RK and SRK), 0.4572 (PR), constant equal to 0.125 (VdW), 0.0866 (RK and SRK), 0.0778 (PR); respectively.

2.1.2.2 Cubic Plus Association (CPA)

The cubic plus association start as a collaboration project with the Research Centre of Shell in Amsterdam in the years of 1995 to 1999. They started with the SRK-EOS and added association term form Wertheim theory as written by Statistical associating fluid theory which known as SAFT (Kontogeorgis et al. 2006a). The CPA-EOS has the following form with respect to the pressure (Michelsen and Hendriks 2001):

$$P = \frac{RT}{V_m - b} - \frac{a}{V_m(V_m + b)} - \frac{1}{2} \left(\frac{RT}{V_m} \right) \left(1 + \frac{1}{V_m} \frac{\partial \ln g}{\partial \left(\frac{1}{V_m} \right)} \right) \sum_i x_i \sum_{A_i} (1 - X_A)_i \quad (2.1-47)$$

$$a = \Omega_a \left(\frac{R^2 T_{cm}^2}{P_{cm}} \right) \left[1 + m_m \left(1 - \sqrt{\frac{T}{T_{cm}}} \right) \right]^2 \quad (2.1-48)$$

$$b = \Omega_b \left(\frac{RT_{cm}}{P_{cm}} \right) \quad (2.1-49)$$

where V_m , T_{cm} , P_{cm} , m_m , g and X_A are molar volume, CPA temperature parameter, CPA pressure parameter, CPA parameter and radial distribution function Fraction of A-sites of molecule i that are not bonded with other sites; respectively.

The association term is taken from the Wertheim theory as in statistical associating fluid theory equation of state (Kontogeorgis et al. 2006a; Michelsen and Hendriks 2001). The association term considers the interaction between site and site because of the hydrogen bonding. This can occur for like molecules which called self-association or unlike molecules which called cross-association. This concept will be more illustrated in the SAFT section. The simplified term of the fraction of A-site of molecule i that are not bonded with other sites is defined as the following:

$$X_{A_i} = \frac{1}{1 + \left(\frac{1}{\sqrt{V_m}}\right) \sum_j x_j \sum_{B_j} X_{B_j} \Delta^{A_i B_j}} \quad (2.1-50)$$

where B_j , X_{B_j} and $\Delta^{A_i B_j}$ are sites of another molecule, fraction of B-sites of molecule j that are not bonded with other sites and association strength between the site A of molecule i with site of molecule j ; respectively.

The association strength is given by the following expression:

$$\Delta^{A_i B_j} = g \left[\exp\left(\frac{\epsilon^{A_i B_j}}{RT}\right) - 1 \right] b_{ij} \beta^{A_i B_j} \quad (2.1-51)$$

where $\epsilon^{A_i B_j}$ and $\beta^{A_i B_j}$ are Association energy and volume; respectively.

The radial distribution function can be estimated by the following expression:

$$g = \frac{2 - \eta}{2(1 - \eta)^3} \quad (2.1-52)$$

$$\eta = \left(\frac{1}{4V_m} \right) b \quad (2.1-53)$$

CPA-EOS gave outstanding results for strongly associating compounds. However, some challenges needed to be investigated more to improve the CPA-EOS such as CPA parameters, the importance of missing terms such as polar contribution, limitation in the critical region, etc. (Kontogeorgis et al. 2006b, 2006a).

2.1.2.3 Statistical Associating Fluid Theory (SAFT)

All the previous EOS provide a fast and straightforward way to estimate the required properties of simple systems such as small molecules and solvent. However, applying these EOS to complex systems (e.g., polymers system) showed theoretical limitations and weaknesses. Statistical associating fluid theory (SAFT) was the result of advancement in several areas such as integral equation theories, radial distribution function and statistical advancement theories. It was developed by Chapman in 1988 (Chapman et al. 1989; Chapman, Jackson, and Gubbins 1988) and it's based on the Wertheim perturbation theory

(Wertheim 1984a, 1984b, 1986b, 1986a). The perturbation theory solves the problem mathematically by approximation. It achieves that by adding correction perturbation term to exact solution terms. The expansion of Helmholtz free energy incorporated with association potential integrals and the molecular distribution functions (Ahmed, 2015).

There are different versions of SAFT that were developed in the past decade and the distinctive features between them could be using different potential, using different formulas for some terms (e.g., dispersion term), simplifying some of the terms (e.g., association term), adding new term (e.g., electrostatic interaction), etc. Nevertheless, they have a similar framework which is combining the intermolecular forces with fluid-structure description by using the radial distribution function in the perturbation theory. The SAFT theory considered as hard-spheres based model where the hard-sphere contains chain and association sites. This can be illustrated more by looking to Figure 2-1 (Ahmed, 2015).

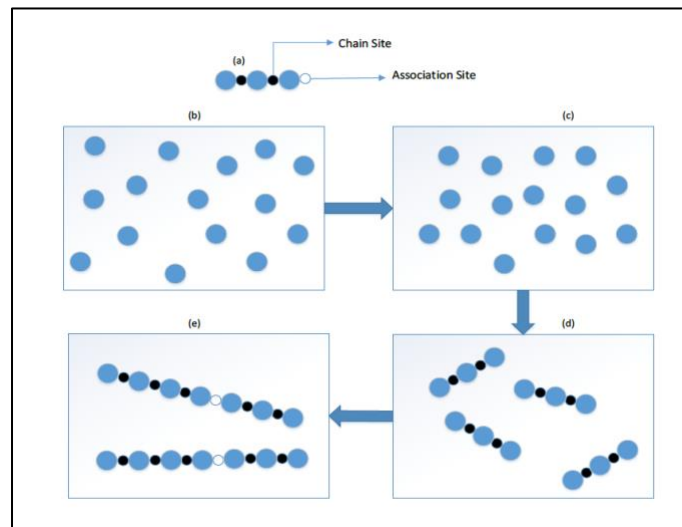


Figure 2-1: Representations of SAFT Theory

The molecules forming procedure in SAFT theory is the following:

- a) The molecules are represented as hard-spheres that were containing initially sites for the chains and the association.
- b) The repulsion forces are exhibited due to the hard sphere molecules assumption.
- c) The attraction forces (dispersive forces) are added.
- d) The chain sites are added; hence, the chain molecules will be formed.
- e) The association sites are added; hence, the association molecules will be formed.

The mathematical representation of the contribution for each step is given by the Helmholtz free energy as the following:

$$a^{res} = a^{seg} + a^{chain} + a^{assoc} \quad (2.1-54)$$

where a^{res} , a^{seg} , a^{Chain} , a^{assoc} are the residual Helmholtz free energy, the segment Helmholtz free energy which include the repulsion and dispersion, the chain Helmholtz free energy and the association Helmholtz free energy; respectively.

The definition of each term could change from version to version of SAFT. In this section, a recent version of SAFT will be highlighted which known as a SAFT-VR Mie (Lafitte et al. 2013). The purpose of developing this version is to overcome the shortcoming of the previous versions as well as increasing the prediction capability. The main limitations in

the previous version are representing thermodynamic second derivative properties and estimating the critical properties (Lafitte et al. 2013). In SAFT-VR Mie, the Mie pair potential (which consider as a general form of the Lenard-Jones potential) was used to describe the repulsion and attraction terms. The Mie pair potential has the following mathematical form for two spheres separated by distance r :

$$u_{ij}^{Mie} = C_{ij}\epsilon_{ij} \left(\left(\frac{\sigma_{ij}}{r_{ij}} \right)^{\lambda_{r,ij}} - \left(\frac{\sigma_{ij}}{r_{ij}} \right)^{\lambda_{a,ij}} \right) \quad (2.1-55)$$

$$C_{ij} = \frac{\lambda_{r,ij}}{\lambda_{r,ij} - \lambda_{a,ij}} \left(\frac{\lambda_{r,ij}}{\lambda_{a,ij}} \right)^{\frac{\lambda_{a,ij}}{\lambda_{r,ij} - \lambda_{a,ij}}} \quad (2.1-56)$$

where u_{ij}^{Mie} , C_{ij} , ϵ_{ij} , σ_{ij} , r_{ij} , $\lambda_{r,ij}$ and $\lambda_{a,ij}$ are Mie pair potential between i and j molecules, pre-factor for i and j molecules, well depth of the Mie potential, segment diameter of molecules i and j , the distance between the i and j molecules, variable repulsion exponent term between the i and j molecules and variable attraction exponent term between the i and j molecules; respectively.

The variable exponent terms used to describe the range of dispersive interactions and the hardness-softness of the repulsive interactions (Dufal et al. 2015). The purpose of using a prefactor term is to guarantee that the minimum value of Mie pair potential is the negative of the well depth ($-\epsilon$). The spheres that Mie pair potential describe called Mie segments

and they can form Mie chain through covalent bonding. Adding the association sites to the Mie segment or chain will form the associating molecule.

The SAFT-VR Mie version contains two more adjustable parameters which are λ_r and λ_a . These parameters raise the number of adjustable parameters to five and seven for non-associating and associating compound, respectfully. These parameters are determined by fitting process against different data including saturated pressure and liquid densities. Improving the predication of SAFT-VR Mie is done using the second derive properties (Lafitte, Bessieres, Piñeiro, and Daridon, 2007; Waseem, 2017).

The SAFT-VR Mie version was developed in term of the Helmholtz free energy and had similar terms to some extent as the previous SAFT versions which represent it mathematically as the following (Lafitte et al. 2013):

$$a^{res} = a^{mono} + a^{chain} + a^{assoc} \quad (2.1-57)$$

where a^{mono} is the mono Helmholtz free energy.

Each of the previous term will be discussed in the following sub sections.

- Mono term

This term accounts for the dispersion interactions and the hard sphere which is the reference fluid in the SAFT-VR Mie. The interactions between these hard spheres (Mie

segment) are represented by perturbed terms (Gil-villegas et al. 1997). These terms expanded following Baker and Henderson theory (Barker and Henderson 1967b) which used a series of temperature inverse in the process of expanding their terms up to the third term. The mathematical representation of the Helmholtz free energy of the Mie segment term is the following:

$$a^{mono} = \left(\sum_{i=1}^n x_i m_i \right) a^M \quad (2.1-468)$$

$$a^M = a^{HS} + \beta a_1 + (\beta)^2 a_2 + (\beta)^3 a_3 \quad (2.1-59)$$

where m_i , a^{HS} , a_1 , a_2 and a_3 are number of Mie segment, Helmholtz free energy of the hard sphere and attraction interaction mean free energy; respectively.

The Helmholtz free energy of the hard sphere is the following (Boublik 1986; Mansoori et al. 1971):

$$a^{HS} = \frac{6}{\pi \rho_s} \left[\left(\frac{\xi_2^3}{\xi_3^2} - \xi_0 \right) \ln(1 - \xi_3) + \frac{3\xi_1 \xi_3}{1 - \xi_3} + \frac{\xi_2^3}{\xi_3(1 - \xi_3)^2} \right] \quad (2.1-60)$$

$$\xi_k = \left(\frac{\pi \rho_s}{6} \right) \sum_i x_{s,i} m_i d_{ii}^k, \quad k = 0,1,2,3 \quad (2.1-61)$$

$$x_{s,i} = \frac{m_i x_i}{\sum_{k=1}^n m_k x_k} \quad (2.1-62)$$

where ρ_s and d_{ii} are number density of the overall segment and the effective diameter of the component segment; respectively.

The effective diameter of the segment is defined by the following expression (Barker and Henderson 1967b, 1967a):

$$d_{ii}(T) = \int_0^{\sigma_{ii}} \left(1 - \exp\left(-\beta u_{ii}^{Mie}(r)\right) \right) dr \quad (2.1-63)$$

The mean free energy of attraction interaction (a_1, a_2, a_3) are expressed by different expressions. The first order perturbation term is the following:

$$a_1 = \sum_{i=1}^n \sum_{j=1}^n x_{s,i} x_{s,j} a_{1,ij} \quad (2.1-64)$$

$$\begin{aligned} a_{1,ij} = & C_{ij} [x_{0,ij}^{\lambda_{a,ij}} (a_{1,ij}^s(\rho_s; \lambda_{a,ij}) + B_{ij}(\rho_s; \lambda_{a,ij})) \\ & - x_{0,ij}^{\lambda_{r,ij}} (a_{1,ij}^s(\rho_s; \lambda_{r,ij}) + B_{ij}(\rho_s; \lambda_{r,ij}))] \end{aligned} \quad (2.1-65)$$

with

$$x_{0,i,j} = \sigma_{ij}/d_{ij} \quad (2.1-66)$$

$$B_{ij}(\rho_s; \lambda_{ij}) = 2\pi\rho_s d_{ij}^3 \epsilon_{ij} \left[\frac{1 - \frac{\zeta_x}{2}}{(1 - \zeta_x)^3} I_{\lambda,ij} - \frac{9\zeta_x(1 + \zeta_x)}{2(1 - \zeta_x)^3} J_{\lambda,ij} \right] \quad (2.1-67)$$

$$\zeta_x = \frac{\pi\rho_s}{6} \sum_{i=1}^n \sum_{j=1}^n x_{s,i} x_{s,j} d_{ij}^3 \quad (2.1-68)$$

$$I_{\lambda,ij} = \frac{-x_{0,ij}^{3-\lambda_{ij}} - 1}{\lambda_{ij} - 3} \quad (2.1-69)$$

$$J_{\lambda,ij} = -\frac{(x_{0,ij})^{4-\lambda_{ij}}(\lambda_{ij} - 3) - (x_{0,ij})^{3-\lambda_{ij}}(\lambda_{ij} - 4) - 1}{(\lambda_{ij} - 3)(\lambda_{ij} - 4)} \quad (2.1-70)$$

The $a_{1,ij}^s$ term in equation (2.1-65) is given by the following expression (Sutherland 1887):

$$a_{1,ij}^s(\rho_s; \lambda_{ij}) = -2\rho_s \frac{(\pi\epsilon_{ij}d_{ij}^3)}{\lambda_{ij} - 3} \frac{1 - \zeta_x^{eff}(\lambda_{ij})/2}{(1 - \zeta_x^{eff}(\lambda_{ij}))^3} \quad (2.1-71)$$

$$\zeta_x^{eff}(\lambda_{ij}) = c_1(\lambda_{ij})\zeta_x + c_2(\lambda_{ij})\zeta_x^2 + c_3(\lambda_{ij})\zeta_x^3 + c_4(\lambda_{ij})\zeta_x^4 \quad (2.1-72)$$

$$\begin{pmatrix} c_1 \\ c_2 \\ c_3 \\ c_4 \end{pmatrix} = \begin{pmatrix} 0.81096 & 1.7888 & -37.578 & 92.284 \\ 1.0205 & -19.341 & 151.26 & -463.50 \\ -1.9057 & 22.845 & -228.14 & 973.92 \\ 1.0885 & -6.1962 & 106.98 & -677.64 \end{pmatrix} \begin{pmatrix} 1 \\ 1/\lambda_{ij}^2 \\ 1/\lambda_{ij}^2 \\ 1/\lambda_{ij}^3 \end{pmatrix} \quad (2.1-73)$$

For $a_{2,ij}$ term in equation (2.1-59), it's given as the following expression:

$$a_2 = \sum_{i=1}^n \sum_{j=1}^n x_{s,i} x_{s,j} a_{2,ij} \quad (2.1-74)$$

where

$$\begin{aligned} a_{2,ij} = & \frac{1}{2} K^{HS} (1 + X_{ij}) \epsilon_{ij} C_{ij}^2 \times [x_{0,ij}^{2\lambda_{a,ij}} (a_{1,ij}^s(\rho_s; 2\lambda_{a,ij}) \\ & + B_{ij}(\rho_s; 2\lambda_{a,ij}) \\ & - 2x_{0,ij}^{\lambda_{a,ij} + \lambda_{r,ij}} (a_{1,ij}^s(\rho_s; \lambda_{a,ij} + \lambda_{r,ij}) \\ & + B_{ij}(\rho_s; \lambda_{a,ij} + \lambda_{r,ij}) \\ & + x_{0,ij}^{2\lambda_{r,ij}} (a_{1,ij}^s(\rho_s; 2\lambda_{r,ij}) + B_{ij}(\rho_s; 2\lambda_{r,ij})))] \end{aligned} \quad (2.1-75)$$

with

$$K^{HS} = \frac{(1 - \zeta_x)^4}{1 + 4\zeta_x + 4\zeta_x^2 - 4\zeta_x^3 + 4\zeta_x^4} \quad (2.1-76)$$

$$X_{ij} = f_1(\alpha_{ij})\zeta_x + f_2(\alpha_{ij})\zeta_x^5 + f_3(\alpha_{ij})\zeta_x^8 \quad (2.1-77)$$

$$\zeta_x = \frac{\pi\rho_s}{6} \sum_{i=1}^n \sum_{j=1}^n x_{s,i} x_{s,j} \sigma_j^3 \quad (2.1-78)$$

$$\alpha_{ij} = C_{ij} \left(\frac{1}{\lambda_{a,ij} - 3} - \frac{1}{\lambda_{r,ij} - 3} \right) \quad (2.1-79)$$

The third order term $a_{3,ij}^s$ in equation (2.1-59) consider as one of the main improvements in the SAFT-VR Mie which is given by the following:

$$a_{3,ij} = -\epsilon_{ij}^3 f_4(\alpha_{ij}) \zeta_x \exp(f_5(\alpha_{ij}) \zeta_x + f_6(\alpha_{ij}) \zeta_x^2) \quad (2.1-80)$$

with

$$f_k(\alpha_{ij}) = \frac{(\sum_{n=0}^{n=3} \phi_{k,n} \alpha_{ij}^n)}{1 + \sum_{n=4}^{n=6} \phi_{k,n} \alpha_{ij}^{n-3}} \quad (2.1-81)$$

- Chain term

The chain term often does not change much between the different versions of SAFT-EOS mathematically. It was developed by Chapman work (Jackson, Chapman, and Gubbins 1988) and they used scaled particle theory radial distribution function (RDF) (Boublík 1970; Chapman et al. 1988). Using different pair correlation function is the main difference between the various versions of SAFT-EOS and the choice laid on the selected reference. The chain term in Mie fluid is represented mathematically by the following:

$$a^{chain} = - \sum_{i=1}^n x_i (m_i - 1) \ln g_{ii}^{Mie}(\sigma_{ii}) \quad (2.1-82)$$

where $g_{ii}^{Mie}(\sigma_{ii})$ is pair correlation function for Mie segment.

It consists of hard sphere term $g_{d,i,j}^{HS}(\sigma_{ij})$, first order radial distribution functions $g_{1,ij}(\sigma_{ij})$ and the second-order radial distribution functions $g_{2,ij}(\sigma_{ij})$. The mathematical representation of pair correlation function for Mie segment is the following:

$$g_{ij}^{Mie}(\sigma_{ij}) = g_{d,ij}^{HS}(\sigma_{ij}) \exp\left(\frac{\beta g_{1,ij}(\sigma_{ij})}{g_{d,ij}^{HS}(\sigma_{ij})} + \frac{(\beta\epsilon)^2 g_{2,ij}(\sigma_{ij})}{g_{d,ij}^{HS}(\sigma_{ij})}\right) \quad (2.1-83)$$

with

$$g_{d,ij}^{HS}(\sigma_{ij}) = \exp(k_0 + k_1 x_{0,ij} + k_2 x_{0,ij}^2 + k_3 x_{0,ij}^3) \quad (2.1-84)$$

$$k_0 = -\ln(1 - \zeta_x) + \frac{42\zeta_x - 39\zeta_x^2 + 9\zeta_x^3 - 2\zeta_x^4}{6(1 - \zeta_x)^3} \quad (2.1-85)$$

$$k_1 = \frac{\zeta_x^4 + 6\zeta_x^2 - 12\zeta_x}{2(1 - \zeta_x)^3} \quad (2.1-86)$$

$$k_2 = \frac{-3\zeta_x^2}{8(1 - \zeta_x)^2} \quad (2.1-87)$$

$$k_3 = \frac{-\zeta_x^4 + 3\zeta_x^2 + 3\zeta_x}{6(1 - \zeta_x)^2} \quad (2.1-88)$$

$$g_{1,ij}(\sigma_{ij}) = \frac{1}{2\pi d_{ij}^3 \epsilon_{ij}} \left[3 \frac{da_{1,ij}}{d\rho_s} - C_{ij} \lambda_{a,ij} x_{0,ij}^{\lambda_{a,ij}} \frac{a_{1,ij}^s(\rho_s; \lambda_{a,ij}) + B_{ij}(\rho_s; \lambda_{a,ij})}{\rho_s} + C_{ij} \lambda_{r,ij} x_{0,ij}^{\lambda_{r,ij}} \frac{a_{1,ij}^s(\rho_s; \lambda_{r,ij}) + B_{ij}(\rho_s; \lambda_{r,ij})}{\rho_s} \right] \quad (2.1-89)$$

$$g_{2,ij}(\sigma_{ij}) = (1 + \gamma_{c,ij}) g_{2,ij}^{MCA} \quad (2.1-90)$$

$$\begin{aligned} \gamma_{c,ij} = & \phi_{7,0} \left(-\tanh \left(\phi_{7,1} (\phi_{7,2} - \alpha_{ij}) \right) + 1 \right) \zeta_x \theta_{ij} \\ & \times \exp(\phi_{7,3} \zeta_x + \phi_{7,4} \zeta_x^2) \end{aligned} \quad (2.1-91)$$

$$\theta_{ij} = \exp(\beta \epsilon_{ij}) - 1 \quad (2.1-92)$$

where $\phi_{7,0}, \phi_{7,1}, \phi_{7,2}, \phi_{7,3}$ and $\phi_{7,4}$ are coefficients depends on VLE data and molecular simulation (Lafitte et al. 2013).

The $g_{2,ij}^{MCA}$ term can be estimated as the following:

$$\begin{aligned} g_{2,ij}^{MCA}(\sigma_{ij}) = & \frac{1}{2\pi d_{ij}^3 \epsilon_{ij}^2} \left[3 \frac{\partial \frac{a_{2,ij}}{1+X_{ij}}}{\partial \rho_s} \right. \\ & - \epsilon_{ij} C_{ij}^2 K^{HS} \lambda_{r,ij} x_{0,ij}^{2\lambda_{r,ij}} \\ & \times \frac{a_{1,ij}^s(\rho_s; 2\lambda_{r,ij}) + B_{ij}(\rho_s; 2\lambda_{r,ij})}{\rho_s} \\ & + \epsilon_{ij} C_{ij}^2 K^{HS} (\lambda_{r,ij} + \lambda_{a,ij}) x_{0,ij}^{\lambda_{r,ij} + \lambda_{a,ij}} \\ & \times \frac{a_{1,ij}^s(\rho_s; \lambda_{r,ij} + \lambda_{a,ij}) + B_{ij}(\rho_s; \lambda_{r,ij} + \lambda_{a,ij})}{\rho_s} \\ & - \epsilon_{ij} C_{ij}^2 K^{HS} \lambda_{a,ij} x_{0,ij}^{2\lambda_{a,ij}} \\ & \times \left. \frac{a_{1,ij}^s(\rho_s; 2\lambda_{a,ij}) + B_{ij}(\rho_s; 2\lambda_{a,ij})}{\rho_s} \right] \end{aligned} \quad (2.1-93)$$

- Association term

The third term in the SAFT equation is the associating term which takes into account the association interactions between the molecules. This term another difference between the SAFT versions since some used simplified association term where others used the full definition of the association or modified term. The full version of the association Helmholtz free energy was developed by Wertheim (Wertheim 1984a, 1984b, 1986b, 1986a). Different potentials can be used in the association term with the square well potential as the most common due to its simplicity compared to the other potentials. The mathematical representation of the Helmholtz free energy is the following:

$$a^{assoc} = \sum_{i=1}^n x_i \sum_{a=1}^{s_i} n_{ai} \left[\ln X_{ai} - \frac{X_{ai}}{2} + \frac{M}{2} \right] \quad (2.1-94)$$

where s_i , M , n_{ai} and X_{ai} are the association site type, number of sites for the molecule, number of type sites on a molecule I and non-bonded fraction of component i at site a ; respectively.

The Non-bonded fraction is defined as the following:

$$X_{ai} = \frac{1}{1 + \rho \sum_{j=1}^n x_j \sum_{b=1}^{s_j} n_{b,j} X_{bj} \Delta_{abij}} \quad (2.1-95)$$

where Δ_{abij} is association strength between component i site 'a' and component j site 'b'.

The mathematical expression for the association strength is the following:

$$\Delta_{abij} = K_{abij} F_{abij} I_{abij} \quad (2.1-96)$$

where K_{abij} , I_{abij} and F_{abij} are bonding volume between component i site 'a' and component j site 'b', association kernel between component i site 'a' and component j site 'b' and Mayer function between component i site 'a' and component j site 'b'; respectively.

The Mayer function represent the hydrogen bonding energy which is estimated by the following equation:

$$F_{abij} = \exp(\beta \epsilon_{abij}^{HB}) - 1 \quad (2.1-97)$$

where ϵ_{abij}^{HB} is hydrogen bonding energy between component i site 'a' and component j site 'b'.

The association strength relies on two parameters; pair potential and the reference fluid type. As it was mention before regarding the potential, the square well potential usually used for describing the association sites. The reference fluid type characterized by radial distribution function which will be utilized in estimating the association kernel. Dufal et

al. (2015) investigated radial distribution functions of diverse reference monomeric systems and ultimately used to estimate the association strength which based on Mie radial distribution function (Mie-RDF). (Dufal et al. 2015).

The Hard-sphere radial distribution function HS-RDF adopted in many studies and different versions of SAFT due to their simplicity computational and reliability for describing the HS fluid (Chapman et al. 1990; Gross and Sadowski 2002), (Galindo et al. 1996). It has the following concept; the reference fluid consists of hard spheres with off-center SW association sites implant on each sphere which used in SAFT-VR Mie (Lafitte et al. 2013) and has the following expression:

$$\Delta_{abij} = K_{abij} F_{abij} g_{d,ij}^{HS}(d) \quad (2.1-98)$$

with

$$\begin{aligned} K_{abij} = & 4\pi d_{ij}^2 \left[\ln \left(\frac{r_{abij}^c + 2r_{abij}^d}{d_{ij}} \right) \right. \\ & \times \left(6r_{abij}^c{}^3 + 18r_{abij}^c{}^2 r_{abij}^d - 24r_{abij}^d{}^3 \right) \\ & + \left(r_{abij}^c + 2r_{abij}^d - d_{ij} \right) \left(22r_{abij}^d{}^2 - 5r_{abij}^c r_{abij}^d \right. \\ & \left. \left. - 7r_{abij}^d d_{ij} - 8r_{abij}^c{}^2 + r_{abij}^d d_{ij} + d_{ij}^2 \right) \right] / (72r_{abij}^d{}^2) \end{aligned} \quad (2.1-99)$$

where r_{ab}^c , r_{ab}^d and $g_{d,ij}^{HS}(d)$ are cutoff range of Square well interaction between site 'a' and site 'b', distance between site 'a' and site 'b' from the segment center and hard-sphere radial distribution function.

Hard sphere radial distribution function evaluated by the following expression (Boublik 1986):

$$g_{d,ij}^{HS}(d) = \frac{1}{1 - \zeta_3} + 3 \frac{d_{jj}d_{ii}}{d_{jj} + d_{ii}} \frac{\zeta_2}{(1 - \zeta_3)^2} + 2 \left(\frac{d_{jj}d_{ii}}{d_{jj} + d_{ii}} \right)^2 \frac{\zeta_2^2}{(1 - \zeta_3)^3} \quad (2.1-100)$$

Dufal et al. (2015) proposed a new association kernel (by utilizing the LJ-RDF reference system (Muert and Gubbins 1995)) for association sites with different fixed geometry. It has the following expression:

$$I(T^*, \rho^*) = \sum_{i=0}^{i+j \leq 10} \sum_{j=0} c_{ij} [\rho^*]^i [T^*]^j \quad (2.1-101)$$

where T^* , ρ^* and c_{ij} are dimensionless temperature, dimensionless density and adjustable parameters; respectively.

The dimensionless temperature can be estimated by the following expression:

$$T_{ij}^* = \frac{k_B T}{\epsilon_{ij}} \quad (2.1-102)$$

where ϵ_{ij} is interaction energy between component i component j.

The dimensionless density can be evaluated by the following mathematical expression:

$$\rho^* = \rho \sigma_{vdW1,x}^3 \quad (2.1-103)$$

with

$$\sigma_{vdW1,x}^3 = \sum_i \sum_j x_i x_j \sigma_{ij}^3 \quad (2.1-104)$$

The Mie association kernel was evaluated based on Mie-RDF by Dufal et al. in 2015 (Dufal et al. 2015). The same approach used to determine the LJ association kernel was utilized to determine the Mie association kernel. The description of the molecular geometry used is a Mie monomeric segment with off-center SW association sites. The following expression used to evaluate the Mie association kernel:

$$I(T^*, \rho^*, \lambda_r) = \sum_{i=0}^{i+j \leq 10} \sum_{j=0} a_{ij}(\lambda_r) [\rho^*]^i [T^*]^j \quad (2.1-105)$$

with

$$a_{ij}(\lambda_r) = \sum_{k=0}^6 b_{i,j,k} [\lambda_r]^k \quad (2.1-106)$$

where λ_r and $b_{i,j,k}$ are repulsive exponent and adjustable coefficients; respectively.

For a pure component system, the SAFT-VR Mie contains the physical parameters to describe the component which could be constant or dependent on other parameters such as temperature and pressure. These parameters are found by fitting to experiment data or other sources of accurate data such as the molecular simulation (Poling, Prausnitz, and O'Connell 1988). The parameters for SAFT-VR Mie of different associating and non-associating compound are taken from the literature which is listed in the following table:

Table 2-2: SAFT-VR Mie parameters for different compounds

Components	m_i	σ_i	ε_i	λ_r	λ_a	ε_{ab}^{HB}	K_{ab}^{HB}	Reference
Methane	1.0000	3.7412	153.36	12.6500	6.0000	N/A	N/A	(Lafitte et al. 2013)
Ethane	1.4373	3.7257	206.12	12.4000	6.0000	N/A	N/A	
Propane	1.6845	3.9056	239.89	13.0060	6.0000	N/A	N/A	
Carbon dioxide	1.5000	3.1916	231.88	27.5570	5.1646	N/A	N/A	
Argon	1.0000	3.4038	117.84	12.0850	6.0000	N/A	N/A	(Dufal et al. 2015)
Ethene	1.7972	3.2991	142.64	9.6463	6.0000	N/A	N/A	
Nitrogen	1.4214	3.1760	72.43	9.8749	6.0000	N/A	N/A	
Oxygen	1.4283	2.9671	81.47	8.9218	6.0000	N/A	N/A	
Hydrogen Sulfide	1.0000	3.7783	387.28	22.4510	6.0000	N/A	N/A	(Perez et al. 2016)
Water	1.0000	3.0063	266.68	17.020	6.0000	1985.4	101.69	(Dufal et al. 2015)

For the mixtures, will be an unlike interaction between the components of the system which will require a combining rule. A combining rule can be defined as a linear function that will describe the unlike molecular interaction potential parameters by utilizing the like molecular interaction parameters (Luongo-ortiz and Starling 1997). All the SAFT-VR Mie parameter except the number of segments need the combining rule for the unlike molecules. One of the most common combining rules is Lorentz-Berthelot combining rules which were utilized in the SAFT-VR Mie. Berthelot combining rule uses a geometric mean sort of expansion while the Lorentz combining rule utilizes the arithmetic mean as the following:

- Segment Diameter (σ):

$$\sigma_{ij} = \frac{\sigma_{ii} + \sigma_{jj}}{2} \quad (2.1-107)$$

- Baker-Henderson effective diameter (d):

$$d_{ij} = \frac{d_{ii} + d_{jj}}{2} \quad (2.1-108)$$

- Cutoff range of SW interaction between association sites a and b (r_{abij}^c):

$$r_{abij}^c = \frac{r_{abii}^c + r_{abjj}^c}{2} \quad (2.1-109)$$

- Distance from the center of the consider segment and each association site (r_{abij}^d):

$$r_{abij}^d = \frac{r_{abii}^d + r_{abjj}^d}{2} \quad (2.1-110)$$

- Bonding volume parameter:

$$K_{abij} = \left(\frac{K_{abii}^{\frac{1}{3}} + K_{abjj}^{\frac{1}{3}}}{2} \right)^3 \quad (2.1-111)$$

While the Berthelot combining rules will be utilized for the energy and interactions-based parameters as the following:

- Energy of association (ϵ_{abij}^{HB}):

$$\epsilon_{abij}^{HB} = \sqrt{\epsilon_{abii}^{HB} \epsilon_{abjj}^{HB}} \quad (2.1-112)$$

- Energy of dispersion with binary interaction parameters (ϵ_{ij}):

$$\epsilon_{ij} = (1 - k_{ij}) \frac{\sqrt{\sigma_{ii}^3 \sigma_{jj}^3}}{\sigma_{ij}^3} \sqrt{\epsilon_{ii} \epsilon_{jj}} \quad (2.1-113)$$

- Attraction or repulsion exponent with binary interaction parameters ($\lambda_{a,ij}$ or $\lambda_{r,ij}$):

$$\lambda_{k,ij} = \sqrt{(\lambda_{k,ii} - 3)(\lambda_{k,jj} - 3) + 3}, \quad k = a, r \quad (2.1-114)$$

2.1.3 Electrolyte Thermodynamics

Electrolyte solutions can be defined as the solutions that contain ions or the solutions that conduct electricity. It encounters in different industries with plenty of applications and high importance. These systems which contain electrolyte are always non-ideal (RONALD FAWCETT 2004). In the following subsections, the ideal and non-ideal solution concept will be illustrated. In addition, some basic electrolyte thermodynamics will be highlighted.

2.1.3.1 Ideal and Non-Ideal Solution

The ideal solution is the solution that the interactions between its species (i.e. A and B) are identical. That means the interaction between A and A is the same as interaction between A and B (RONALD FAWCETT 2004). From a thermodynamic point of view, the chemical potential of one species in one phase will equal the chemical potential of the same species in the other phase, that is,

$$\mu_i^v = \mu_i^l \quad (2.1-115)$$

The chemical potential of the vapor phase could be written in this format:

$$\mu_i^v = \mu_i^{v.o} + RT \ln P_i \quad (2.1-116)$$

$$P_i = x_i P_i^o \quad (2.1-117)$$

where $\mu_i^{v.o}$, P_i and P_i^o are the chemical potential of the vapor phase for component i in the ideal solution, Partial pressure for species i and Vapor pressure for species i ; respectively.

Equation (2.1-117) is known as Raout's law which applies for the ideal solution (RONALD FAWCETT 2004). On the other hand, the non-ideal solution is the solution with different interactions between its species which most of solutions, in reality, falls in this category.

By using the equality of the chemical potential, the non-ideal solution is representing it mathematically as the following:

$$\mu_i^v = \mu_i^{v,o} + RT \ln P_i \quad (2.1-118)$$

$$P_i = \gamma_i x_i P_i^o \quad (2.1-119)$$

where γ_i is the activity coefficient for species i .

The activity coefficient work as a correction factor for the non-ideal solution (e.g., Modified Raoul's law) (RONALD FAWCETT 2004). The activity coefficient in the ideal solution will be unity.

2.1.3.2 Electrolyte Framework

The macroscopic properties are calculated from the microscopic properties for the system in the statistical thermodynamics (Kontogeorgis and Folas 2009). This is done by what's known as the ensemble. It's defined as a big number of microstates which share in common between them that all have similar properties as the microscopic system (Raabe 2016). There are several ensembles in the statistical thermodynamic (Lee, 1988):

- Microcanonical ensemble (NVE): the number of particles (N), the volume of the system (V) and the internal energy (E) are constant.
- Canonical ensemble (NVT): the number of particles (N), the volume of the system (V) and the temperature of the system (T) are constant.
- Grand canonical ensemble (μ VT): the chemical potential (μ), the volume of the system (V) and the temperature of the system (T) are constant.
- Isothermal-isobaric ensemble (NPT): the number of particles (N), the pressure of the system (P) and the temperature of the system (T) are constant.

For the electrolyte, there are several scales and the most common are Lewis-Randall scale (LR) and McMillan-Mayer scale (MM). Lewis-Randall scale treats the solvent explicitly and it yields an expression in term of the Gibbs excess energy when it is used for the calculation. On the other hand, the McMillan-Mayer scale treats the solvent molecules implicitly by a dielectric constant. Using the MM framework in deriving models yield expression in the excess Helmholtz free energy. Theories such as Debye-Huckel and primitive means spherical approximation are derived in the MM framework. On the other hand, models such as the NRTL model and UNIQUAC model are derived in the LR framework (van Bochove 2003; Chen and Evans 1982; Debye and Hückel 1923; Lee 2008; McMillan and Mayer 1945; Sanchez-Castro and Blum 1989; Sander, Fredenslund, and Rasmussen 1986).

2.1.3.3 Electrolyte Solution Properties

The dissociation of the salt in a solvent will result in positively charged ions (cations) and negatively charged ions (anions). The dissociation degree depends on the salt and the solvent. The salt could dissociate completely, and the solution will have the ions and the solvent. On the other hand, it could dissociate partially and the solution will contain the salt as molecular form beside the ions and the solvent (Wright 2007). The following equation for the dissociation reaction:



where $M_{v_+}X_{v_-}$, M , X , v_+ , v_- , z_+ and z_- are a salt, cation, anion, the stoichiometric coefficient for the cation, the stoichiometric coefficient for the anion, valance of the cation and valance of the anion; respectively.

Also, the electroneutrality must maintain with no net charge exist in the solution which represented mathematically by the following expression:

$$v_+z_+ + v_-z_- = 0 \quad (2.1-121)$$

The concentration of the electrolyte in solution can be expressed in different format; molality (m_i) which is the number of moles of the salt per 1 kg of the solvent, molarity (c_i)

which can be defined as the number of moles of the salt per volume of the solvent and mole fraction (x_i).

The conversion between them is important since the mole fraction usually used for modeling where the molarity and the molality for the experiment. The following equations can be used for the conversions:

$$x_i = \frac{1}{\frac{v}{v_i} + \frac{1000 \frac{g}{kg}}{M_{solv} v_i m_i}} \quad (2.1-122)$$

$$m_i = c_i \left(\frac{n_s W_s + 1000}{1000 d_m} \right) \quad (2.1-123)$$

where v , M_{solv} , d_m and n_s are the total stoichiometric coefficient, the molecular weight of the solvent, the density of the solution and the number of moles of the solute; respectively.

2.1.3.4 Activity Coefficient

The activity defined as the ratio of the fugacity of the component in the solution over the fugacity of the same pure component at the same conditions, it can be expressed mathematically as the following:

$$a_i = \frac{\hat{f}_i}{f_i} \quad (2.1-124)$$

where a_i is the activity for component i

The activity coefficient is a correction factor for deviation from the ideality. It can be calculated by the following expression:

$$\gamma_i = \frac{a_i}{x_i} = \frac{\hat{f}_i}{x_i f_i} = \frac{\hat{\varphi}_i}{\varphi_i} \quad (2.1-125)$$

where $\hat{\varphi}_i$ and φ_i are fugacity coefficient component i in the solution and fugacity coefficient of pure component i , respectively.

Equation (2.1-125) can be used to calculate the activity coefficient of the solvent or the solute. For the solvent, it will be the same and for the solute will be the following expression:

$$\gamma_i^* = \frac{\gamma_i}{\gamma_{i,o}} = \frac{\varphi_i}{\varphi_{i,o}} \quad (2.1-126)$$

where γ_i^* , $\gamma_{i,o}$ and $\varphi_{i,o}$ are the activity coefficient for the ion species i in the electrolyte solution, the activity coefficient for the ion species i in the infinite diluted solution and the fugacity coefficient for the ion species i in the infinite diluted solution; respectively.

When the concentration of the salt goes to zero, it is called diluted infinite solution. It can be expressed mathematically as the following:

$$\gamma_i(x_0) = \lim_{x_0 \rightarrow 0} \gamma_i, i = ion \quad (2.1-127)$$

$$\varphi_i(x_0) = \lim_{x_0 \rightarrow 0} \varphi_i, \quad i = ion \quad (2.1-128)$$

where x_0 is the mole fraction of each component in the infinite diluted solution.

All the previous activity equations (2.1-125) - (2.1-127) are mole fraction based, however, most experiment measurement data usually presented in molality based. Therefore, the molality-based activity coefficient can be calculated from the mole fraction activity coefficient as the following:

$$\gamma_i^m = \left(\sum_{solvent} x_{solvent} \right) * \gamma_i^* \quad (2.1-129)$$

where γ_i^m and γ_i^* are the activity coefficient in molality based and in mole fraction based for component i.

2.1.3.5 Mean Ionic Activity Coefficient

Another way to express the deviation from ideality is the mean ionic activity coefficient (MIAC) (Robinson and Stokes 1960). The data in the literature usually are presented in this format. It can be calculated using the following expression:

$$\gamma_{-,+}^m = [(\gamma_c^m)^{v_c} (\gamma_a^m)^{v_a}]^{\frac{1}{v}} \quad (2.1-4730)$$

where $\gamma_{-,+}^m$, γ_c^m and γ_a^m are the mean ionic activity coefficient, the activity coefficient for cation and the activity coefficient for anion; respectively.

2.1.3.6 Osmotic Coefficient

The osmotic coefficient is a different method to estimate the deviation from the ideality. It can be calculated in Lewis-Randall framework (Pitzer n.d.):

$$\Phi^{LR} = -\frac{x_{solvent}}{x_{solute}} \ln a_{solvent} \quad (2.1-4831)$$

where Φ^{LR} is the osmotic coefficient in the Lewis-Randall framework.

In the McMillan-Mayer framework, the osmotic coefficient can be calculated by the following equation:

$$\Phi^{MM} = \frac{\Pi}{\Pi_{id}} \quad (2.1-132)$$

where Φ^{MM} , Π and Π_{id} are osmotic coefficient in the McMillan-Mayer framework, the real osmotic pressure and the ideal osmotic pressure; respectively.

2.2 Electrolyte Modeling

The phase behavior of the system is very crucial in the oil and gas industry (e.g., avoiding gas hydrate formation) and it is profoundly impacted by the presence of the electrolyte in the system (Loehe and Donohue 1997). As a result, it is important to use a model that can predict the properties of a system that contains electrolytes. However, modeling the electrolyte with high accuracy is a challenging task because the ions in the system have longer range interaction compared to a neutral system which will make the system close to the non-ideality (Lin & Thomsen, 2007; Loehe & Donohue, 1997). There are two approaches in modeling both the solvent and the ions from the physical perspective. For the solvents, it can be treated as a dielectric continuum where the solvent molecules replace with dielectric constant. This approach called the primitive model. On the other hand, the solvent can be treated as a collective of hard-sphere with embedded point dipoles which called non-primitive model. For the ions, there are two ways to model them: a restricted

model where all the ions are restricted to one dimension and a non-restricted where each ion has its real dimension (Sultan 2017). The following sections will discuss electrolyte solution theories, dielectric models and the solvation models.

2.2.1 Electrolyte Solution Theories

There are many theories for the electrolyte solution, most of them exist in quantum mechanics and statistical mechanics. The exact theory is the solution of the Schrödinger equation which considered as the basis of quantum mechanics theory. It solves for the nuclei and the electrons in the solution and it considers all the interaction between them. Even though that this method is the exact solution, it is complicated in term of mathematical equations and this is the reason of avoiding this method for complex systems (Friedman, 1981; Loehe & Donohue, 1997; Donald McQuarrie, 1976). In terms of Hamiltonians level (interaction within the system), using the Schrödinger equation called the Schrödinger level and it can be considered as the most accurate level (Friedman, 1981; Loehe & Donohue, 1997; Donald McQuarrie, 1976). There is another level such as the Born-Oppenheimer level and the McMillan-Mayer level. The Born-Oppenheimer level solves for the molecules of the solvent, the ions and the molecules of the solute (Friedman 1981). For the McMillan-Mayer level, the ions of the solute are considered only where the solvent is treated as continuum (primitive model) (Friedman 1981). Most of theories in the statistical thermodynamics are either the Born-Oppenheimer level or the McMillan-Mayer level. The most important theories will be discussed.

2.2.1.1 Integral Equation Theory

Integral equation theory is one of the statistical mechanics theories and it can be used to obtain the pair correlation function (radial distribution function). It is a function that describes the distribution of a particle (i.e. ion) around a central particle (e.g., ion) (Wright 2007). One of the methods to calculate the pair correlation function is by solving the Ornstein-Zernicke (OZ) equation which is given by:

$$h_{12} = c_{12} + \rho \int c_{13} h_{13} dr_3 \quad (2.2-1)$$

$$h_{ij} = g_{ij} - 1 \quad (2.2-2)$$

where c_{ij} , g_{ij} , h_{ij} and $\int dr_3$ are the direct correlation function between particle i and j , the radial distribution function for i particle around central j particle, the total correlation function and integral over the coordinates of a third particle; respectively.

It consists of two parts: a direct part and an indirect part. The direct part concerns with the direct relation of two molecules and their impact on each other ignoring the other molecules which is represented by direct correlation function c_{ij} . On the other hand, the indirect part accounts for the influence of one molecule (molecule 1) on the other molecule (molecule 3) which then will affect the other molecule (molecule 2) which is represented by the integration term (RONALD FAWCETT 2004). The solution of this equation required

relation between the radial distribution function and direct correlation function which is called the closure (Loehe and Donohue 1997). It is provided by a different equation such as the Percus-Yevick equation, Hypernetted Chain (HNC) integral equation and the mean spherical approximation (MSA) (Friedman, 1981; Loehe & Donohue, 1997; Donald McQuarrie, 1976).

- Hypernetted chain (HNC) approximation

HNC approximation considers the most accurate closure compared to MSA and PY equation in describing the electrolyte solutions (Loehe and Donohue 1997; RONALD FAWCETT 2004), (Wei and Blum 1987). Their closure expression as the following:

$$c(r) = h(r) - \ln g(r) - \beta u(r) \quad (2.2-3)$$

where $u(r)$ is the potential or the interaction energy as a function of r .

Its main drawback that it does not have an analytical solution which means a numerical method must be used. Because the equations are non-linear, computation difficulties drew the scientists of using it (Corti HR and Prini R 1987), (Lin & Thomsen, 2007; Ronald Fawcett, 2004).

- Mean Spherical Approximation (MSA)

Mean spherical approximation is one of the most popular closures for the OZ equation which has the following expression:

$$c(r) = -\beta u(r), \quad r > \sigma \quad (2.2-4)$$

$$g(r) = 0, \quad r < \sigma \quad (2.2-5)$$

where σ is the closest distance of approach for the pair.

The development of MSA started with Lewis and Wannier in 1952; they proposed a continuum model that was generalized by Lebowitz and Percus (1966) for Ising ferromagnets which resulted in the mean spherical model (MSM) (Lebowitz and Percus 1966; Lewis and Wannier 1952). Wertheim (1964) worked on an analytical solution for the PY equation which was extended by Waisman and Lebowitz (1970) to solved the restricted primitive model for the electrolyte by the perturbation theory (Waisman 1972; Waisman and Lebowitz 1970, 1972; Wertheim 1964). Blum (1975) worked on primitive MSA and came with a solution method for the OZ equation (Blum 1975). In 1977, Blum and Hoeye derived an expression for the internal energy and Helmholtz free energy for primitive case which is given by:

$$\Delta E = -\frac{e^2}{\epsilon} \left\{ \Gamma \sum_{i=1}^n \frac{\rho_i z_i^2}{1 + \Gamma \sigma_i} + \frac{\pi}{2\Delta} \Omega P_n^2 \right\} \quad (2.2-6)$$

$$\alpha^{MSA} = -\frac{e^2}{\epsilon} \left\{ \Gamma \sum_{i=1}^n \frac{\rho_i z_i^2}{1 + \Gamma \sigma_i} + \frac{\pi}{2\Delta} \Omega P_n^2 \right\} + \frac{\Gamma^3}{3\pi} \quad (2.2-7)$$

with

$$2\Gamma = \alpha \left(\sum_{i=1}^n \rho_i \left[\frac{z_i - \frac{\pi}{2\Delta} \sigma_i^2 P_n}{1 + \Gamma \sigma_i} \right]^2 \right)^{0.5} \quad (2.2-8)$$

$$\Omega = 1 + \frac{\pi}{2\Delta} \sum_k \frac{\rho_k \sigma_k z_k}{1 + \Gamma \sigma_k} \quad (2.2-9)$$

$$P_n = \frac{1}{\Omega} \sum \rho_k \sigma_k z_k / (1 + \Gamma \sigma_k) \quad (2.2-10)$$

$$\alpha^2 = 4\pi\beta e^2 / \epsilon_0 \quad (2.2-11)$$

$$\Delta = 1 - \pi\zeta_3/6 \quad (2.2-12)$$

$$\zeta_n = \sum \rho_k (\sigma_k)^n, \quad n = 0, 1, 2, 3 \quad (2.2-13)$$

$$\sigma_{ij} = \left(\frac{1}{2}\right)(\sigma_i + \sigma_j) \quad (2.2-14)$$

with the following restriction:

$$\sum_{i=1}^n \rho_i z_i = 0 \quad (2.2-15)$$

where e , ϵ_0 , ρ_i and σ_i are the elementary charge, the permittivity of the medium, the ions density, the ions diameter; respectively

Equations (2.2-8) to (2.2-10) will be solved simultaneously to obtain the MSA parameters (P_n, Ω, Γ) which will be needed to calculate the energies. The previous model was used in many researches for the electrolyte system and it exhibited an excellent accuracy (Wu and Prausnitz 1998). The main improvement of the MSA on the DH is the fact that DH assumes the ions as point charges with no volume where the MSA considers the size of the ions which is closer to the real picture (Lee 1988).

Blum and Wei (1987) worked on a non-primitive case where the solvent is treated as a collective of molecules (Blum and Wei 1987; Wei and Blum 1987). They came up with an analytical solution for this case which is obtained by solving equations in three different parameters: screening parameter Γ , ion-dipole interaction parameter B^{10} and dipole-dipole interaction parameter b_2 . This method is better in term of accuracy compared to the other methods since it represents the reality in term of the physics where ions and the solvent molecules are treated separately (Liu, Li, & Lu, 1998).

Different simplification and models were derived from and done to the MSA over the last years such as explicit MSA. Copeman and Stein derived in 1986 an explicit form of the MSA for non-primitive case (Copeman and Stein 1986, 1987). They used the Debye-Huckel radial distribution function and derived a non-iterative screening factor. In 1988, Harvey et al. worked on a primitive-explicit case by using a linear mixing rule for the ion size (Harvey, Copeman, and Prausnitz 1988). Sanchez-Castro and Blum (1989) derived a new scheme to approximate the primitive MSA by using mean diameter (Sanchez-Castro and Blum 1989). It used the weight average method for ions diameters and the Newton-Raphson improvement method.

2.2.1.2 Poisson-Boltzmann (PB) Equation Theory

Debye-Huckel theory (1923) considered as the first theory for the electrolyte solution which is based on Poisson-Boltzmann equations (Debye and Hückel 1923; RONALD FAWCETT 2004). Poisson equation is a partial differential equation that is used to describe the variation of micro-potential (local potential) in space by the following equation (RONALD FAWCETT 2004):

$$\nabla^2 \Phi = -\frac{\rho_z}{\varepsilon \varepsilon_0} \quad (2.2-16)$$

where ∇ , Φ , ε_s and ε_0 are Laplace operation, electrostatic local potential, the permittivity of the medium and the free space permittivity; respectively.

On the other hand, the Boltzmann equation used to determine the charge density. It links different parameters such as the concentration of the ions, potential, charge number and the ion density as the following equation (RONALD FAWCETT 2004):

$$\rho_z = \sum_{i=1}^n z_i F c_i^* \exp(-z_i f \Phi) \quad (2.2-17)$$

where F , c_i^* and f are the Faraday constant, the concentration of the i ion and a constant; respectively.

The radial distribution function $g_{ij}(r)$ is defined as the following:

$$g_{ij}(r) = \exp[-z_i e \beta \Phi] \quad (2.2-18)$$

where β equal to $\frac{1}{k_B T}$.

By substituting the previous definition of the radial distribution function in the Boltzmann equation to become as the following:

$$\rho_z = \sum_{i=1}^n z_i F c_i^* g_{ij}(r) \quad (2.2-19)$$

The combining of the Possion equation and the Boltzmann gives the Possion-Boltzmann equation as the following:

$$\nabla^2\Phi = -\sum_{i=1}^n \frac{z_i F c_i^*}{\epsilon_s \epsilon_0} g_{ij}(r) \quad (2.2-20)$$

The previous equation has two main problems; the solution is not consistent with fundamental laws of electrostatics and the equation is not a linear equation. Debye-Huckle solves this problem which will be illustrated in the following subsection (Debye and Hückel 1923; RONALD FAWCETT 2004; Wright 2007).

- Debye-Huckle Theory

Since the electrostatic energy is insignificant compared to the kinetic energy, they expanded the exponential term (radial distribution function) in the right-hand side of the Possion-Boltzmann equation by Taylor series and used two terms to represent it as the following:

$$g_{ij}(r) = 1 - \frac{z_j e \Phi}{k_B * T} + \frac{1}{2} \left[\frac{z_j e \Phi}{k_b T} \right]^2 - \dots \quad (2.2-21)$$

By keeping the first two terms, the radial distribution function will be as the following:

$$g_{ij}(r) \approx 1 - \frac{z_j e \Phi}{k_B * T} \quad (2.2-22)$$

By substituting the new radial distribution function in the Poisson equation it will become as the following:

$$\rho_z = \sum_{i=1}^n z_i F c_i^* - \sum_{i=1}^n -z_i^2 F c_i^* f \Phi \quad (2.2-23)$$

The first part of the previous equation in the right-hand side will be zero since it is the summation of the ions in the solution (RONALD FAWCETT 2004). The second part defined to describe the electrolyte solution called the ionic strength defined as the following:

$$I = \frac{1}{2} \sum_{i=1}^n z_i^2 c_i^* \quad (2.2-24)$$

By using the previous simplification and the ionic strength definition then substituting them in the Poisson-Boltzmann equation to get the following equation:

$$\nabla^2 \Phi = \frac{2FfI}{\epsilon_s \epsilon_0} \Phi = \kappa^2 \Phi \quad (2.2-25)$$

Where the constant κ called Debye–Huckel reciprocal distance with the following definition:

$$\kappa = \left(\frac{2FfI}{\varepsilon_s \varepsilon_0} \right)^{1/2} \quad (2.2-26)$$

By assuming the ions are spherical, applying boundary conditions and solving the second order differential equation (RONALD FAWCETT 2004), the solution of the Poisson-Boltzmann equation is the following:

$$\Phi = \frac{z_i e}{4\pi \varepsilon_s \varepsilon_0 r} \frac{\exp(\kappa a - \kappa r)}{r} \quad (2.2-27)$$

where κ , r and a are the Debye–Huckel reciprocal distance, any point in the solution in which the electric potential is being measured and the distance from the center of ion i to the center of ion j ; respectively.

One of the important assumptions that Debye-Huckle (Debye and Hückel 1923) made that the electric potential of a point inside the solution is the sum of two electric potential; the self-electric potentials (Φ_{self}) generated by the ion and the electric potential of the ion atmosphere ($\Phi_{atmosphere}$) (RONALD FAWCETT 2004). The previous equation represents the sum of the two potentials. By using the total electric potential energy various

ions, Debye-Huckel reached to the following equation to calculate the excess Helmholtz free energy:

$$-\frac{A^E}{T} = \frac{kV}{4\pi \sum x_i z_i^2} \sum \frac{x_i z_i^2}{a_i^3} \left(\frac{3}{2} + \ln(1 + a_i \kappa) - 2(1 + a_i \kappa) + \frac{(1 + a_i \kappa)^2}{2} \right) \quad (2.2-28)$$

The electric potential energy of a single ion is given by the following:

$$u = -\frac{e^2 z_i^2 \kappa}{8\pi \epsilon \epsilon_0 (1 + \kappa a)} \quad (2.2-29)$$

By assuming that the reason non-ideality is the interaction between the ions and the excess Helmholtz free energy equal to Gibbes free energy, the following expression is reached:

$$RT \ln(\gamma_i) = \Delta \mu_i \approx N_A u = -\frac{e^2 z_i^2 \kappa}{8\pi \epsilon \epsilon_0 (1 + \kappa a)} \quad (2.2-30)$$

$$\ln(\gamma_i) = -\frac{e^2 z_i^2 \kappa}{8\pi \epsilon \epsilon_0 K T (1 + \kappa a)} \quad (2.2-31)$$

where u is electric potential energy.

The average activity coefficient can be calculated as the following:

$$\ln(\gamma_{+,-}) = -\frac{Az^2\sqrt{I}}{1 + Ba\sqrt{I}} \quad (2.2-32)$$

$$A = \frac{\sqrt{2\pi N_A d}}{(4\pi\epsilon\epsilon_0 kT)^{3/2}} e^3 \quad (2.2-33)$$

$$B = \sqrt{\frac{2e^2 N_A d}{4\pi\epsilon\epsilon_0^2 kT}} \quad (2.2-34)$$

where I and d are molality based ionic strength and solvent density.

There is another form for the Debye-Huckle law which is for the diluted solution (ionic strength less than 0.001 M) called the limiting Debye-Huckle law (Wright 2007). It is represented by the following equation:

$$\log(\gamma_{+,-}) = -Az^2\sqrt{I} \quad (2.2-35)$$

The extended version of Debye-Huckle law is used to improve the accuracy of the limiting version which is represented as the following (Robinson and Stokes 1960):

$$\ln(\gamma_{+,-}) = -\frac{Az^2\sqrt{I}}{1 + Ba\sqrt{I}} + 0.1I \quad (2.2-36)$$

Even though the Debye-Huckle law is well known in the literature for estimating the activity coefficient, it fails for a high concentration solution (RONALD FAWCETT 2004). The reasons behind that can be illustrated as the following; Debye-Huckle law ignores the extra work needed to introduce new ions in the system while minting the volume constant and the law account for central ion size while ignoring the size of the other ions (RONALD FAWCETT 2004). There are many modifications made over the years to improve the DH model (Kjellander 2005; Loehe and Donohue 1997; Nordholm 1983; Outhwaite 1969; Quarati and Scarfone 2007; Robinson and Stokes 1960; Stokes 1972; Xiao and Song 2017). One of the modification was made by Aasberg-Petersen et al. (1991) (Aasberg-Petersen, Stenby, and Fredenslund 1991) in which they calculated the activity of the component in the system by the following expressions:

$$\ln \gamma_i^{EL} = \frac{2AM_m h_{is}}{d_i B^3} f(BI^{\frac{1}{2}}) \quad (2.2-37)$$

$$A = 1.37757 \frac{10^5 d_m^{\frac{1}{2}}}{\epsilon_m T} \quad (2.2-38)$$

$$B = 6.359696 \times \frac{d_m^{\frac{1}{2}}}{\epsilon_m T} \quad (2.2-39)$$

$$f(z) = 1 + z - \frac{1}{1+z} - 2 \ln(1+z) \quad (2.2-40)$$

where γ_i^{EL} , M_m , h_{is} , d_m are the activity coefficient of the non-electrolyte component i , the molecular weight of the mixture, the interaction coefficient between the salt and the non-electrolyte components and mixture density; respectively.

- Pitzer extension

One of the well-known extensions for Debye-Huckel law is Pitzer work in 1973 where he used virial expansion (Pitzer 1973; Pitzer and Mayorga 1973). He truncated the radial distribution function at the second order to become as the following:

$$g_{ij}(r) \approx 1 - \frac{z_j e \Phi}{k_B * T} + \frac{z_j^2 e^2 \Phi^2}{2 k_b^2 T^2} \quad (2.2-41)$$

The average activity coefficient can be calculated as the following (Rowland and May 2015):

$$\ln(\gamma_{+,-}) = f^\gamma + B^\gamma m + C^\gamma m^2 \quad (2.2-42)$$

$$f^\gamma = -A \left[\frac{\sqrt{I}}{1 + Ba\sqrt{I}} + \left(\frac{2}{1.2} \right) \ln I + 1.2 \sqrt{I} \right] \quad (2.2-43)$$

$$B^\gamma = 2\beta^0 + \beta^1 \left(\frac{2(1 - (1 + 2\sqrt{I}) \exp(-2\sqrt{I}))}{4I} + \exp(-2\sqrt{I}) \right) \quad (2.2-44)$$

where $C^\gamma, \beta^0, \beta^1$ are adjustable parameters.

Pitzer theory is more general and flexible compared to the Debye-Huckle law when it comes to the application but they have a similar accuracy (Rowland and May 2015).

2.2.1.3 Perturbation Theory

The perturbation theory is expressing the total potential energy of a system as a sum of two potential energy; unperturbed system potential energy which is represented by the hard-sphere potential and perturbed system potential energy which is represented by attractive potential (Barker and Henderson 1967a). Zwanzig in 1954 proposed this concept and many scientists worked on it since then such Smith and Alder (1959), Frisch et al. (1966), McQuarrie and Katz (1967) with no success at low temperature for different reasons (Barker and Henderson 1967a, 1967b; McQuarrie and Katz 1966; Smith and Alder 1959; W. 1954). Baker and Henderson expand the Helmholtz free energy by using Taylor series

containing two Taylor expansion in two parameters (Barker and Henderson 1967a, 1967b). Applying this concept on a system that containing electrolyte faced two problems which are slow convergence and divergence in some configuration in the expansion (Loehe and Donohue 1997). These problems were solved by different scientists using different techniques (Henderson and L. Blum 1980; Stell and Lebowitz 1968). It was an initial step for this theory to be used extensively for different electrolyte systems.

Jin and Donohue (1988) developed an electrolyte EOS by combining the Perturbed Anisotropic Chain theory (PACT) with the Henderson's restricted primitive model (RPM). PACT was used to account for the short-range interaction and the Henderson's RPM was used to account for long-range interaction. The Helmholtz free energy is calculated in PACT by including three terms; ideal gas term, repulsion term and attraction term. The attraction term includes the molecule-molecule interaction, charge-charge interaction and molecule-charge interaction. The molecule-molecule interaction considers the following; the Lennard-Jones interaction, the dipole-induced-dipole interaction, the dipole-dipole interaction, the quadrupole-quadrupole interaction and the dipole-quadrupole interaction. The Charge-charge interaction is obtained by using perturbation expansion and MSA correction form the DH theory. The charge-molecule interaction includes two interactions which are: the charge-dipole interaction and the charge-induced-dipole interaction. Where the definition of each term is presented in their work. They used one adjustable parameter for the ion. They tested their EOS on 50 strong electrolytes in the water system with one adjustable parameter (Jin and Donohue 1988a, 1988b, 1991).

2.2.2 Dielectric Models

There are several models for calculating the dielectric constants available in the literature. They are a function of different parameters and the development is different as well. Some of these models are:

Uematsu and Franck (Uematsu and Frank 1980) in 1980 developed a model to calculate the dielectric constant. It is function of temperature and the density as the following equation:

$$\epsilon = 1 + \left(\frac{A_1}{T^*}\right)\rho^* + \left(\frac{A_2}{T^*} + A_3 + A_4T^*\right)\rho^{*2} + \left(\frac{A_5}{T^*} + A_6T^* + A_4T^{*2}\right)\rho^{*3} + \left(\frac{A_8}{T^{*2}} + \frac{A_9}{T^*} + A_{10}\right)\rho^{*4} \quad (2.2-45)$$

$$\rho^* = \frac{\rho}{\rho_0} \quad (2.2-46)$$

$$T^* = \frac{T}{T_0} \quad (2.2-47)$$

where ρ_0 , T_0 and A_i are numerical constants given in the following table:

Table 2-3: Numerical Constants of Uematsu and Franck Model

A_1	A_2	A_3	A_4	A_5	A_6	A_7	A_8	A_9	A_{10}	$\rho_0, Kg/m^3$	T_0, K
7.62571	2.44003×10^2	-1.405693×10^2	2.77841×10^1	-9.62805×10^1	4.17909×10^1	-1.02099×10^1	-4.52059×10^1	8.46395×10^1	-3.58644×10^1	1000	298.15

Maribo-mogensen et al., (2013) developed a model for the dielectric constant and its function of temperature, composition and density (Maribo-mogensen, Kontogeorgis, and Thomsen 2013). It has shown accurate predictions for complex hydrogen bonding fluid and it has the following expression:

$$\frac{(2\varepsilon_r^2 + \varepsilon_\infty)(\varepsilon_r - \varepsilon_\infty)}{\varepsilon_r} = \left(\frac{\varepsilon_\infty + 2}{3}\right)^2 \frac{N_A}{\varepsilon_0 k_B T v} \sum_i x_i g_i \mu_{i,0}^2 \quad (2.2-48)$$

where ε_∞ , ε_r , ε_0 , v , g_i and $\mu_{i,0}$ are the permittivity at infinite frequency, the static permittivity, the vacuum permittivity, the molar volume, the Kirkwood g-factor taking into account local dipolar correlations due to the fluid structure, the vacuum dipole moment of component i ; respectively.

Schreckenberget al. (2014) developed simple model that showed excellent results and it takes in the account the temperature change, solvent density and composition (Schreckenberget al. 2014). It has the following expression:

$$D = 1 + \rho_{solv} d \quad (2.2-49)$$

where d is the solvent-dependent parameter.

The solvent-dependent parameter is a function of temperature and solvent parameters which represent it as the following:

$$d = d_V \left(\frac{d_T}{T} - 1 \right) \quad (2.2-50)$$

where d_V and d_T are solvent specific parameters.

Table (2-4) shows the solvent parameters that will be used in this work (Schreckenberget al. 2014).

Table 2-4: Solvent parameters

Guest	MW (g/mol)	$d_V \left(\frac{dm^3}{mol} \right)$	$d_T (K)$
Water	18.02	0.3777	1403.0
Methanol	32.05	0.5484	1011.0
Ethanol	46.07	0.9480	732.1
Propan-1-ol	60.10	1.269	641.7
Propan-2-ol	60.10	1.667	550.1
n-Butan-1-ol	74.12	1.515	593.3
n-Butan-2-ol	74.12	2.555	461.6
t-Butanol	74.12	2.616	417.1
n-Pentan-1-ol	88.15	1.991	527.8
n-Hexan-1-ol	102.17	2.860	457.1
Carbon dioxide	44.01	0.025	0.0

2.2.3 Solvation Model

The presence of the ions inside the medium affects the interaction of the system which is represented by the free energy of solvation (Eriksen et al. 2016). Solvation can be defined as the energy needed to take the ion from the ideal gas to the pure solvent (Ahmed et al., 2017). This free energy can be accounted for by utilizing the Born Model which consists of a discharging and charging cycle (Born 1920). It can be calculated by the following expression:

$$a^{\text{Born}} = -\frac{e^2}{4\pi\epsilon_0} \left(1 - \frac{1}{D}\right) \sum_{i=1}^{n_{\text{ion}}} \frac{N_i Z_i}{\sigma_i} \quad (2.2-51)$$

where σ_i is ion diameters.

2.3 Hydrate Modeling

The impotence of the hydrate modeling raised very rapidly in recent years due to a leap in knowledge (i.e., statistical thermodynamics) and its applications. The beginning was at the macroscopic level experiment which is expensive in resources (Sloan, 2004; Willcox, Carson, & Katz, 1941). The work in microscopic level such XRD data was the basis for establishing the different gas structure (I and II) (Pauling & Marsh, 1952; Waseem, 2017). There was some empirical model to predict the gas hydrate formation conditions. The first attempt was by using the K-value by Katz (1945) as the following expression (Carson and Katz 1941):

$$K_i = \frac{y_i}{x_i} \quad (2.3-1)$$

where y_i and x_i are mole fraction of the i component in the gas phase and the solid phase for free water; respectively.

The model must satisfy the following conditions:

$$\sum_i^n \frac{y_i}{K_i} = 1 \quad (2.3-2)$$

Building K-charts for a different range of pressure and temperature was another method for modeling the gas hydrate, but it was not accurate for some components (Carson & Katz, 1941; Mann, 1988; Tabatabaei, Tohidi, & Todd). There was some attempt to use the empirical correlation; the first was by Holder et al. (1988) which was developed for pure gases (Chapoy 2004; Holder, Zetts, and Pradhan 1988). Markogon (1981) correlated different correlations for natural gases by accounting for the gas gravity (Makogon 1981).

All the previous correlations were not accurate and had many limitations since they all missed the physical sense (Makogon 1981). This fact led to one of the most significant milestones in the gas hydrate modeling which is van der Waals and Platteeuw (vdWP) model (Van der Waals & Platteeuw, 1959). Their model was developed in the statistical thermodynamics and considered as the link between the microscopic level and the macroscopic level for the gas hydrate structure (Haghighi 2009). Their model has the following assumption:

- The cavity of the structure contains no more than one guest molecule.
- The guest molecule inside the cavity or the cage is free to rotate and there no interaction between the guest molecule and the cage molecules.
- Lennard-Jones and Devonshire potential (Lennard-Jones and Devonshire 1937, 1938) was used to describe the guest molecules relation with cage molecules in term of energy at distant r from the cage center.

Even though there are some studies showed there are some errors in the assumption could affect the prediction accuracy of the gas hydrate, it still used abundantly in the gas hydrate modeling (Ballard 2002; Khan et al. 2018; Martin and Peters 2009c, 2009b, 2009a). It was

built on the concept of equality between the phases in term of the chemical potential. These phases could include the hydrate phase, the ice phase and the liquid phase of water. The equilibrium condition can be expressed mathematically as the following:

$$\Delta\mu_w^H = \mu_w^\beta - \mu_w^H = \mu_w^\beta - \mu_w^\pi \quad (2.3-3)$$

where $\Delta\mu_w^H$, μ_w^β , μ_w^H and μ_w^π are the difference in the chemical potential for the gas hydrate, the chemical potential of reference phase which is empty hydrate phase, the chemical potential of hydrate phase and the chemical potential of coexisting phase; respectively.

The difference in the chemical potential for the gas hydrate can be calculated by the following equation:

$$\Delta\mu_w^H = -RT \sum_i^n \lambda_i \ln \left(1 - \frac{\sum_k f_k C_{ki}}{1 + \sum_k f_k C_{ki}} \right) \quad (2.3-4)$$

where λ_i , f_k and C_{ki} are the number of cavities of type I per water molecule in the structure, fugacity of component i in the gas phase and the Langmuir constant; respectively.

The Langmuir constant is calculated by the following expression:

$$C_{ki} = \frac{4\pi}{kT} \int_0^{\infty} \exp\left(\frac{w(r)}{kT}\right) r^2 dr \quad (2.3-5)$$

where $w(r)$ and r are spherical cell potential and distance from the center of the structure.

The Langmuir constant is estimated by inserting the spherical cell potential in equation (2.3-5). The spherical cell potential is important to describe the interaction between the guest molecule and the host molecules. It obtains by the cell theory of Lenard-Jones-Devonshire which sum the host-guest pair potential for the whole structure. The original vdWP utilize the famous the Lenard-Jones 12-6 potential which is limited in term of accuracy to monoatomic gases and spherical molecules (Van der Waals & Platteeuw, 1959). Different researchers investigate the model to improve it, especially the assumption which made some limitation to the model (McKoy & Sinanoğlu, 1963; Parrish & Prausnitz, 1972; S. R. Zele, S.-Y. Lee, & Holder, 1999). Mckoy and Sinonglu in 1963 compared between the different pair potentials for monoatomic molecules (spherical and rod molecules) (McKoy and Sinanoğlu 1963). They found that the Kihara model (Kihara 1953) has better results to describe both spherical and rod-like molecules. Parrish and Prausnitz work in 1972 was a tremendous improvement (Parrish and Prausnitz 1972) in gas hydrate modeling for gas mixtures. They used the Kihara model (Kihara 1953) to describe the guest and host interaction and extended the vdWP from a single gas molecule to multiple gas molecules (gas mixture) which is more practical. The spherical potential can be calculated by using the Kihara model (Kihara 1953) as the following:

$$w(r) = 2z\varepsilon \left[\frac{\sigma^{12}}{R^{11}r} \left(\delta^{10} + \frac{a}{R} \delta^{11} \right) - \frac{\sigma^6}{R^5 r} \left(\delta^4 + \frac{a}{R} \delta^5 \right) \right] \quad (2.3-6)$$

$$\delta^N = \frac{\left[\left(1 - \frac{r}{R} - \frac{a}{R} \right)^{-N} - \left(1 + \frac{r}{R} - \frac{a}{R} \right)^{-N} \right]}{N} \quad (2.3-7)$$

where R , z , r , a , σ and ε are the cell radius, the coordination numbers, the radial distance, the core radius (Kihara parameter), the core diameter (Kihara parameter) and the characteristic energy (Kihara parameter); respectively.

Kihara potential parameter can be determine by different methods (Avlonitis 1994; Parrish and Prausnitz 1972; Saito et al. 1964). The two important methods are; using the experimental virial coefficient and the viscosity data for the pure compound and fitting Kihara parameters with hydrate dissociation data. The first method was incapable of predicting the hydrate equilibrium or gas mixtures (Klauda & Sandler, 2003; Jeffery Klauda & Sandler, 2000). The other side of the coin was much better. It resulted a superior outcomes since it abolishes the need for mixing rules which help in improving the result. The Kihara potential parameters for hydrate formers from the literature presented in table 2-5. Simplifying the calculation is done by some researchers such as Munck et al. in 1988 (Munck, Skjold-Jørgensen, and Rasmussen 1988). They came up with the following expression for Langmuir constant:

$$C_i(T) = \frac{A}{T} \exp\left(\frac{B}{T}\right) \quad (2.3-8)$$

where A and B are and adjustable parameters.

These adjustable parameters that used for each gas molecules for small and large cavities are presented in table 2-6 (Parrish and Prausnitz 1972; Waseem 2017).

Table 2-5: Kihara potential parameters for different hydrate formers.

Guest	a, Å	σ , Å	ϵ/k , K	Reference
Argon	0.184	2.9434	170.5	(Parrish and Prausnitz 1972)
Methane	0.3	3.2398	153.17	
Ethane	0.4	3.318	174.97	
Propane	0.68	3.303	200.94	
Iso-butane	0.8	3.1244	220.52	
Nitrogen	0.35	3.6142	127.95	
Carbon dioxide	0.31	2.9681	169.09	
Hydrogen Sulfide	0.31	3.1558	205.85	
Oxygen	0.31	2.7673	166.37	
Ethylene	0.47	3.291	172.87	
Ethyne	0.363	3.255	171.94	(Tumba et al. 2013)

Table 2-6: Langmuir constant adjustable parameters by Parrish & Prausnitz, 1972

Guest	Small	Large	Small	Large
	Aml × 103, K	Bml × 10-3, K	Aml × 102, K	Bml × 10-3, K
Structure – I hydrates				
Methane	3.7237	2.7088	1.8372	2.7379
Propane	0	0	0	0
Iso-butane	0	0	0	0
Nitrogen	3.8087	2.2055	1.842	2.3013
Ethylene	0.083	2.3969	0.5448	3.6638
Structure – II hydrates				
Argon	21.8923	2.3151	186.6043	1.5387
Methane	2.956	2.6951	7.6068	2.2027
Ethane	0	0	4.0818	3.0384
Propane	0	0	1.2353	4.4061
Iso-butane	0	0	1.3136	4.6534
Nitrogen	3.0284	2.175	7.5149	1.8606
Ethylene	0.0641	2.0425	3.494	3.1071
Carbon dioxide	0.9091	2.6954	4.8262	2.5718
Oxygen	14.4306	2.3826	15.382	1.5187

The existing of excess free water in gas production increases the probability of hydrate formation. This excess free water is an aqueous liquid phase which considered most often as the interacting phase. The hydrate formations take place in the system by the interaction of the gas phase and the hydrate phase. The aqueous phase could contain the inhibiting liquid, condensate hydrocarbon liquid or in some cases ice (Davidson et al. 1981). This is accounted for in calculating the difference in chemical potential for the liquid phase in the water. It can be expressed as the following (Anderson & Prausnitz, 1986; Englezos, Huang, & Bishnoi, 1991):

$$\frac{\Delta\mu_w^L(T, P)}{RT} = \frac{\Delta\mu_w(T_0, P_0)}{RT_0} - \int_{T_0}^T \frac{\Delta h_w^L(T)}{RT^2} dT + \int_{P_0}^P \frac{\Delta v_w^L(T)}{RT} dP - \ln x_w \quad (2.3-9)$$

$$\Delta h_w^L(T) = \Delta h_w^0(T_0) + \int_{T_0}^T \Delta C_{pw} dT \quad (2.3-10)$$

$$\Delta C_{pw} = \Delta C_{pw}^0(T_0) + \beta(T - T_0) \quad (2.3-11)$$

where $\Delta\mu_w^L(T, P)$, $\Delta\mu_w(T_0, P_0)$, $\Delta h_w^L(T)$, $\Delta v_w^L(T)$, $\Delta h_w^0(T_0)$, ΔC_{pw} , $\Delta C_{pw}^0(T_0)$, x_w , T_0 and P_0 are the difference in the chemical potential between the empty hydrate and liquid water, the difference in the chemical potential between the empty hydrate and liquid water at the reference conditions, the difference in the molar enthalpy between the empty hydrate and liquid water, the difference in the molar volume between the empty hydrate and liquid water, the difference in the molar enthalpy between the empty hydrate and liquid water at the reference conditions, the difference in heat capacity between the empty hydrate and liquid water, the difference in heat capacity between the empty hydrate and liquid water at the reference conditions, the solubility of gas in the liquid water term, the reference temperature and the reference pressure; respectively.

The reference conditions for the previous parameters are $T_0 = 273.15$ K and zero absolute pressure. The different parameters are reported in the literature which is shown in Table-2-7. The last term in equation (2.3-9) is accounting for the solubility of the gas in the liquid phase of the water which only consider at relatively high pressure (more than 10 MPa) (Holder, Corbin, and Papadopoulos 1980).

Table 2-7: Literature values of reference thermodynamic properties

Parameters	Structure I	Structure II	Reference
$\Delta\mu_w^o$ $\left(\frac{J}{mol}\right)$	1235±10	-	(Holder et al. 1980)
	1297	937	(Dharmawardhana, Parrish, and Sloan 1980)
	1264	883	(Parrish and Prausnitz 1972)
	1299.5±10	-	(Holder, Malekar, and Sloan 1984)
	1287	1068	(Handa and Tse 1986)
Δh_w^o $\left(\frac{J}{mol}\right)$	-4327	-	(NG and Robinson 1985)
	-4622	-4986	(Dharmawardhana et al. 1980)
	-4860	-5203.5	(Parrish and Prausnitz 1972)
	-4150	-	(Holder et al. 1984)
	-5080	-5247	(Handa and Tse 1986)
$\Delta C_{p_w}^o$ $\left(\frac{J}{mol} \cdot K\right)$	-38.13	-38.13	(Parrish and Prausnitz 1972)
	-34.583	-36.8607	(John, Papadopoulos, and Holder 1985)
β $\left(\frac{J}{mol} \cdot K^2\right)$	0.141	0.141	(Parrish and Prausnitz 1972)
	0.189	0.1809	(John et al. 1985)
Δv_w $\left(\frac{cm^3}{mol}\right)$	4.6	5.0	(Parrish and Prausnitz 1972)

From a computational methodology perspective, Englezos et al. (1991) method is one of the most common algorithms for the gas hydrate (Englezos et al. 1991). It can be divided into two main parts; the first is responsible for calculating the vapor-liquid equilibrium for each component. The known parameters are assumed which include the pressure, the temperature and the feed composition (the flash calculation). The second part used to calculate the water fugacity in the hydrate phase at the assumed pressure and equate it to fugacities that were calculated from the flash calculation (first part) as the following equation:

$$f_i^V = f_i^L = f_i^H \quad (2.3-12)$$

The fugacity of the hydrate phase for the water can be calculated by the following expression (van der Waals & Platteeuw, 1959):

$$f_w^H = f_w^\beta \exp\left(\frac{-\Delta\mu_w^H(T, P)}{RT}\right) \quad (2.3-13)$$

$$f_w^\beta = f_w^L \exp\left(\frac{\Delta\mu_w^L(T, P)}{RT}\right) \quad (2.3-14)$$

Where f_w^H , f_w^β and f_w^L are the water hydrate phase fugacity, the empty hydrate fugacity and the pure water liquid fugacity; respectively

The fugacities are compared to the hydrate fugacity calculated from the second part through a tolerance criterion. While the tolerance less the tolerance criterion, the algorithm will keep updating the pressure until the tolerance criterion is fulfilled.

CHAPTER 3

LITERATURE REVIEW

This chapter summarizes the literature review that related to modeling the electrolyte and modeling the gas hydrate in the presence of electrolytes.

3.1 Modeling the Electrolyte

This section highlights the previous work done in modeling the electrolyte. It starts with electrolyte equations of state and ends with using the perturbation theory for electrolyte modeling.

3.1.1 Electrolyte Equation of State

Many researchers and scientists tried to develop and improve the existing equations of state for the electrolyte system. The reason for that is the interaction in the electrolyte solution made the accuracy of equations of state decrease drastically. In the following sections, the development of the important electrolyte equations of state will be highlighted starting with cubic EOS, CPA-EOS and SAFT-EOS.

3.1.1.1 Electrolyte Cubic EOS

Starting with the electrolyte cubic equation of state, Simon et al. (1991) presented an electrolyte equation of state which contains the following; the SRK-EOS as a parent model, the Debye-Huckel model for the electrostatic interactions and the Born model to discharge and charge the ions. They used the Buckingham model for the dielectric constant. They tested their EOS in predicting the activity coefficient, the mean activity coefficient and K-values. (Simon et al. 1991).

Zuo and Guo (1991) utilized the PT-EOS and extended it to electrolyte systems. The extension was done by adding the Debye-Huckel term for the long-range interaction. Maryott and Smith model (1951) was used to estimate the dielectric constant. They used two binary interaction parameters to predict the phase equilibrium of different systems at high pressure (Zuo & Guo, 1991).

Furst and Renon's (1993) have developed a new equation of state for the electrolyte solution. It consists of two parts; the non-electrolyte part and the electrolyte part. The non-electrolyte term is described by the Schwartzentruber EOS (modified SRK EOS) and it contains two terms; repulsion term and attractive short arrange term. For the electrolyte part, it consists of simplified a MSA term to account for the long-range interactions and addition term to account for the ions short-range interactions which is taken from Planches and Renon model (modified non-primitive MSA). Their EOS was fitted for the osmotic coefficient for 28 electrolyte solution at conditions of 25 °C and 1 bar. They used six parameters and they predicted the osmotic coefficient result without using any adjustable parameters (Fürst and Renon 1993).

Myers et al. (2002) worked on developing an equation of state (EOS) for electrolyte solution which included three terms for three types of interactions: interactions between uncharged species, interactions resulting from charging free energy of ions and the interactions between ions (electrostatic). It has the following expressions: ideal gas term, Peng Robinson term, Born term and MSA term. They used the Franck and Uematsu model to calculate the permittivity of the medium. The restricted primitive version of the mean spherical approximation model was used to describe the long-range ion interaction (Coulomb interaction). Their EOS was fitted to experimental data of 138 electrolyte solution for the range of 25 C and 1 bar to 300 C and 120 bar. They used three different adjustable parameters for the salts (Myers, Sandler, and Wood 2002).

Lin et al. (2007) compared different EOS with different electrolyte terms to evaluate their performance in predicting the apparent molar volume, the mean activity coefficient, the osmotic coefficient and the solid-liquid equilibrium (Lin, Thomsen, and de Hemptinne 2007). They used the SRK-EOS, the PR-EOS and the CPA-EOS to describe the short-range interaction. The long-range interactions were described by simplified explicit restricted MSA, simplified implicit non-restricted MSA and the simplified Debye-Huckel. They found that there no significant difference between the electrolyte terms in the predictability of the mention properties and the simplified Debye-Huckel model was the best in the computational time compared to the other model (Lin et al., 2007).

3.1.1.2 Electrolyte Cubic Plus Association EOS

The development of the cubic plus association equation of state helped in advancing the electrolyte modeling. Wu and Prausnitz (1998) extended the Peng-Robinson equation of state by adding the contribution of the association term and the electrostatic term. Their EOS was developed in term of Helmholtz free energy. The Helmholtz free energy of the association bond was used from the SAFT EOS assuming there are three sites for water. Helmholtz free energy of Born model concern with the energy needed for recharging the ions in the solution was used. The contribution of Helmholtz free energy due to Coulombic ion-ion interactions is given by the non-restricted primitive version of MSA. One adjustable parameter was used in their work for the ion. The proposed EOS predict the behavior of simple systems that contain hydrocarbon, water and sodium chloride (Wu and Prausnitz 1998).

Inchekel et al. in 2008 presented an extension for the CPA-EOS for electrolyte systems. It contained the following term; the Born model for charging and discharging the ions, the SRK-EOS for repulsion, the simplified explicit MSA for long-range interaction and the solvation interaction was added from Planche and Renon work (Planche and Renon 1981). They used Simon et al. (1997) model and the Pottel model for the dielectric constant. They utilize two interaction parameters and three adjustable parameters. Their EOS predicted the apparent molar volume and the osmotic coefficient for different salts (Inchekel, de Hemptinne, and Fürst 2008).

Courtail et al. (2014) used the electrolyte CPA to study a system that could be encounter in deep reservoirs. Their system contains; CH₄, CO₂, H₂O and NaCl at high pressure and

temperature conditions (up to 200 MPa and 573 K). Their CPA-EOS consisted of the SRK-EOS for the repulsion and dispersion term, the simplified explicit MSA for the long-range interactions and the Born model for charging and discharging the ions. The Simonin's model was coupled with the Schmidt correlation for the dielectric constant estimation. Up to three binary interaction parameters were used. The electrolyte CPA-EOS was tested by predicting the phase densities, the salting-out effect, the gas solubility and the critical points which were predicted (Courtial et al. 2014).

Carvalho et al. (2015) worked on the solubility of CO₂ in an aqueous solution of NaCl experimentally and theoretically. They utilize the CPA-EOS which contained the cubic term (SRK-EOS), the association term and an ionic term (DH theory). They generated a phase equilibrium data for CO₂+H₂O+NaCl system then modeled it using the CPA-EOS (Carvalho et al. 2015).

Mogensen et al. (2015) extended the CPA-EOS for mixed electrolyte systems by using the SRK-EOS for repulsion and dispersion terms, the Debye-Huckel model for the electrostatic term and the Born model for turning on and off the charges. Maribo-Mogensen et al. (2013) model was used for the static permittivity calculation. Their e-CPA-EOS can use parameters that are salt specific or ion specific which gave an advantage in term of the feasibility for the users. They predicted the vapor-liquid equilibrium, the solid-liquid equilibrium and the liquid-liquid equilibrium for different systems using one binary interaction parameters (Maribo-mogensen, Thomsen, and Kontogeorgis 2015).

Schlaikjer et al. (2017) compared the salt parameters in CPA-EOS to the extended UNIQUAC model. Their EOS consisted of the following: the SRK-EOS, the Debye-

Huckle model and the association term from the Wertheim's association theory. They used Maribo-Mogensen et al., (2014) model for the dielectric constant. They compared their EOS with extended UNIQUAC model in predicting the solubility and the activity coefficient. They found that the overall performance for both of them is almost similar (Schlaikjer, Thomsen, and Kontogeorgis 2017).

3.1.1.3 Electrolyte Statistical Associating Fluid Theory EOS

The improvement in accuracy of SAFT-EOS compared to other EOS (e.g., cubic EOS) and simplicity to other theories (lattice fluid theory) were the reasons for the scientists and researchers to apply it for electrolyte systems. Many researchers tried different versions of the SAFT-EOS and applied it for the electrolyte systems with some modification. In the following subsection, some of these developments are discussed.

- SAFT-VR

Galind et al. (1999) extended their previous work (Gil-villegas et al. 1997) of statistical associating fluid theory for variable range (SAFT-VR) by using the restricted primitive mean spherical approximation model (MSA-RPM) to account for the ion-ion interaction which known as SAFT-VRE. They studied ten systems (nine single salt and one mixed salts) in a temperature range of 273 – 373 K. One adjustable parameter was used for the ion. They compared the Debye-Huckle theory for one system with the MSA-RPM and found the result almost similar (Galindo et al. 1999).

Patel et al. (2003) investigated the salting-out phenomena for n-alkanes in water with strong electrolytes. They used the SAFT-VRE (Galindo et al. 1999) to perform this study

with the assumption of complete dissociation and they have two adjustable parameters for the interactions. They predict the salting-out effect for different systems (. Patel, Paricaud, Galindo, & Maitland, 2003).

Zhao et al., (2007) developed an equation of state for electrolyte fluids by using the statistical associating fluid variable range theory (SAFT-VR) with non-primitive non-restricted mean spherical theory (MSA) to yield the statistical associating fluid theory for potentials of variable range plus dipole and electrolyte (SAFT-VR+DE). The general MSA was used to account explicitly for the ion-ion, ion-dipole and dipole-dipole interactions. They performed molecular simulation (NPT ensemble) to generate some data and compared their EOS with it. Different models were coupled with the SAFT-VRE including the Debye-Huckel theory, the primitive MSA, the restricted non-primitive MSA, the semi-restricted non-primitive MSA to compare them with their approach. They find that their approach gave very excellent results compared to the simulation results and the other models. They tested it for dilute electrolyte solutions and their approach can be applied for more concentrated solutions (Zhao, Dos Ramos, and McCabe 2007).

Anvari et al. (2013) used the SAFT-VR to study the amino acid solutions in term of the phase behavior for aqueous and aqueous electrolyte solutions. Their EOS consist of the mono term, chain term, association term and the ionic term. They used the Yukawa potential to calculate the modified pair potential function. The ionic term was estimated by utilizing the simplified-implicit MSA for different ion sizes (non-restricted). They estimated the solubility and the activity coefficient of different amino acids in aqueous electrolyte solutions (Anvari et al. 2013).

Schreckenberget al. (2014) developed an improved version of the SAFT-VR (Zhao et al. 2007) by including the Born model and using a new model to calculate the dielectric constant that depends on the density, temperature and the composition of the solvent. They modified the Uematsu and Franck (1980) model to be a function of temperature, density and solvent composition. They used the restricted primitive version of MSA (MSA-RPM) to describe the Coulombic interactions. They studied different electrolyte systems that contain single and mixed salts. They predicted the osmotic coefficient, the solution density and the mean ionic activity coefficient for their system. They observed that the parameters of the ion were following the physical trends in both the dispersion energies and the sizes of the ions which give more confidence for their model (Schreckenberget al. 2014).

Das et al., (2015) extended the SAFT-VR+DE to study nineteen different aqueous electrolyte solutions for fully and partially dissociated salts. They added an ionic association term to account for the high electrostatic interaction at high salt concentration. They found that considering the ion association or enhancing the anion solvent interaction could improve the predicting ability of the model. They predict the osmotic coefficient, the density and the mean ionic activity coefficient at different conditions for full dissociated and partially dissociated salts. They predicted the dielectric constant using the SAFT-EOS. They used two fitted parameters and compared their result with Monto-Carlo simulation (Das, Hlushak, Dos Ramos, et al. 2015; Das, Hlushak, and McCabe 2015).

Eriksen et al. (2016) used the SAFT-VR Mie EOS and incorporated it with the non-restricted primitive version of MSA. They studied different systems of single and mixed salts. In addition, they used the Born model and only one adjustable parameter was used

for the ion. They predicted the density, the vapor pressure, the mean ionic activity coefficient and the osmotic coefficient (Eriksen et al. 2016).

Das et al. (2018) used the SAFT-VR+DE to study mixed solvent electrolyte systems for different solvent composition and ionic concentration. The non-primitive EOS was used to predict the vapor-liquid equilibria and the dielectric properties for different systems. Their model, in general, captured the equilibrium properties for binary and ternary systems without the fitting parameters in good qualitative representation. The achievement of better quantitatively representation needed an accurate capture of the effect of the ions on the solvent molecules. They fitted an effective radius for the ions to improve the quantitative representation. Also, the salt effect on the dielectric constant was investigated for several methanol-salt systems. (Das, dos Ramos, and McCabe 2018).

- PC-SAFT

Cameretti et al. (2005) utilized perturbed-chain statistical associated fluid theory (PC-SAFT) (Gross and Sadowski 2001) to predict the liquid densities and the vapor pressure for single electrolyte systems. They studied twelve systems of single electrolyte. They used the Debye-Huckel theory for the electrostatic interaction. They used two adjustable parameters for each ion. (Cameretti, Sadowski, and Mollerup 2005).

Held et al. (2008) used the ePC-SAFT (Cameretti et al. 2005) and came up with a new set of parameters to improve the prediction ability of the EOS. They determined their ionic specific parameter by a fitting process to the experimental measurements of the density and the mean ionic activity coefficient. On the other hand, their previous work used the liquid density and the saturated vapor pressure in the parameterization process. They predicted

the solute activity coefficient, the liquid densities and the vapor pressure for 115 aqueous electrolyte systems (Held, Cameretti, and Sadowski 2008).

Held and Sadowski (2009) applied the ePC-SAFT to weak electrolyte systems. They used the association/dissociation equilibrium to account for ion association (ion pairing). This phenomenon is proved experimentally for some weak electrolyte systems. By considering the ion pairing, the model predictability for the mean ionic activity coefficient and the density were improved (Held and Sadowski 2009).

Lee and Kim (2009) used the PC-SAFT and coupled it with the non-restricted primitive MSA and the Born model to model different aqueous electrolyte solutions. They predicted the mean ionic activity coefficient, the osmotic coefficient, the solution density and the solubility without any adjustable parameters (Lee & Kim, 2009).

Herzog et al. (2010) coupled the PC-SAFT with the semi-restricted non-primitive MSA to model different aqueous electrolyte solutions for different concentrations. They included the association between the solvent and the ions. They predicted the system pressure and the liquid density (Herzog, Gross, and Arlt 2010).

Doozandeh et al. (2012) used the SAFT and coupled it with the restricted-primitive MSA model to study the protein partitioning in polymer-salt aqueous systems. They used the Nelder-Mead simplex method to derive the adjustable parameters. They used the mean ionic activity coefficient in the ions parameterization (Doozandeh, Pazuki, and Asghar 2012).

Held et al. (2012) applied the ePC-SAFT to model alcohol-mixed solvent salt systems. They used solvent specific parameters with a physical meaning. They predicted the phase

behavior, the solution density and the mean ionic activity coefficient of different mixture solvent electrolyte systems (Held et al. 2012).

Rozmus et al. (2013) extended the PPC-SAFT (NguyenHuynh et al. 2008; Rozmus, de Hemptinne, and Mougin 2011; Tamouza et al. 2004, 2005) to study strong electrolyte systems. They used the Born model and the primitive MSA for the electrolyte contributions. They predicted the mean ionic activity, vapor pressure, density and solubility of different systems (Rozmus et al. 2013).

Held et al (2014) modified the ePC-SAFT to account for the dispersion between the ions. They explicitly considered the dispersion between the anion-cation where the dispersion between the anion-anion and cation-cation were neglected. Also, they used three binary interaction parameters for anion-cation, anion-solvent and cation-solvent interaction. These modifications improve the accuracy in predicting the phase behavior especially for weak electrolyte solution and at high salt concentration systems (Held et al. 2014).

Mohammad et al. (2015) measured the salt influence on the liquid-liquid equilibrium for methyl isobutyl ketone- water systems with different salts. They used modified COSMO-RS (Ingram et al. 2012; Klamt, Eckert, and Arlt 2010) and the ePC-SAFT to model the liquid-liquid equilibria. The ePC-SAFT was better than the modified COSMO-RS in predicting the salting effect since the modified COSMO-RS does not have specific system parameter which make it suitable for industrial applications due to its easiness (Mohammad et al. 2015). Also, they studied the impact of the lithium and sodium salts on the liquid-liquid equilibria of water/1-butanol systems at 298.15 K and 1 bar. They used the ePC-SAFT to predict the influence of these salts on the system and on the partitioning of 5-

hydroxymethylfurfural (HMF) in the system. They succeed in predicting the influence of the salts on the system compared to the experiment results (Mohammad et al. 2016).

Shadloo et al. (2016) evaluated the ePC-SAFT (Cameretti et al. 2005) for different electrolyte systems by estimating the density. They tried two strategies and compared their results: the first is the association interactions are only between the water molecules and the second includes the association forces that exist between the water molecules and the ions (the ions have fixed association sites). They used two adjustable parameters in the first strategy and three in the second strategy. They found that the second strategy is slightly better compared to the first in predicting the liquid density (Shadloo, Abolala, and Peyvandi 2016). In 2017, they extended the investigation to calculate the MIACs, the osmotic coefficients and the water activities of aqueous electrolyte solutions at different temperatures for both strategies. They found an improvement in the result using the second strategy (Shadloo and Peyvandi 2017).

Ahmed et al., (2018) used the group contribution polar perturbed chain statistical association fluid theory (GC-ePPC-SAFT) (Rozmus et al. 2012) and coupled it with the Born model and the ionic association to study different mixed electrolyte systems. They worked on the parameters and the dielectric constant to improve the model. They evaluated their model by predicting the vapor-liquid equilibrium and the density for different single and mixed salts systems (Ahmed et al., 2017).

- LJ-SAFT

Liu et al. (1999) used the statistical associating fluid theory with Lennard-Jones potential for strong electrolyte systems. Their equation has the following contributions; ion-ion

interaction term, ion-dipole interaction term, dipole-dipole interaction term, dispersion term, hydrogen bonding term and repulsing term. The implicit simplified MSA was used for the ion-ion interaction term. The ion-dipole interaction and dipole-dipole interaction were taken from the Henderson et al. work (Henderson, Blum, and Tani 1986). The dispersion term was described by Cotterman et al. work (Cotterman, Schwarz, and Prausnitz 1986). The SAFT-EOS was used to describe the hydrogen bonding between the water molecules and the repulsion term was described by Mansoori et al. equation (Mansoori et al. 1971). They investigated 30 electrolyte systems where they predicted the densities and the mean ionic activity coefficients (Liu, Li, & Lu, 1999).

Liu et al. (2005) developed an equation of state by combining a low-density expansion of MSA and the statistical associating fluid theory. Their EOS consist of the following contributions which is written in term of Helmholtz free energy; hard sphere contribution, Lennard-Jones contribution, electrostatic contribution and the associating contribution. The hard sphere contribution was estimated by using the equation from Mansoori et al. work (Mansoori et al. 1971). Cotterman et al. equation for the Lennard-Jones term was used (Cotterman et al. 1986). The low-density expansion of the non-primitive MSA was adopted in their work to describe the electrostatic interactions which include ion-ion interaction, ion-dipole interaction and dipole-dipole interaction. They tested their EOS by predicting mean activity coefficient, osmotic coefficient and the density for 15 aqueous alkali halide solutions (Liu, Wang, & Li, 2005).

- SAFT1 and SAFT2

Ji et al., (2005) extended the SAFT1 (Adidharma and Radosz 1998) to electrolyte systems by coupling it with the restricted primitive MSA model (SAFT1-RPM). Their EOS contains one salt specific adjustable parameter. They predicted the solubility, the osmotic coefficient and the density of multiple different systems (Ji et al. 2005). They investigated more systems by the same model in another work and used the dielectric model of Fernandez et al. (Tan, Adidharma, and Radosz 2005).

In 2006, Tan et al., presented the SAFT2 which is based on the SAFT1 with some modification in its terms. It consists of the following contributions; hard sphere term, dispersion term, chain term, association term and the restricted primitive MSA model for the ionic term. They adjusted the boundary conditions for the hard sphere term. The dispersion term, also, was adjusted by changing its correction coefficients. The chain term became temperature independent where it was temperature dependent in the SAFT1 for nonionic segments. They used binary interaction terms between the anion-cation. They predicted the activity coefficient, the osmotic coefficient, the density and the vapor pressure. (Ji, Tan, et al. 2006; Ji, Adidharma, and Engineering 2006; Tan et al. 2006).

In 2008, Ji and Adidharma extended their SAFT2 to a higher range of temperature and pressure. They improve their EOS by including the interactions between the cations by adjustable parameters and neglected the anion-anion. They predicted the activity coefficient, the osmotic coefficient and the density of different electrolyte systems (Ji and Adidharma 2008).

Jiang et al. (2016) modeled the CO₂ solubility in different single and mixed electrolyte solutions by using the SAFT2. They used a corrected version of MSA (KMSA (Jiang and Adidharma 2015)) instead of using the restricted-primitive MSA which used in the original SAFT2 work (Ji, Adidharma, et al. 2006; Tan et al. 2006). The corrected version of the MSA contains an empirical correction factor for the internal energy. They used interaction parameters between the CO₂-H₂O and CO₂-ion to predict the solubility (Jiang, Panagiotopoulos, and Economou 2016).

- SAFT-HR

Najafloo et al., (2015) modeled different aqueous solutions by using the SAFT-HR (Huang & Radosz, 1990), (Huang & Radosz, 1991). They coupled it with the explicit non-restricted primitive of MSA and the Born model to obtain the eSAFT-HR. They used two approaches in obtaining the parameters; salt approach and ion approach. They studied 61 different single electrolyte systems and they predicted the mean activity coefficient, the osmotic coefficient and the liquid densities (Najafloo, Feyzi, and Zoghi 2014). They modeled the solubility of the CO₂ in aqueous N-methyldiethanolamine solutions by using the eSAFT-HR (Najafloo, Feyzi, and Zoghi 2015).

3.1.2 Perturbation Theory for Electrolyte

Starting with Jin and Donohue work in 1988, they worked on electrolyte EOS for strong and weak salts (Jin and Donohue 1988a, 1988b, 1991). They used the Perturbed Anisotropic Chain Theory (PACT) (Vimalchand and Donohue 1985; Vimalchand, Donohue, and Celmins 1986) to describe the short-range interaction. The PACT considers

the translation, rotational and vibrational motions of the molecules. The repulsion term was adopted from Carnahan and Starling work (Carnahan and Starling 1972). For the long-range interaction term, they used the Henderson restricted primitive model (RPM) (Henderson 1983). They studied 50 strong electrolytes in water and calculated the mean activity coefficient for them. In addition, the specific volume for several binary electrolyte solutions was evaluated with two fitting parameters.

Harvey and Prausnitz (1989) used the Baker-Henderson perturbation theory for mixtures and extended to electrolyte systems. They used the simplified explicit MSA model to describe the long interaction and the Born model for the charging and discharging processes. They used Uematsu and Franck model to estimate the dielectric constant. They used two ion specific parameters and three binary interaction parameters. They examined their work by predicting the osmotic coefficient and the salt-out effect for different systems (Harvey and Prausnitz 1989).

The summary for all the previous discussions is presented in Table 3-1. It includes the reference, year, the parent model for each work, the electrolyte model, do they include the Born model in their work, the dielectric model with its variables, the parameters for their model and the association contributions details.

Table 3-1: Summary of the literature for electrolyte modeling

Model	Reference	Parent Model	Electrolyte Model	Born	Di-electric Model		Parameters		Association		
					Model	Variables	Pure Parameter	Interaction Parameter	Ion Association	Association	Association parameter
Cubic	(Simon et al., 1991)	SRK	DH	Yes	Buckingham Model	T, V, ion, η	1	1: Ion-Solvent	No	No	---
	(Y. X. Zuo & Guo, 1991)	Petal-Teja	DH	No	Maryott and Smith (1951)	T	---	1: Ion-Solvent 1: Ion-Solute	No	No	---
	(Furst & Renon, 1993)	mSRK	PMSA: nR: electrostatic + short range term (SR2)	No	Pottel	V, Ion	---	1-2: Ion-Ion 1: Ion-Solvent	No	No	---
	(Myers et al., 2002)	PR	PMSA: R	Yes	Uematsu and Franck Model (1980)	T, V	3	1: Ion-Solvent	No	No	---
	(Yi Lin et al., 2007)	PR	PMSA: R	Yes	Uematsu and Franck Model (1980)	T, V	3	1: Ion-Ion 1: Ion-Solvent	No	No	---
		PR	PMSA: nR	Yes		T, V	3	1: Ion-Ion 1: Ion-Solvent	No	No	---
Perturbation	(Jin & Donohue, 1988b)	PACT	Perturbation Term for the charge-molecules and charge-charge interactions	No	Malmberg and Maryott Model (1956)	T	1	---	No	No	---
		Barker-Henderson: Perturbation	PMSA: nR	Yes	Uematsu and Franck Model (1980)	T, V	2	1: Ion-Solvent 1: Ion-Solute	No	No	---
	(W.-B. Liu et al., 1999)	Perturbation terms	PMSA: nR	No	---	---	1	---	No	Yes: Self	$\epsilon^{AB}, \kappa^{AB}$
CPA	(Wu & Prausnitz, 1998)	PR	PMSA: nR	Yes	---	T, x	1-3	---	Yes: Ion-Solvent	Yes: Self	$\epsilon^{AB}, \kappa^{AB}$
	(Yi Lin et al., 2007)	SRK	PMSA: nR	Yes	Uematsu and Franck Model (1980)	T, V	3	1: Ion-Ion 1: Ion-Solvent	No	Yes: Self	$\epsilon^{AB}, \kappa^{AB}$
CPA	(Inchekel et al., 2008)	SRK	PMSA: nR: electrostatic + short range term (SR2)	Yes	Simonin's model	T, V, ion	4	1: Ion-Solvent	No	Yes: Self	ϵ^{AB}
	(Courtial et al., 2014)	SRK	PMSA: nR	Yes	Simonin's model (1997) + Schmidt correlation (1982)	T, V, ion	---	3: System Components 3: Ion-Components	No	Yes: Self + Cross	$\epsilon^{AB}, \kappa^{AB}$
	(Carvalho et al., 2015)	SRK	DH	No	---	---	---	---	No	Yes	$\epsilon^{AB}, \kappa^{AB}$
	(Maribo-mogensen et al., 2015)	SRK	DH	Yes	Maribo-Mogensen et al. (2013)	T, V, x_i	2	1: Salt-Solvent 1: System Components	No	Yes: Self	$\epsilon^{AB}, \kappa^{AB}$
	(Schlaikjer et al., 2017)	SRK	DH	Yes	Maribo-Mogensen et al. (2013)	T, V, x_i	3	1: Salt-Solvent	No	Yes: Self	$\epsilon^{AB}, \kappa^{AB}$
SAFT	(Galindo et al., 1999)	SAFT-VR	PMSA: R	No	---	T	1	1: Ion-Solvent	No	Yes: Self	κ^{AB}
	(B. H. Patel et al., 2003)	SAFT-VR	PMSA: R	No	---	T	1	1: Ion-Solvent	No	Yes: Self	$\epsilon^{AB}, \kappa^{AB}$
	(Tan et al., 2005)	SAFT1	PMSA: R	No	Ferna'ndez et al. (1997)	T	5	---	No	Yes: Self	$\epsilon^{AB}, \kappa^{AB}$
	(Z. Liu et al., 2005)	LJ-SAFT	LDE-MSA: nR	No	Wertheim (1971)	T, V, x_i	2	---	Yes: Ion-Solvent	Yes: Cross and Self	$\epsilon^{AB}, \kappa^{AB}$
	(Ji et al., 2005)	SAFT1	PMSA: R	No	---	T	5	1: Salt-Salt	No	Yes: Self	$\epsilon^{AB}, \kappa^{AB}$
	(Cameretti et al., 2005)	PC-SAFT	DH	No	Floriano and Nascimento (2004)	T	2	---	No	Yes: Self	$\epsilon^{AB}, \kappa^{AB}$
	(Ji, Adidharma, et al., 2006), (Ji, Tan, et al., 2006)	SAFT2	PMSA: R	No	Ferna'ndez et al. (1997)	T	2	---	No	Yes: Self	$\epsilon^{AB}, \kappa^{AB}$
	(Zhao et al., 2007)	SAFT-VR+DE	MSA: nR	No	---	---	5	---	No	Yes: Self and Cross	$\epsilon^{AB}, \kappa^{AB}$
	(Ji & Adidharma, 2008)	SAFT2	PMSA: R	No	Ferna'ndez et al. (1997)	T	1	1: Ion-Ion	No	Yes: Self	$\epsilon^{AB}, \kappa^{AB}$

Table 3-1: Summary of the literature for electrolyte modeling (continue)

Model	Reference	Parent Model	Electrolyte Model	Born	Di-electric Model		Parameters		Association		
					Model	Variables	Pure Parameter	Interaction Parameter	Ion Association	Association	Association parameter
SAFT	(Held et al., 2008)	PC-SAFT	DH	No	---	---	2	---	No	Yes: Self	$\epsilon^{AB}, \kappa^{AB}$
	(Held & Sadowski, 2009)	PC-SAFT	DH	No	---	---	2	---	Yes: Ion-Ion	Yes: Self	$\epsilon^{AB}, \kappa^{AB}$
	(B. Lee & Kim, 2009)	PC-SAFT	PMSA: nR	Yes	Fernández et al. (1997)	T	4	---	Yes: Ion-Solvent	Yes: Self	$\epsilon^{AB}, \kappa^{AB}$
	(Herzog et al., 2010)	PC-SAFT	NPMSA: sR	No	---	---	3	1: Ion-solvent	Yes: Ion-Solvent	Yes: Self	$\epsilon^{AB}, \kappa^{AB}$
	(Held et al., 2012)	PC-SAFT	DH	No	Fitting Correlation	T	2	3: Solvent-Solvent	No	Yes: Cross	$\epsilon^{AB}, \kappa^{AB}$
	(Doozandeh et al., 2012)	SAFT	RP-MSA	No	---	---	3	---	No	Yes: Self	$\epsilon^{AB}, \kappa^{AB}$
	(Anvari et al., 2013)	SAFT-VR	PMSA: nR	No	---	---	2	---	No	Yes	$\epsilon^{AB}, \kappa^{AB}$
	(Justyna Rozmus et al., 2013)	PPC-SAFT	PMSA: nR	Yes	Simonin's model (1982)	T, V, ion	2	---	Yes: Ion-Solvent, Ion-Ion	Yes: Self and Cross	$\epsilon^{AB}, \kappa^{AB}$
	(Schreckenber et al., 2014)	SAFT-VR	PMSA: R	Yes	Modified Uematsu and Frank	T, V, x_i	1	3: Ion-Ion 5: Solvent-Solvent	No	Yes: Self	$\epsilon^{AB}, \kappa^{AB}$
	(Held et al., 2014)	PC-SAFT	DH	No	---	---	2	1: Ion-Solvent 2: Solvent-Solvent	No	Yes: Cross	$\epsilon^{AB}, \kappa^{AB}$
	(Najafloo et al., 2014)	SAFT-HR	PMSA: nR	No	Maryott and Smith (1951)	T	2	---	No	Yes	$\epsilon^{AB}, \kappa^{AB}$
	(Das et al., 2015)	SAFT-VR+DE	cMSA: nR	No	---	---	3	---	Yes: Ion-Solvent	Yes: Self and Cross	$\epsilon^{AB}, \kappa^{AB}$
	(Hao Jiang et al., 2016)	SAFT2	KMSA	No	---	---	5	1: Solvent-Ion	No	Yes: Self	$\epsilon^{AB}, \kappa^{AB}$
(Mohammad et al., 2016)	ePC-SAFT and COSMO-RS	DH	No	No model	---	3	2: Solvent-Ion 2: Solvent-Solvent	No	Yes: Self and Cross	$\epsilon^{AB}, \kappa^{AB}$	
SAFT	(Najafloo et al., 2015)	SAFT-HR	PMSA: nR	Yes	---	T, x_i	3	3	No	Yes	$\epsilon^{AB}, \kappa^{AB}$
	(Eriksen et al., 2016)	SAFT-VR Mie	PMSA: nR	Yes	Modified Uematsu and Frank	T, V, x_i	5	1: Ion-Solvent	Yes: Ion-Solvent	Yes: Self and Cross	$\epsilon^{AB}, \kappa^{AB}$
	(Mohammad et al., 2016, 2015)	ePC-SAFT	DH	No	No model	---	3	2: Solvent-Ion 2: Solvent-Solvent	No	Yes: Self and Cross	$\epsilon^{AB}, \kappa^{AB}$
	(Shadloo et al., 2016)	PC-SAFT	DH	No	Fernández et al.	T	4	---	No and Yes: Ion-Solvent	Yes: Self	$\epsilon^{AB}, \kappa^{AB}$
	(Das et al., 2018)	SAFT-VR+DE	cMSA: nR	No	---	V, ion, μ	3	1: Ion-Solvent	No	Yes	$\epsilon^{AB}, \kappa^{AB}$
	(S. Ahmed et al., 2017)	GC-ePPC-SAFT	PMSA: nR	Yes	Schreckenber et al.	T, V, ion	3	2: Cross association	Yes: Ion-Ion and Ion-Solvent	Yes: Self and Cross	$\epsilon^{AB}, \kappa^{AB}$

3.2 Modeling the Gas Hydrate with Electrolyte

Modeling the gas hydrate has been an interest for many researchers around the world due to its importance. Many methods and theories were developed to estimate the phase behavior of the gas hydrate. K-values chart method was developed and used to estimate the hydrate formation conditions. It's the ratio between the vapor-solid equilibrium ratio but this method received a low acceptance (Carroll 2003; Carson and Katz 1941; Elgibaly and Elkamel 1998; Mann et al. 1989; Shahnazar and Hasan 2014; Willcox et al. 1941). Another method is the gas gravity method which is temperature-pressure charts that require the gravity of the gas to determine the formation conditions. Katz chart is one of the most common type used in this method (Katz 1945). However, since only one parameter is needed for this method the deviation is expected especially for gas gravity higher than 0.9 (Loh and James 1983; Shahnazar and Hasan 2014). Some correlations were developed by using different regression methods (Bahadori, 2008; A Bahadori, Vuthaluru, Tade, & Mokhatab, 2009; Alireza Bahadori, 2011; Alireza Bahadori, Mokhatab, & Towler, 2008; Alireza Bahadori & Vuthaluru, 2009; Berge, 1986; Ghiasi, 2012; Kadyshevich, Song, & Sloan, 1987). Group of researchers used the artificial neural network (ANN) model. By training the model with input data, a pattern will be generated and used to estimate the remaining data (Chouai, Laugier, and Richon 2002; Schmitz, Zemp, and Mendes 2006). Different studies used the ANN models to predict the hydrate formation conditions (Mohammadi, Belandria, & Richon, 2010; Mohammadi & Richon, 2010; Moradi, Nazari, Alavi, & Mohaddesi, 2013) or to estimate how many water molecules attached to hydrate structure (Torrecilla et al. 2013a, 2013b). Statistical methods, also, were used to come up with different correlation for hydrate equilibrium (Ameripour and Barrufet 2009), surface

tension during hydrate formation (Zarenezhad 2014) and the inhibition of salts or KHI to hydrate structure (Rashidabad, Hatami, and Ebrahimi 2013; Shadravanan, Schaffie, and Ranjbar 2014).

Due to the pioneering work of van der Waals and Platteeuw (vdWP) (van der Waals & Platteeuw, 1959) in addition to the extension work of Parrish and Prausnitz (Parrish and Prausnitz 1972), the thermodynamic modeling of the hydrate phase had colossal advancement. Their works were considered as the ground for modeling the gas hydrate phase (Bakker 1998; Ballard and Sloan 2002; Jeffery B. Klauda and Sandler 2000; Klauda and Sandler 2003). Many scientists coupled the vdWP model with different equations of state to predict the hydrate formation conditions or the effect of different inhibitors (Abolala, Karamoddin, & Varaminian, 2014; El Meragawi, Diamantonis, Tsimpanogiannis, & Economou, 2016; Hejrati Lahijani & Xiao, 2017; Jäger, Vinš, Gernert, Span, & Hrubý, 2013; Moradi & Khosravani, 2012, 2013; Renault-Crispo, Lang, & Servio, 2014; Waseem & Alsaifi, 2018). This section focuses on the gas hydrate modeling literature in the presence of the electrolyte.

Starting with Englezos work in 1992, he presented a method that can be used to predict the incipient conditions of high soluble gas (CO_2) in an aqueous electrolyte solution. They used the vdWP model for the gas hydrate phase, Trebble- Bishnoi EOS (Trebble and Bishnoi 1988a) for the vapor phase and Aasberg-Petersen et al. (1991) model (Tobergte and Curtis 2013) for the fugacity in the liquid phase (Englezos 1992).

Javanmardi and Moshfeghian (1998) work in which they proposed a thermodynamic model to predicate the hydrate formation condition for natural gas with single component and

mixed weak electrolyte solution. They used the van der Waals and Plateeuw model that describes the adsorption of gas into a liquid solution and they used the Pitzer and Mayorga model for water activity in the electrolyte solution. They assumed that the enthalpy of hydrate formation per water molecule in the hydrate lattice can be calculated by correlation that depends on ionic strength, pressure and the number of moles (Javanmardi et al. 1998).

In 2001, Javanmardi et al. proposed a thermodynamic model that estimate hydrate formation conditions in the presence of electrolyte and alcohol. They used Aasberg-Petersen et al. (1991) method in modeling with the Peng-Robinson EOS for the water fugacity, Margules model for the water activity in the presence of an alcohol and Javanmardi and Moshfeghian (2000) correlation for water activity in the presence of an electrolyte. They used Holder et al. (1980) (Holder et al. 1980) modification to the vdWP model. They studied many systems include NaCl, CaCl₂, methanol with different percentages (Javanmardi, Moshfeghian, and Maddox 2001).

Nasrifar and Moshfeghian (2001) proposed a model to estimate the gas hydrate conditions in the presence of electrolyte and alcohol. They used Holder et al. (1988) modification to the vdWP, the water activity in the presence of alcohol calculated by the Margules activity model, water activity in the presence of electrolyte is estimated by a derived expression. They investigated different systems include NaCl, KCl, CaCl₂ with different combinations of the previous salts (Nasrifar and Moshfeghian 2001).

Vu et al. (2002) used the Pénélox's EOS (Abdoul, Rauzy, and Pénélox 1991) (modified PR-EOS) to investigate the effect of the salts on the hydrate formation when methanol

present in the system. They coupled it with the vdWP model for the gas hydrate and tested it for CH₄ and CO₂ systems with salt (Vu, Suchaux, and Fürst 2002).

Clarke and Bishnoi (2004) developed an equation of state that was tested for hydrate-vapor-liquid equilibrium. Their equation of state include; the Trebble–Bishnoi EOS term (Trebble and Bishnoi 1987, 1988b), the Born model term, the non-restricted primitive explicit MSA term and the solvation term. They used the Holder model for the difference in chemical potential in water between the hydrate phase and in the empty hydrate while using the Holder model (Holder et al. 1980). They predicted the hydrate formation conditions for different systems (includes NaCl, KCl and methanol) (Clarke and Bishnoi 2004).

Marion et al. (2006) worked on modeling gas hydrate equilibria in electrolyte solutions. They used the solid solution model which is based on the classical thermodynamics to describe the solid hydrate phase. They developed a gas hydrate model and included it into the FREZCHEM model (an equilibrium chemical thermo-dynamic model) which calculates the equilibrium between the ice and water and between the dissolve and the solid salts (Marion and Grant 1994). Pitzer approach was used to get the activity coefficients that depend on the temperature and they used pressure dependence term for the ion activity coefficient. The model was validated for different data set for methane hydrate and carbon dioxide hydrate. Duan model that has been used in defining the fugacity coefficient has a lower temperature limit equal to 0 C°. Also, the model was developed for methane and CO₂ hydrate only, the other gases that form hydrate will need similar parametrization (Marion et al. 2006).

Mohammadi et al. (2007) modeled the salt precipitation, the salt solubility, and its hydrate inhibition ability thermodynamically by using a modified version of the Patel-Teja equation of state (Zuo & Guo, 1991). They treated the salt as a pseudo-component and used the solid-liquid equilibrium theory to model the equilibrium between the aqueous phase and the precipitated salt. By using water freezing point depression data along with boiling point elevation data, the binary interaction between the salt and water were optimized. The van der Waals-Platteeuw theory was used to model the gas hydrate. The model was tested for methane in the presence of NaCl and NaCl + KCl aqueous solution (Mohammadi & Richon, 2007).

Jiang and Adidharma (2012) used the ion-based statistical associating fluid theory (Ion-based SAFT2) to describe the hydrate dissociation conditions for different gases in the presence of single and mixed electrolyte solutions. They coupled it with the van der Waals and Platteeuw model to describe the hydrate phase (the chemical potential of water in hydrate). The ion based-SAFT2 has less parameter and therefore it can handle the electrolyte solution better than the other models. The systems that have been studied are methane, ethane, and propane hydrate phase equilibrium in the presence of single and mixed salt solutions containing NaCl, KCl, and CaCl₂ (H Jiang and Adidharma 2012a, 2012b).

Valavi and Dehghani (2012) worked on coupling the modified perturbed hard-sphere equation of state (PHSC-EOS) (Lee & Kim, 2015) with the vdWP model to predict the gas hydrate formations conditions. They include the restricted-primitive implicit version of the MSA model to account for the long-range interaction in the system. They

investigated 102 systems of different gases with different inhibitors and salts such as Methanol, Ethanol, MEG, NaCl, KCl and CaCl₂ (Valavi and Dehghani 2012).

Mohammadi et al., (2014) modeled the hydrogen sulfide hydrate dissociation condition in the presence of different inhibitors and salts. They used the vdWP concept with some modification in calculating some of the parameters (Sloan & Koh, 2008). They used the extended UNIQUAC model to estimate the activity of water. They investigated H₂S with different inhibitors and salts including; Methanol, ethanol, EG, NaCl, KCl and CaCl₂ (Mohammadi et al., 2014).

Kwaterski and Herri (2014) presented a thermodynamic model for gas hydrate in the presence of an electrolyte. Their model consists of the following; the vdWP model for the gas hydrate phase, the SRK-EOS for gas phase, Henry law for the gas solubility and the electrolyte non-random two-liquid (eNRTL) excess Gibbs energy model for the electrolyte. The eNRTL model contains two contributions; short-range contribution and long-range contribution. The Long-range contribution is represented by Debye–Hückel modified version by Pitzer (Pitzer 1973, 1980) while the short-range contribution represented by the modified version of the non-random-two-liquid model of Renon and Prausnitz (Renon and Prausnitz 1968). They investigated different systems with different single and mixed salts including: NaCl, KCl, CaCl₂ (Kwaterski and Herri 2014).

Osfouri et al., (2015) developed a model to predict gas hydrate in the presence of different thermodynamics inhibitors and salts. Their model has the following contributions; the vdWP model for the gas hydrate phase, modified Patel–Teja equation of state for the vapor phase, short ranger term represent it by the non-electrolyte NRTL-NRF local composition

model (Haghtalab, Shojaeian, and Mazloumi 2011), long range represent it by the Pitzer–Debye–Huckel equation and the water activity in the presence of polar inhibitor by the Margules equation. Holder et al., (1980) expression was used for chemical potential in aqueous phase (Holder et al. 1980). Their model was tested for many systems that contain single or mixed salts include NaCl, KCl, CaCl₂ and thermodynamics inhibitors such as MEG, DEG and TEG (Osfouri et al. 2015).

Sirino et al., (2016) used the flash calculation method to predict the mole fraction of different hydrate systems with the presence of inhibitors and salts. They coupled the CPA-EOS with the vdWP model. The CPA-EOS based model was the SRK-EOS and they used the Debye-Huckel equation to account for the electrostatic interaction. They readjust the Langmuir constants for each gas hydrate former. Their model was able to predict the hydrate formation conditions for different systems that contain different inhibitors (CH₃OH, C₂H₅OH, C₂H₆O₂) and different salt (NaCl, KCl, CaCl₂) (Sirino et al. 2018).

CHAPTER 4

ELECTROLYTE PROPERTIES USING SAFT-VR MIE

COUPLED WITH PRIMITIVE MSA

4.1 Introduction

The electrolyte compounds could inhibit the hydrate formation by shifting the pressure-temperature curve to higher pressure and lower temperature. The accuracy in predicting them plays a significant role in the accuracy of gas hydrate calculation in the presence of these salts.

This chapter includes the methodology section which highlights the methodology used in optimizing the SAFT-VR Mie parameters for the salts in particular the dispersion energy between the ion the solvent. Also, the results obtained from this model will be shown in the results section which includes the following properties; mean ionic activity coefficient (MIAC), osmotic coefficient (Φ) and the vapor pressure of different aqueous solutions.

4.2 Methodology

The methodology that was used is similar to Eriksen et al., (2016) work (Eriksen et al. 2016). They modified equation (2.1.2.3-4) to include the electrostatic contribution by adding the primitive MSA term and born term. The equation becomes the following:

$$a^{res} = a^{mono} + a^{chain} + a^{assoc} + a^{MSA} + a^{Born} \quad (4.2-1)$$

The first two terms are used for the components in the systems and the association term to account for the hydrogen bonds. The last two terms account for the electrostatic forces in the system. The definition of these terms can be found in Chapter 2.

The ions treated as fully dissociated in the solution which agrees with the equilibrium reaction equation (2.1-) while the dissociation of the solvent was ignored. The ions diameters were selected experimentally from Shannon (Shannon 1976) work where he reported the crystal ionic radii for different coordination numbers. The coordination number was chosen as six since it was reported for all the ions that were in a place of interest in this work. The crystal ionic radii do not take into account the effect of the solvent and represent the real case of the ions with no influence which is the reason to have distinctive Born diameter. The Born diameter was taken from Rashin and Honig (Rashin and Honig 1985) work in which they made the ion cavity experience a minimum contribution dielectric medium as the definition for the Born diameter cavity. The dispersion attraction forces between the like and unlike ions (ϵ_{ii} and ϵ_{ij}) were calculated using the following equations (Eriksen et al. 2016):

$$\epsilon_{ij} = \frac{(\lambda_{r,ij} - 3)(\lambda_{a,ij} - 3)}{2C(\lambda_{r,ij} - \lambda_{a,ij})} \frac{\alpha_{0,i}\alpha_{0,j}}{(4\pi\epsilon_0)^2\sigma_{ij}^6} \frac{I_i I_j}{I_i + I_j} \quad (4.2-2)$$

$$C = \left(\frac{\lambda_{r,ij}}{\lambda_{r,ij} - \lambda_{a,ij}} \right) \left(\frac{\lambda_{r,ij}}{\lambda_{a,ij}} \right)^{\lambda_{r,ij}/(\lambda_{r,ij} - \lambda_{a,ij})} \quad (4.2-3)$$

$$\lambda_{k,ij} = 3 + \sqrt{(\lambda_{k,ii} - 3)(\lambda_{k,jj} - 3)} , \quad k = a, r \quad (4.2-4)$$

where $\lambda_{r,ij}$, $\lambda_{a,ij}$, $\alpha_{0,i}$ AND I_i are Mie exponent for the unlike repulsion ion and attraction ion, electronic polarizability for ion i and ionization potential for ion I; respectively

The electronic polarization and ionization potential were collected from the literature and used in calculating the dispersion forces (Al-Joboury and Turner 1967; Branscomb 1966; DR Lide 2005; Klein, Kochanski, and Strich 1996; Pyper, Pike, and Edwards 1992). The dispersion forces between the water and the ions were considered as an adjustable parameter that is fitted to the experimental data. These experimental data include the vapor pressure of the electrolyte solution, osmotic coefficient and mean ionic activity coefficient. The parameters used for the ions are listed in Table 4-1 while unlike dispersion attraction energies between the ions are listed (Eriksen et al. 2016).

Table 4-1: SAFT-VR Mie parameters for different ions

Ion, i	σ_{ii}/A	σ_{ii}^{Born}/A	$\lambda_{r,i}$	$\lambda_{a,i}$	$(\epsilon_{ii}/k_B)/K^o$
Li+	1.8	2.632	12	6	6.1039
Na+	2.23	3.36	12	6	31.711
K+	3.04	4.344	12	6	90.097
Rb+	3.32	4.622	12	6	130.35
Mg2+	1.72	2.91	12	6	89.264
Ca2+	2.28	3.724	12	6	261.28
Sr2+	2.64	4.108	12	6	305.79
Ba2+	2.98	4.238	12	6	401.26
F-	2.38	2.846	12	6	66.059
Cl-	3.34	3.874	12	6	113.77
Br-	3.64	4.174	12	6	107.38
I-	4.12	4.686	12	6	102.9

Table 4-2: Dispersion attractive energies between the unlike ions

	F-	Cl-	Br-	I-
Li+	7.6879	8.2904	7.1802	5.8749
Na+	22.891	27.938	24.99	21.383
K+	43.681	61.01	56.592	50.963
Rb+	53.634	78.254	73.489	67.344
Mg2+	28.051	29.6	25.498	20.708
Ca2+	63.572	76.936	68.645	58.536
Sr2+	73.57	95.805	87.132	76.321
Ba2+	88.214	122.051	112.837	101.148

The estimation of the dispersion between the water and ions is achieved by minimizing the objective function which involves the relevant difference between the experimental data and the result from the model. The Levenberg-Marquardt method was utilized with least-square objective function as shown in the following equation (Levenberg and Arsenal 1943; Marquardt 1963):

$$\min F_{obj} = \sum_o \left(\frac{\omega_o}{n_{p,o}} \sum_j^{n_{p,o}} \left[\frac{X_{o,j}^{exp} - X_{o,j}^{calc}}{X_{o,j}^{exp}} \right]^2 \right) \quad (4.2-5)$$

where F_{obj} , ω_o , $n_{p,o}$, $X_{o,j}^{exp}$ and $X_{o,j}^{calc}$ are the objective output, the weight given for each property \mathbf{o} , the number of data points, the experiment value of the property and the calculated value of the property.

The model accuracy was assessed by comparing the electrolyte SAFT-VR Mie results with experimental data for different properties. This was done by calculating the percent absolute average deviation (%AAD) with respect to the experimental data for each property:

$$\%AAD = \frac{100}{np_o} \sum_o \left| \frac{X_{o,j}^{exp} - X_{o,j}^{calc}}{X_{o,j}^{exp}} \right| \quad (4.2-6)$$

The salts that were investigated are; LiCl, LiBr, LiI, NaF, NaCl, NaBr, NaI, KF, KCl, KBr, KI, MgBr₂, MgCl₂, CaBr₂, CaCl₂, CaI₂, BaBr₂, BaCl₂. The results of the SAFT-VR Mie for the mean ionic activity coefficient, osmotic coefficient and the vapor pressure for each of the salts that were mention are shown in the result and discussion section.

4.3 Results and Discussion

Evaluating the SAFT-VR Mie plus MSA predictability was achieved by the mean ionic activity coefficient, osmotic coefficient and the vapor pressure of the electrolyte solutions. As these terms were defined in Chapter 2, they are directly related to the fugacity which means they are related to the other thermodynamic properties which help in assessing the model (Eriksen et al. 2016). The optimization process was done using equation (4.2-5) with one property, either the MIAC or Osmotic coefficient depending on the better representation of the other properties. The purpose of this is to use the remaining properties as criteria of the model physical representation. Even though using more than one property in the optimization will improve the results, it could jeopardize the physical representation and the aim of using the least data in the optimization. Choosing the property for the optimization and the comparison is subject to the availability of the data. Starting with Lithium salts which include Lithium Chloride, Lithium Bromide and Lithium Iodide. The comparison with experimental data of these salts is shown in Figure 4-1 through Figure 4-6 for MIAC, Osmotic Coefficient and vapor pressure. All of them showed a good match with experimental data while the highest AAD is % 20.05 for the Lithium Bromide vapor pressure. The optimization process for these salts was varying by using Osmotic Coefficient or MIAC data. Never the less, both of them showed a good match for the other estimated properties. Keeping in mind that Lithium-ion is one of the smallest ions which is an indication of the excellence of the model especially for the hard sphere term (Eriksen et al. 2016). The %AAD of the different properties, optimized dispersion parameter between the ion and the water, the data used for the optimization and in comparison with experimental data for the Lithium salts are listed in Table 4-3. The next salts set is the

sodium salts which include Sodium Fluoride, Sodium Chloride, Sodium Bromide and Sodium Iodide. The match with experimental data agrees with very low absolute average deviation as shown in Table 4-3 for all the properties. As shown in Figure 4-7 through Figure 4-13, the match is excellence compared to the experimental data. The potassium salts (potassium fluoride, potassium chloride, potassium bromide and potassium iodide) gave excellence match compared to the experimental data as shown from Figure 4-14 to Figure 4-20. All the optimized dispersion parameters for the cation and the anion for the divalent salt that were mention are shown in Table 4-3.

For the divalent cation, the calcium and barium were investigated. The Calcium salts that were studied: Calcium Bromide, Calcium Chloride and Calcium Iodide which are shown from Figure 4-21 to Figure 4-25. The agreement with experiment data is fair with the highest percentage absolute average deviate of %22.5 for the Calcium chloride mean ionic activity coefficient. The other information on the Calcium salts is shown in Table 4-3. The Barium salts that were considered include Barium Bromide and Barium Chloride. The match with experimental data is excellent for all the available properties as shown from Figure 4-26 through Figure 4-29 and the data used in the optimization with AAD% for each property are shown in Table 4-3.

Comparing the overall results of the model to different model, there are some improvement compare to some work for several salt and in the same there is accuracy deteriorated for others. However, most of the previous works optimized more than one parameter such as the ion diameters, the dispersion parameters and fitting parameter which improve the accuracy of the model. Furthermore, the model was able to capture the osmotic coefficient better than the mean ionic activity coefficient in most cases. This can be contributed to the

fact that osmotic coefficient represents the solvent better than the mean ionic activity coefficient. The model is established on good base to represent the solvent (SAFT-VR Mie). On the other hand, determining the parameters of SAFT-VR Mie for the ions was done using different approach than the original approach.

- Lithium Chloride (LiCl)

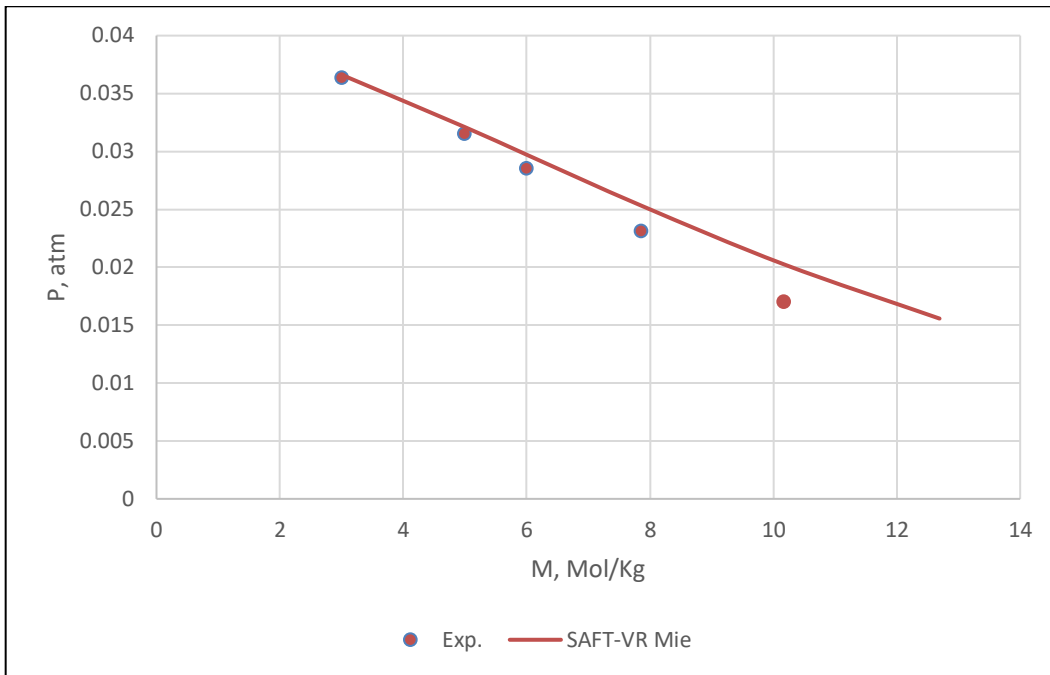


Figure 4-1: Comparison between the Experimental Results and SAFT-VR Mie EOS for the Vapor Pressure of Lithium Chloride as function of Salt Concentration at T = 303 K

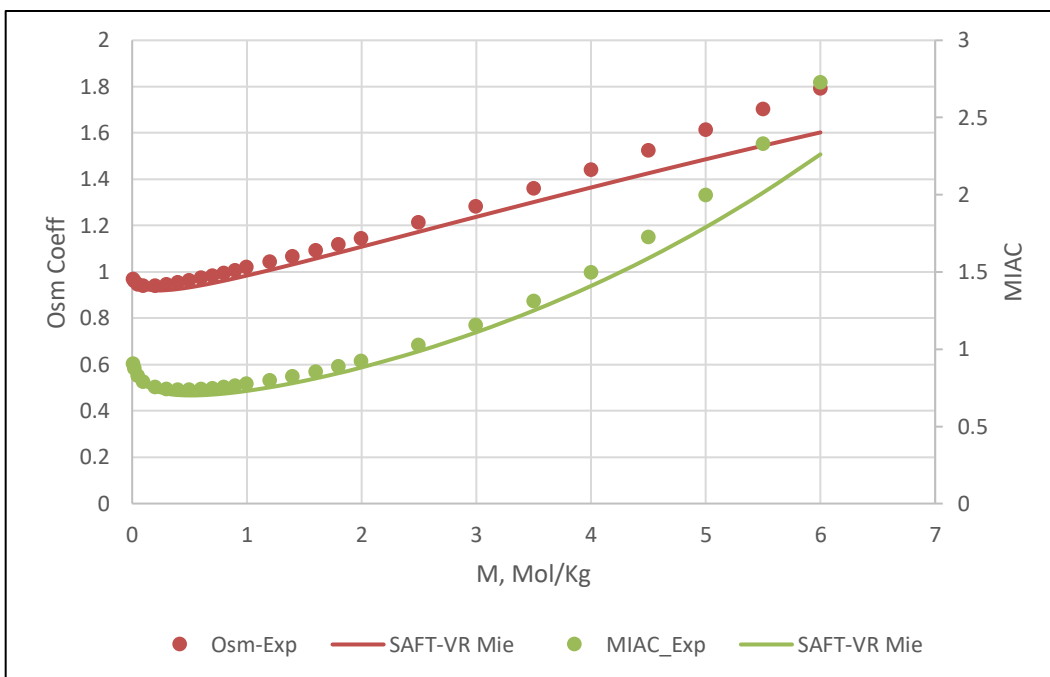


Figure 4-2: Comparison between the Experimental Results and SAFT-VR Mie EOS for the Osmotic Coefficient and Mean Ionic Activity Coefficient (MIAC) of Lithium Chloride as function of Salt Concentration at T = 298 K

- Lithium Bromide (LiBr)

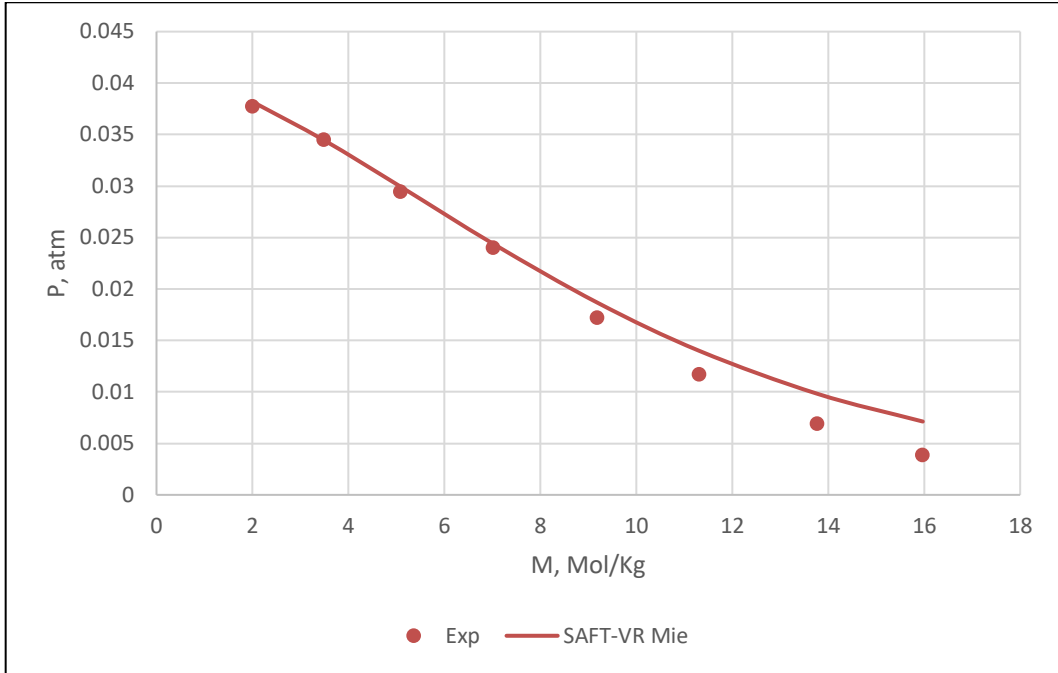


Figure 4-3: Comparison between the Experimental Results and SAFT-VR Mie EOS for the Vapor Pressure of Lithium Bromide as function of Salt Concentration at T = 298 K

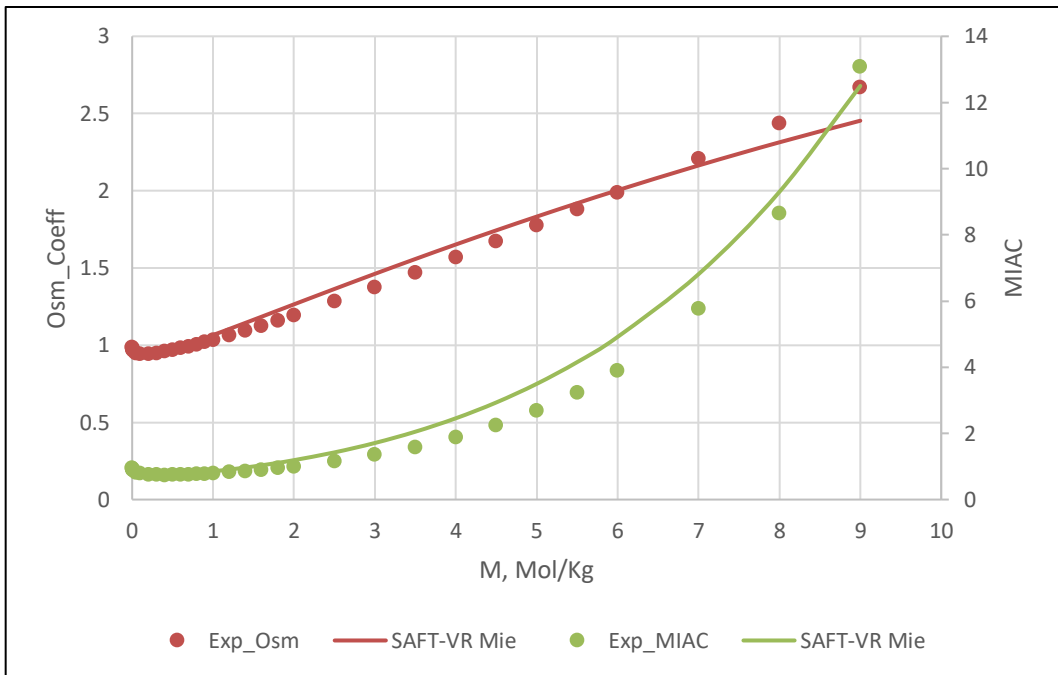


Figure 4-4: Comparison between the Experimental Results and SAFT-VR Mie EOS for the Osmotic Coefficient and Mean Ionic Activity Coefficient (MIAC) of Lithium Bromide as function of Salt Concentration at T = 303 K

- Lithium Iodide (LiI)

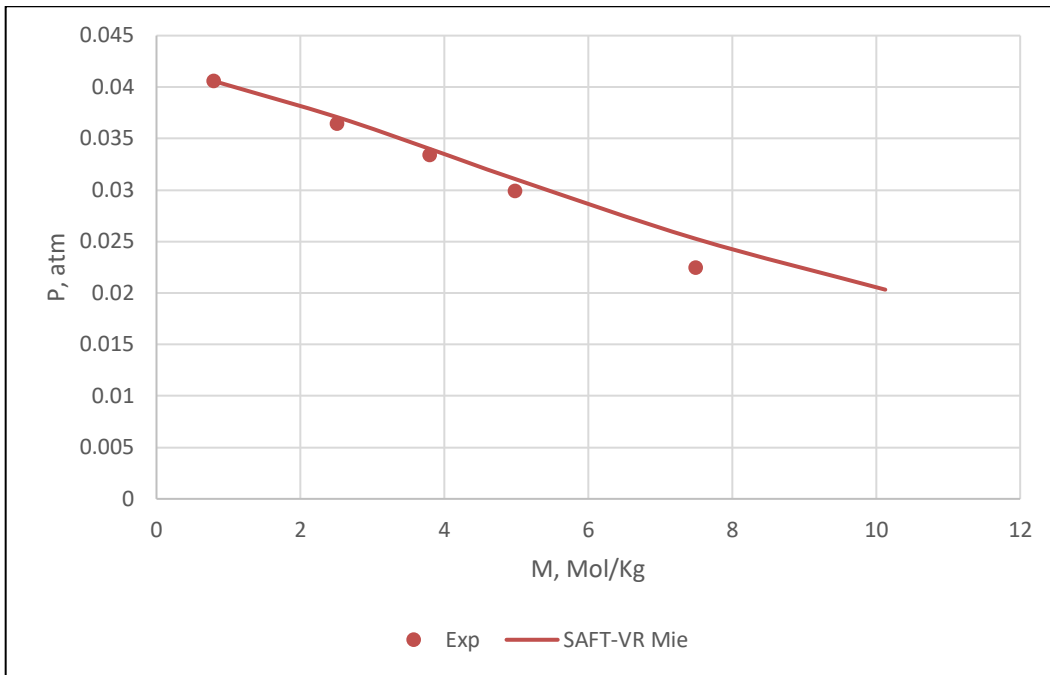


Figure 4-5: Comparison between the Experimental Results and SAFT-VR Mie EOS for the Vapor Pressure of Lithium Iodide as function of Salt Concentration at T = 298 K

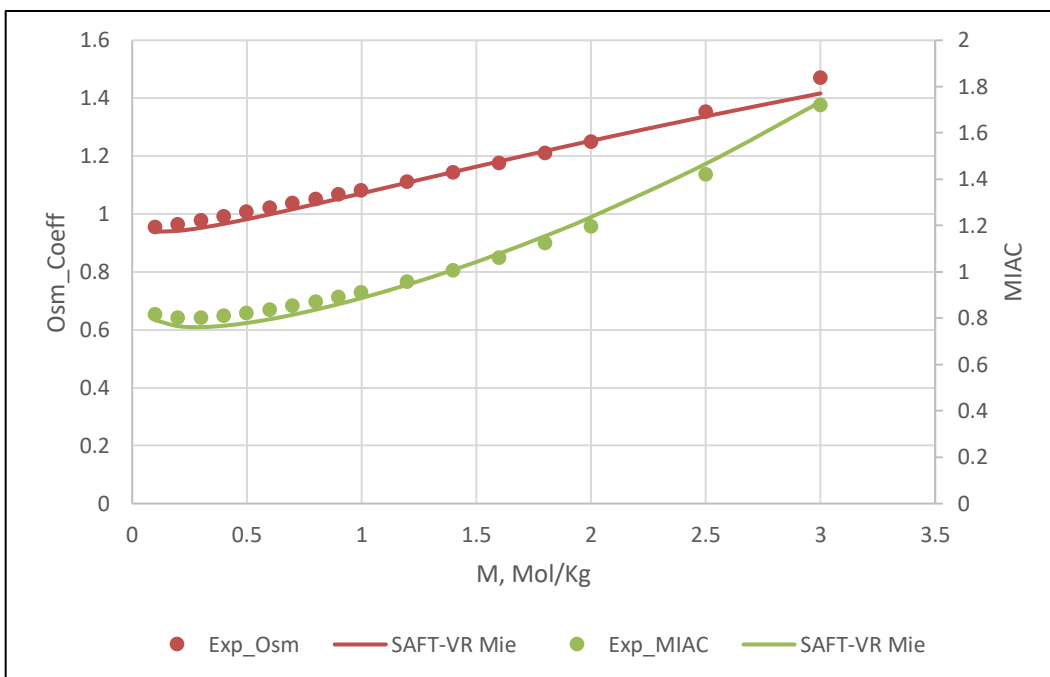


Figure 4-6: Comparison between the Experimental Results and SAFT-VR Mie EOS for the Osmotic Coefficient and Mean Ionic Activity Coefficient (MIAC) of Lithium Iodide as function of Salt Concentration at T = 303 K

- Sodium Fluoride (NaF)

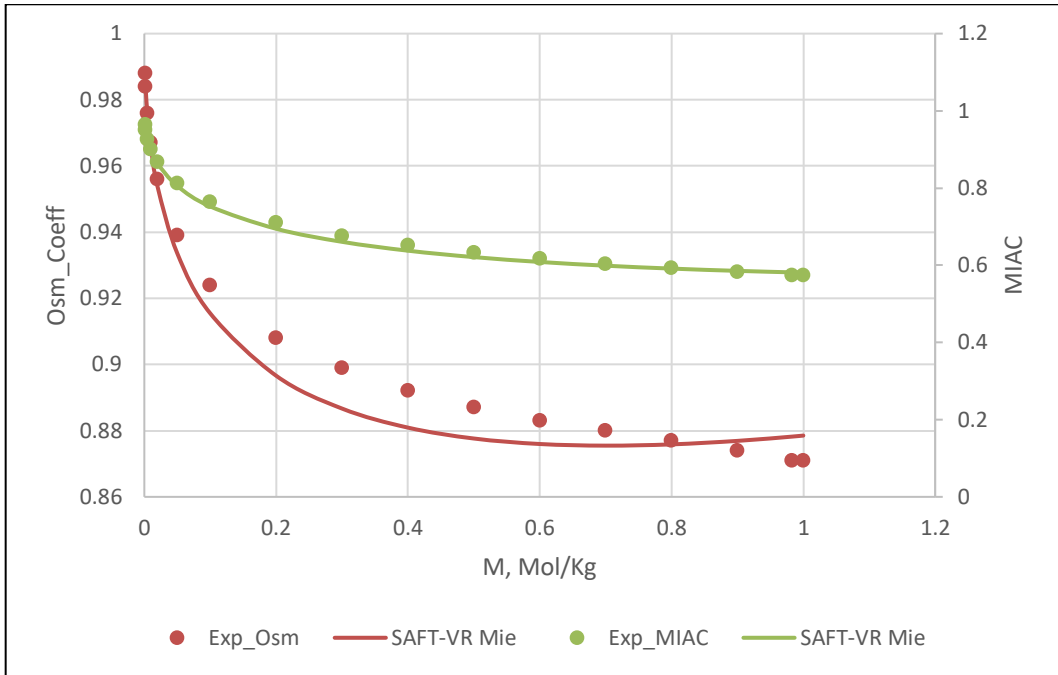


Figure 4-7: Comparison between the Experimental Results and SAFT-VR Mie EOS for the Osmotic Coefficient and Mean Ionic Activity Coefficient (MIAC) of Sodium Fluoride as function of Salt Concentration at T = 298 K

- Sodium Chloride (NaCl)

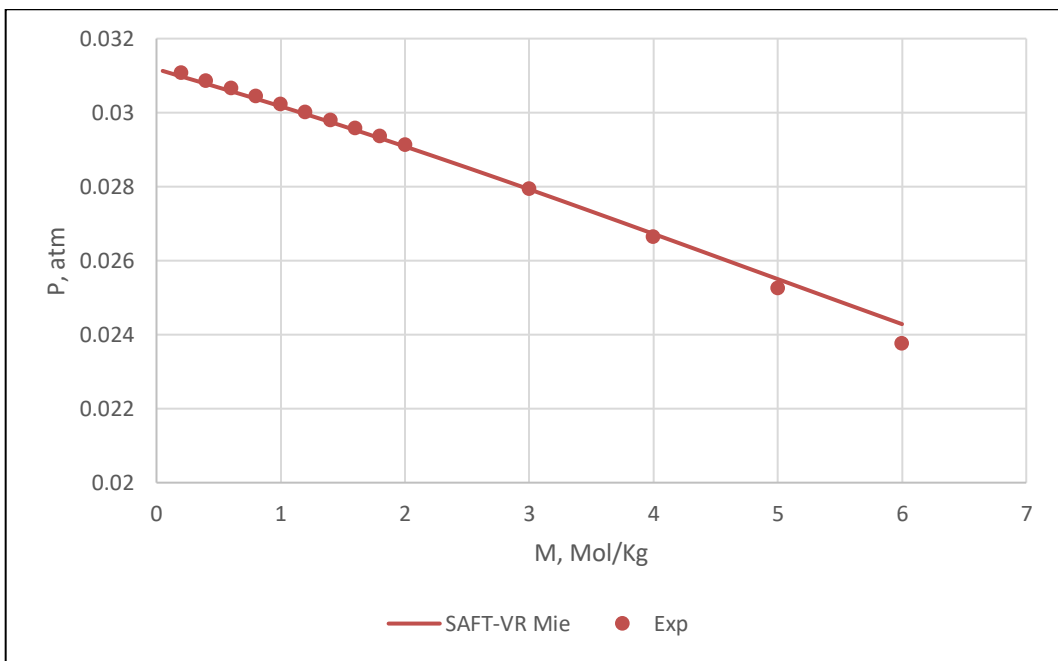


Figure 4-8: Comparison between the Experimental Results and SAFT-VR Mie EOS for the Vapor Pressure of Sodium Chloride as function of Salt Concentration at T = 298 K

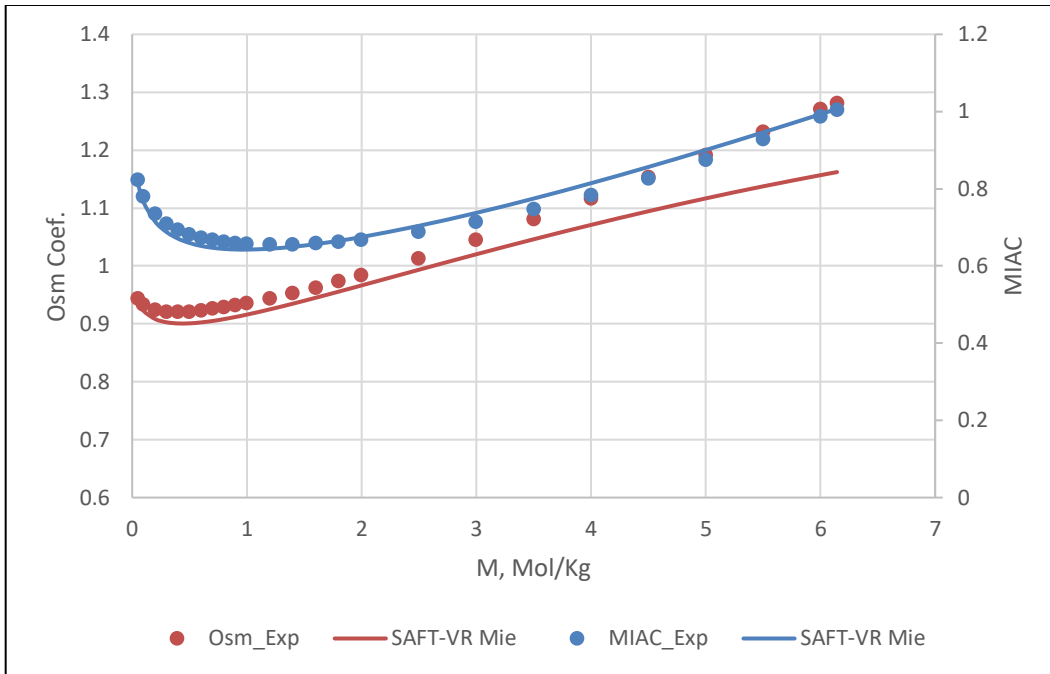


Figure 4-9: Comparison between the Experimental Results and SAFT-VR Mie EOS for the Osmotic Coefficient and Mean Ionic Activity Coefficient (MIAC) of Sodium Chloride as function of Salt Concentration at T = 298 K

- Sodium Bromide (NaBr)

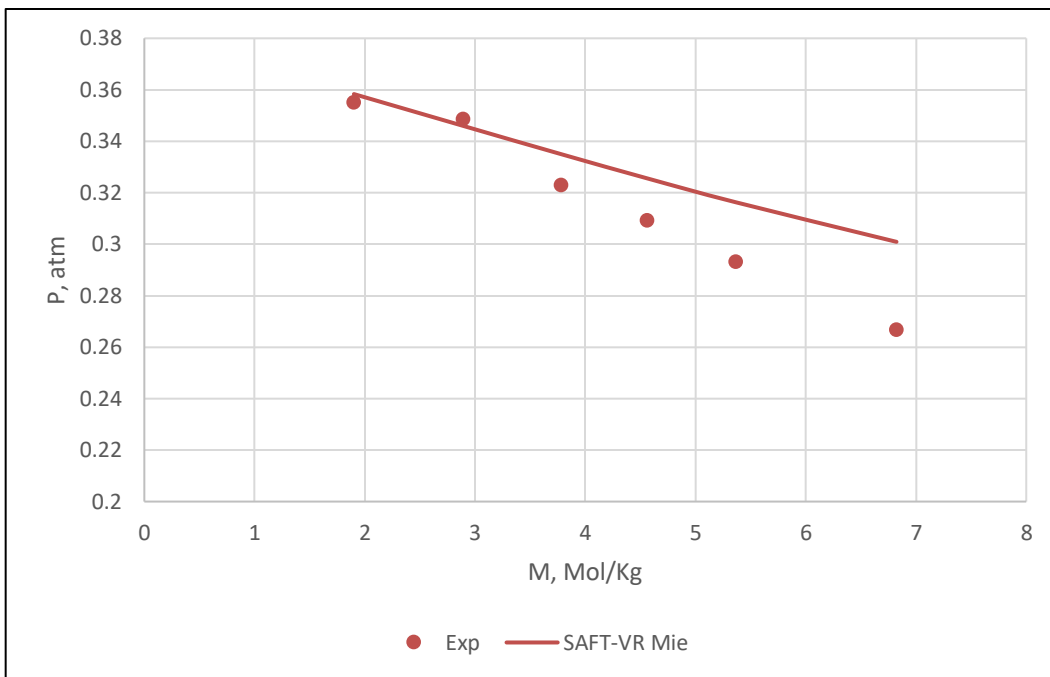


Figure 4-10: comparison between the Experimental Results and SAFT-VR Mie EOS for the Vapor Pressure of Sodium Bromide as function of Salt Concentration at T = 348 K

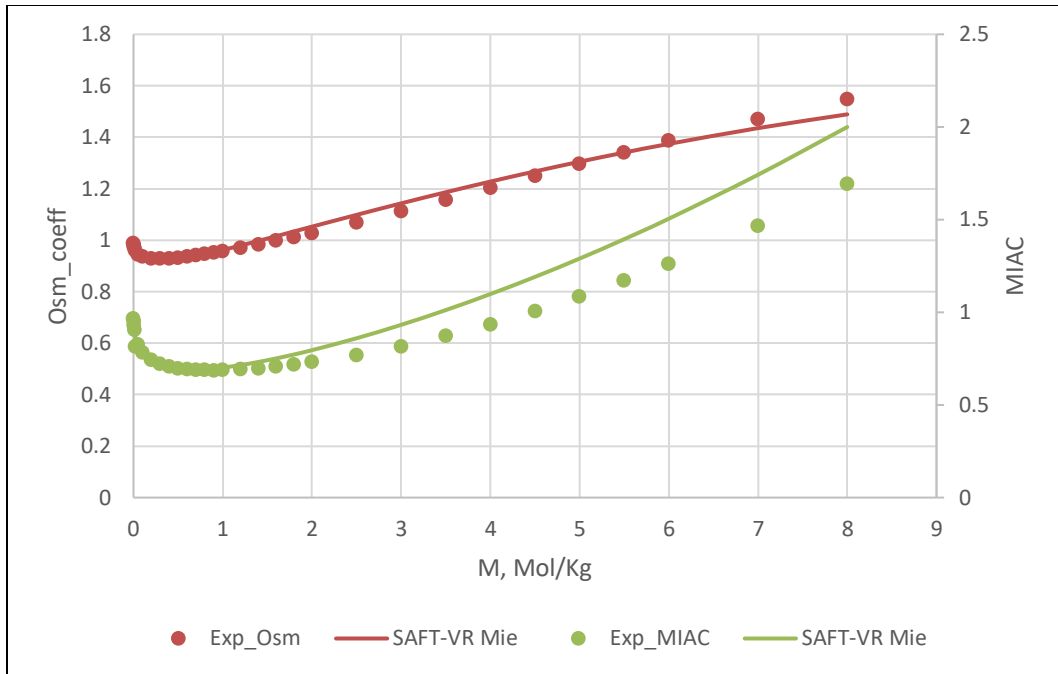


Figure 4-11: Comparison between the Experimental Results and SAFT-VR Mie EOS for the Osmotic Coefficient and Mean Ionic Activity Coefficient (MIAC) of Sodium Bromide as function of Salt Concentration at T = 298 K

- Sodium Iodide (NaI)

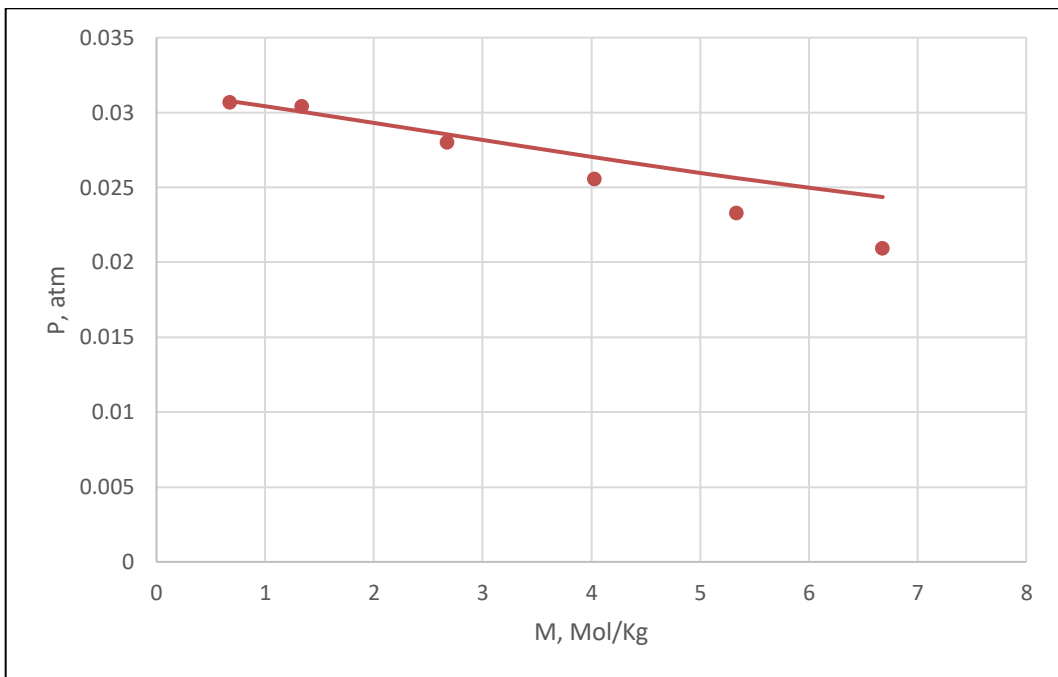


Figure 4-12: Comparison between the Experimental Results and SAFT-VR Mie EOS for the Vapor Pressure of Sodium Iodide as function of Salt Concentration at T = 298 K

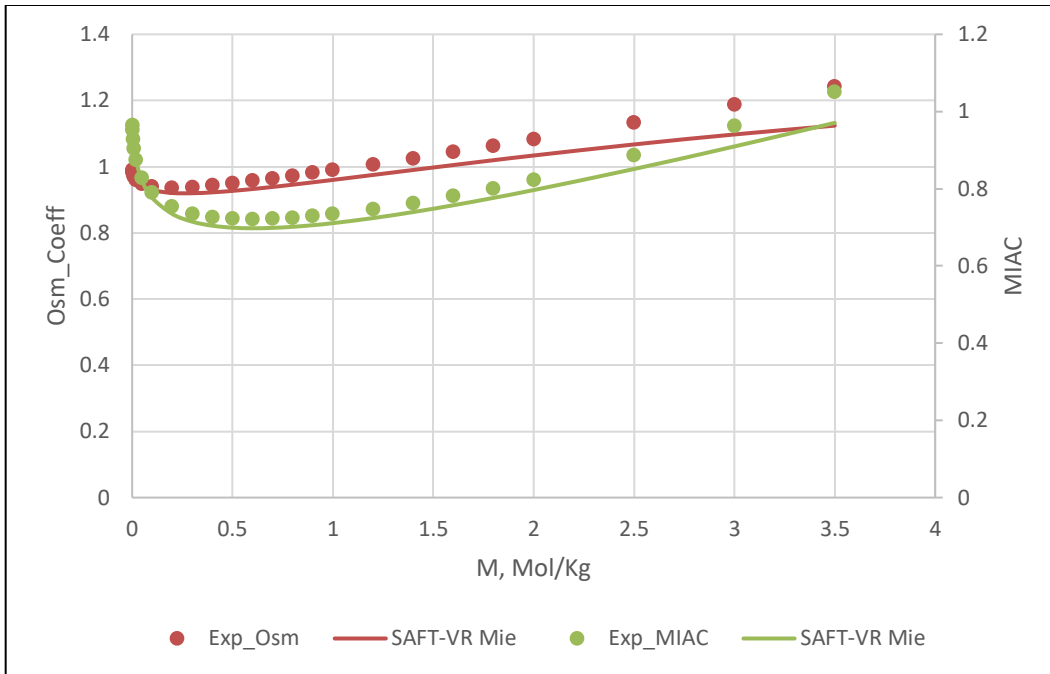


Figure 4-13: Comparison between the Experimental Results and SAFT-VR Mie EOS for the Osmotic Coefficient and Mean Ionic Activity Coefficient (MIAC) of Sodium Iodide as function of Salt Concentration at T = 298 K

- Potassium Fluoride (KF)

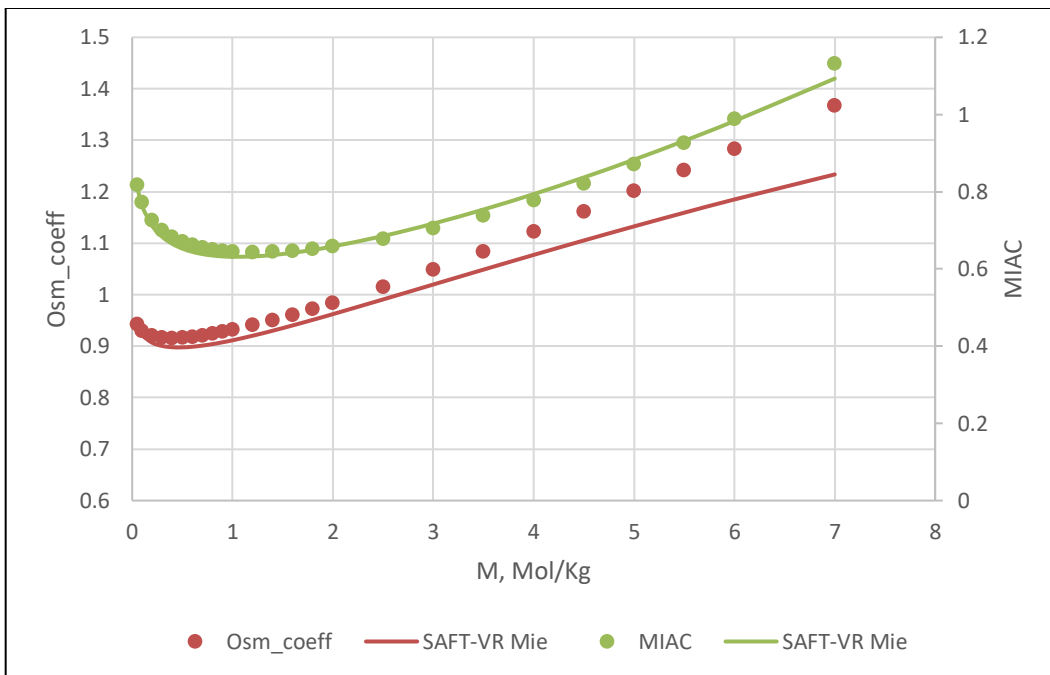


Figure 4-14: Comparison between the Experimental Results and SAFT-VR Mie EOS for the Osmotic Coefficient and Mean Ionic Activity Coefficient (MIAC) of Potassium Fluoride as function of Salt Concentration at T = 298 K

- Potassium Chloride (KCl)

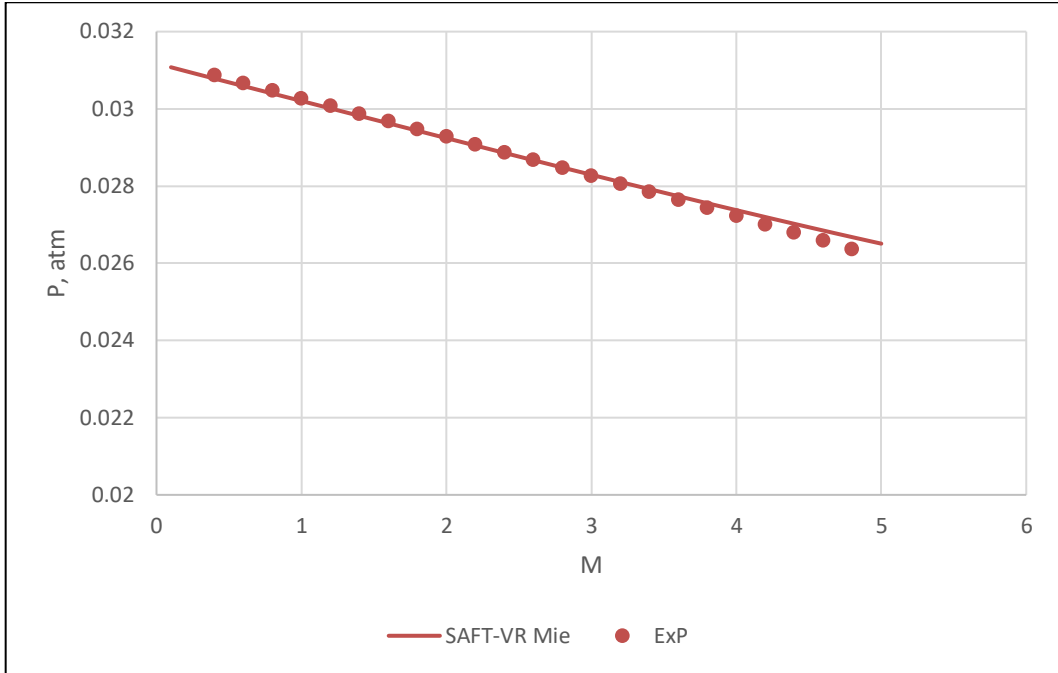


Figure 4-15: Comparison between the Experimental Results and SAFT-VR Mie EOS for the Vapor Pressure of Potassium Chloride as function of Salt Concentration at T = 298 K

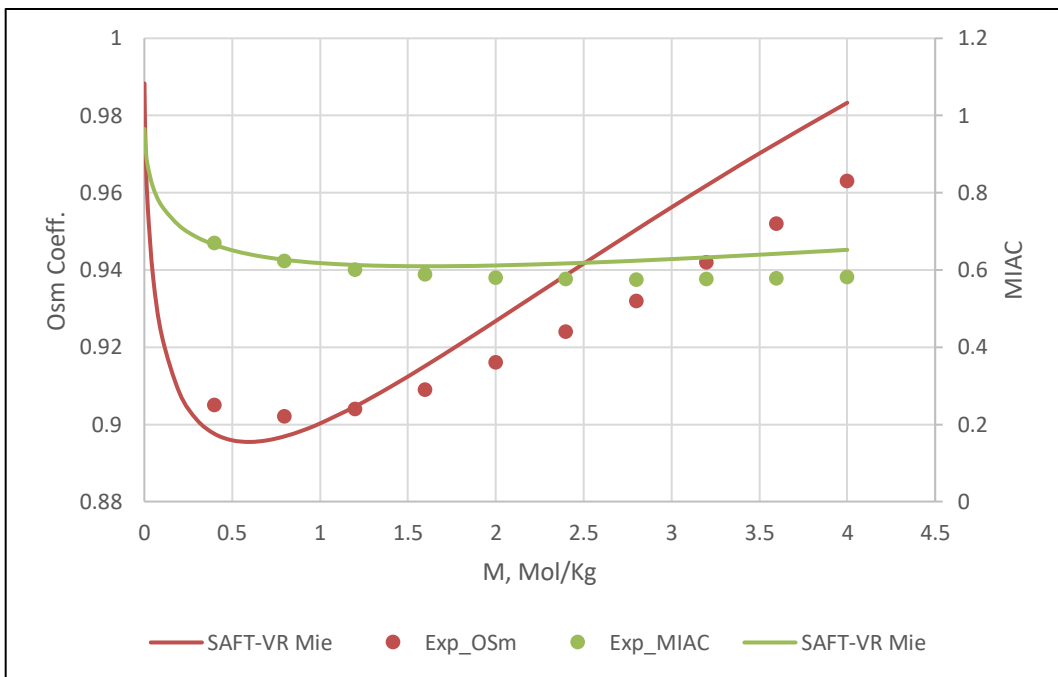


Figure 4-16: Comparison between the Experimental Results and SAFT-VR Mie EOS for the Osmotic Coefficient and Mean Ionic Activity Coefficient (MIAC) of Potassium Chloride as function of Salt Concentration at T = 298 K

- Potassium Bromide (KBr)

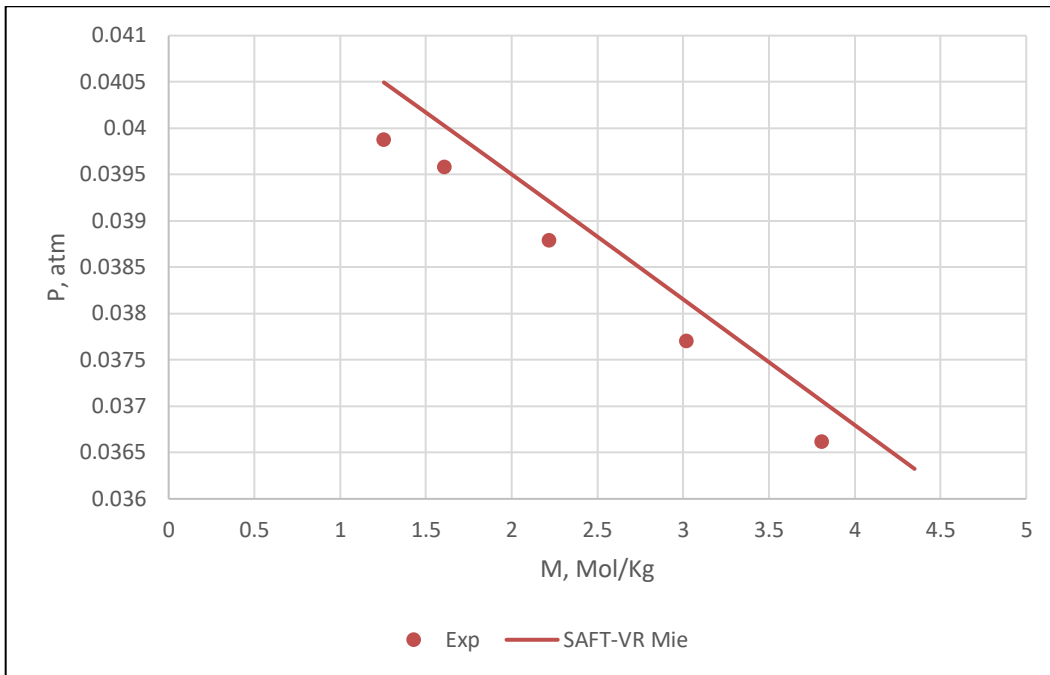


Figure 4-17: Comparison between the Experimental Results and SAFT-VR Mie EOS for the Vapor Pressure of Potassium Bromide as function of Salt Concentration at T = 303 K

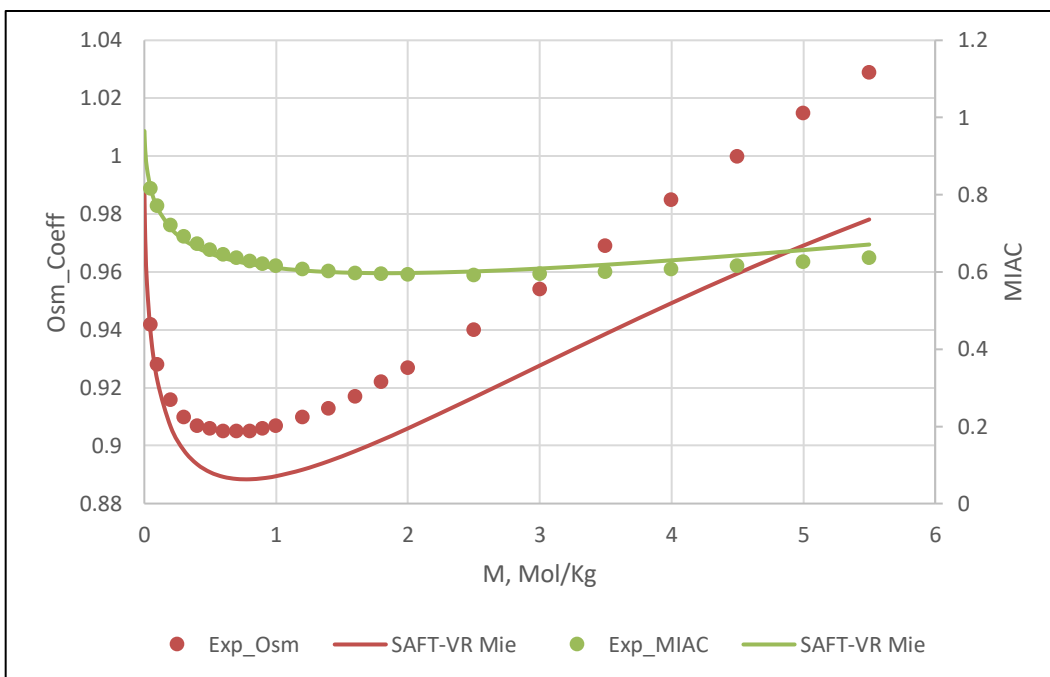


Figure 4-18: Comparison between the Experimental Results and SAFT-VR Mie EOS for the Osmotic Coefficient and Mean Ionic Activity Coefficient (MIAC) of Potassium Bromide as function of Salt Concentration at T = 298 K

- Potassium Iodide (KI)

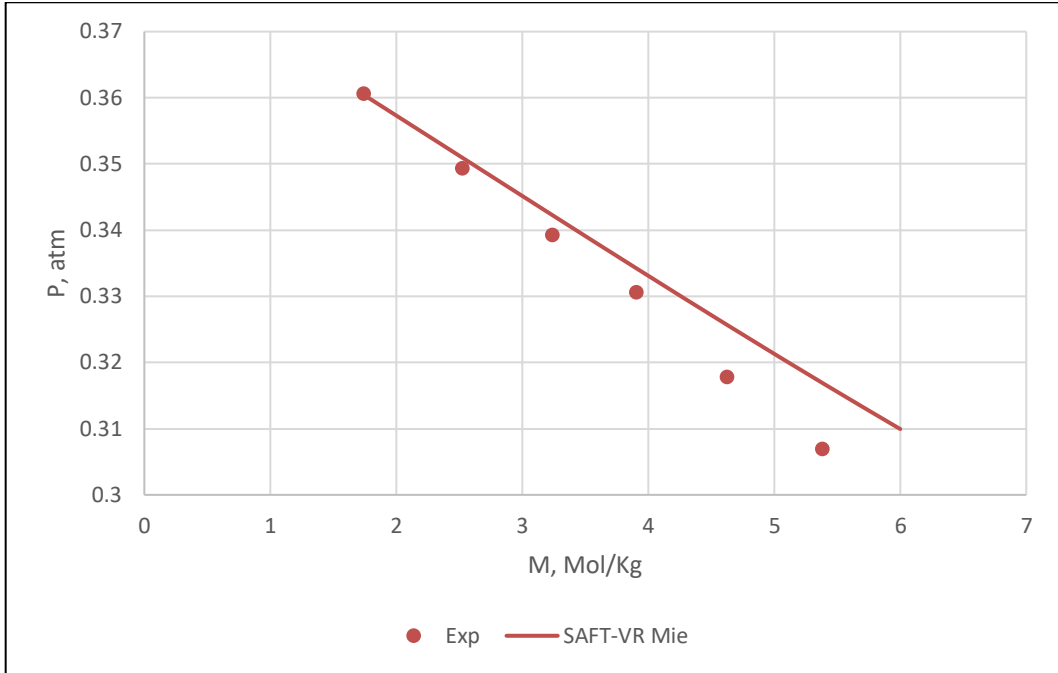


Figure 4-19: Comparison between the Experimental Results and SAFT-VR Mie EOS for the Vapor Pressure of Potassium Iodide as function of Salt Concentration at T = 348 K

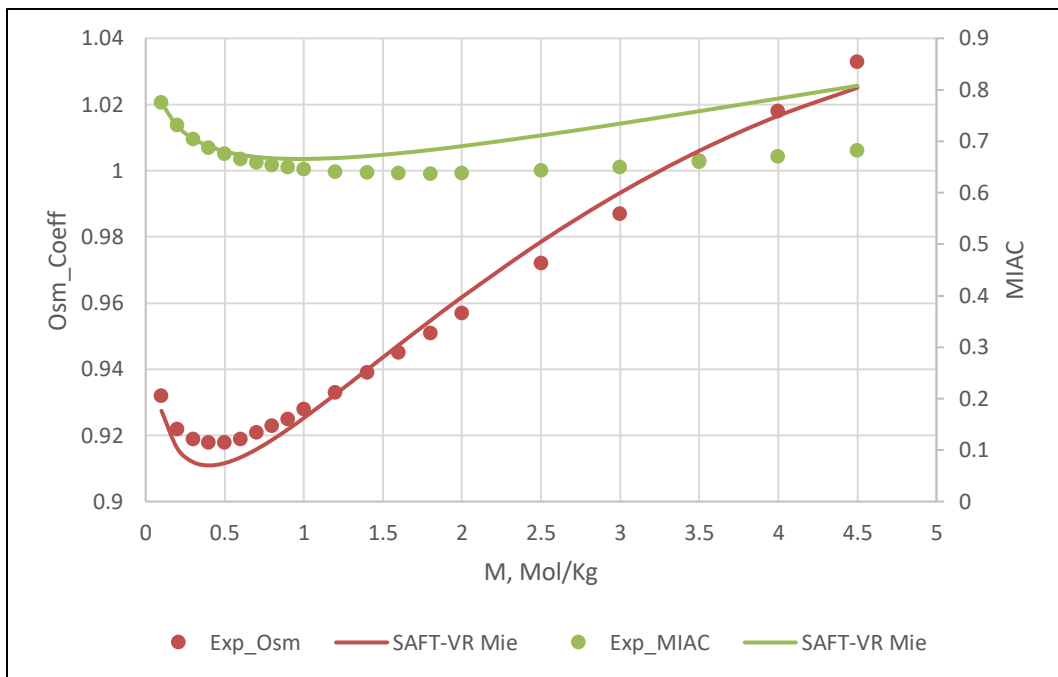


Figure 4-20: Comparison between the Experimental Results and SAFT-VR Mie EOS for the Osmotic Coefficient and Mean Ionic Activity Coefficient (MIAC) of Potassium Iodide as function of Salt Concentration at T = 298 K

- Calcium Bromide (CaBr₂)

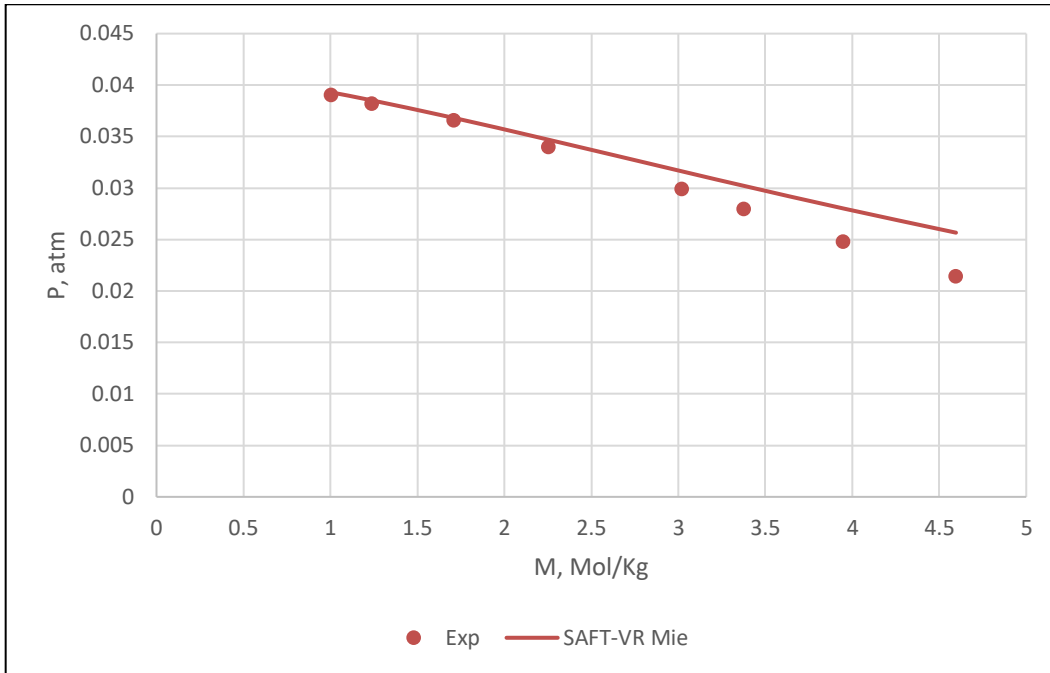


Figure 4-21: Comparison between the Experimental Results and SAFT-VR Mie EOS for the Vapor Pressure of Calcium Bromide as function of Salt Concentration at T = 303 K

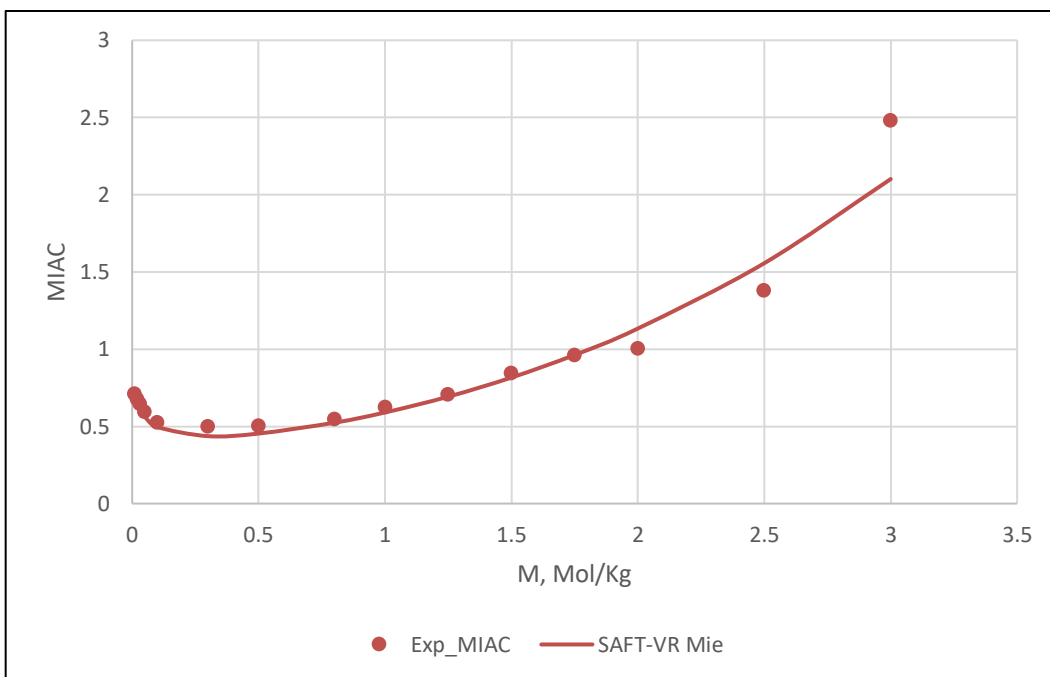


Figure 4-22: Comparison between the Experimental Results and SAFT-VR Mie EOS for the Mean Ionic Activity Coefficient (MIAC) of Calcium Bromide as function of Salt Concentration at T = 298 K

- Calcium Chloride (CaCl₂)

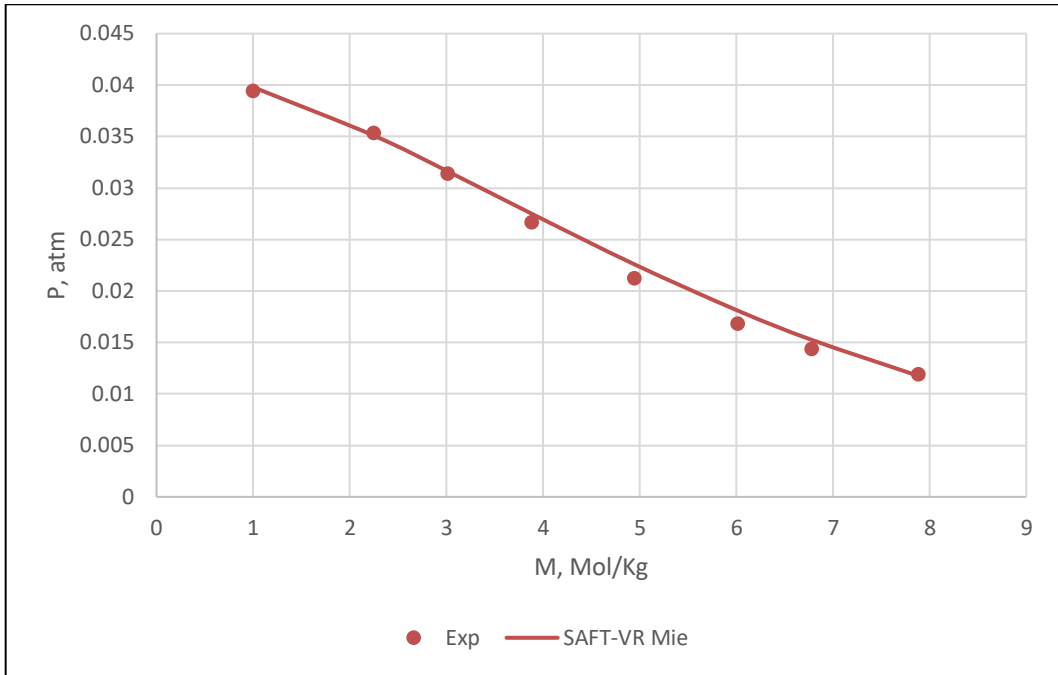


Figure 4-23: Comparison between the Experimental Results and SAFT-VR Mie EOS for the Vapor Pressure of Calcium Chloride as function of Salt Concentration at T = 303 K

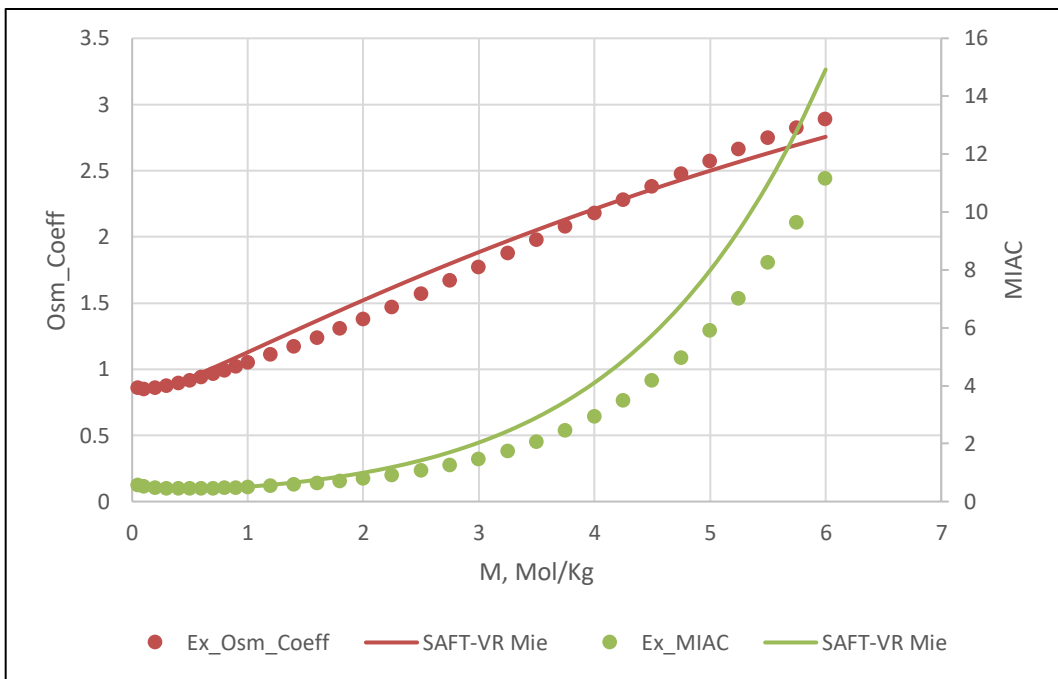


Figure 4-24: Comparison between the Experimental Results and SAFT-VR Mie EOS for the Osmotic Coefficient and Mean Ionic Activity Coefficient (MIAC) of Calcium Chloride as function of Salt Concentration at T = 298 K

- Calcium Iodide (CaI₂)

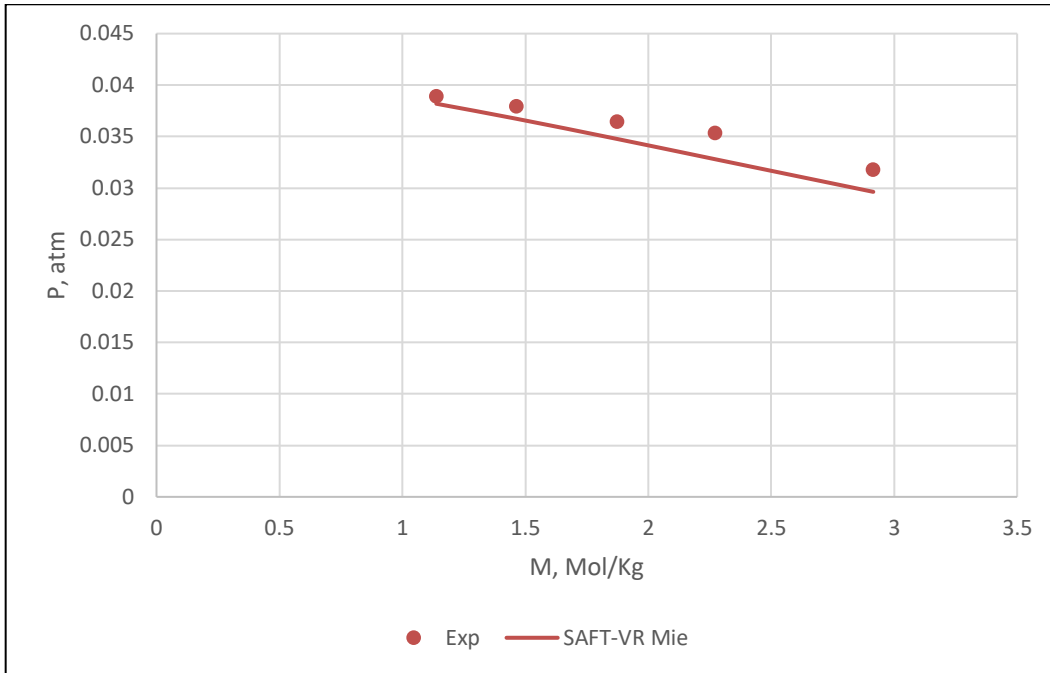


Figure 4-25: Comparison between the Experimental Results and SAFT-VR Mie EOS for the Vapor Pressure of Calcium Iodide as function of Salt Concentration at T = 303 K

- Barium Bromide (BaBr₂)

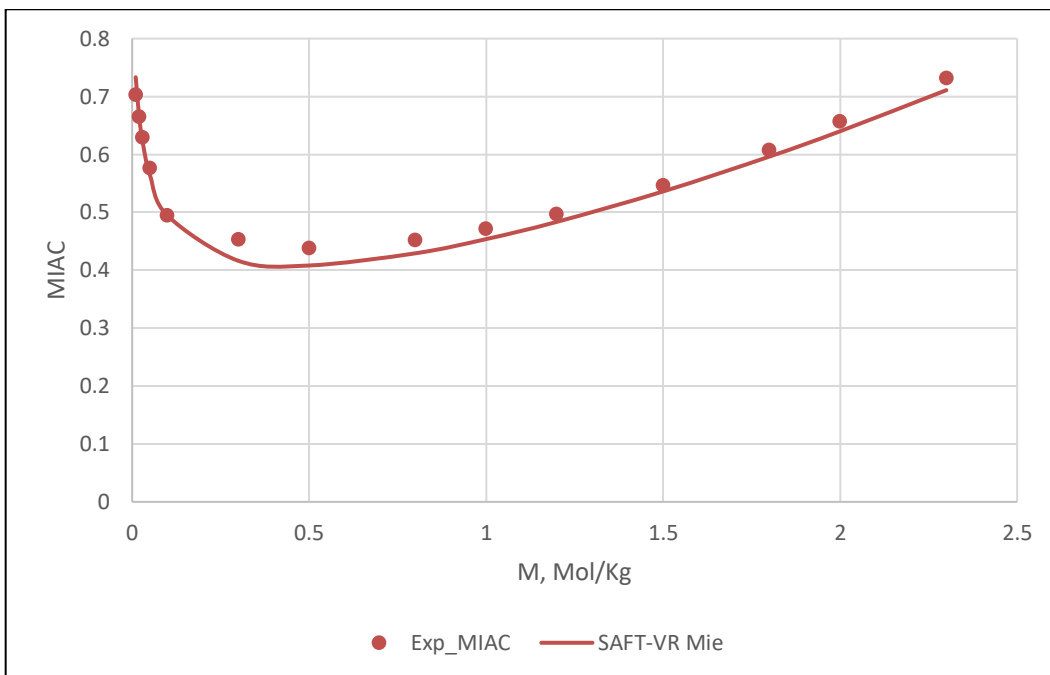


Figure 4-26: Comparison between the Experimental Results and SAFT-VR Mie EOS for the Mean Ionic Activity Coefficient (MIAC) of Barium Bromide as function of Salt Concentration at T = 298 K

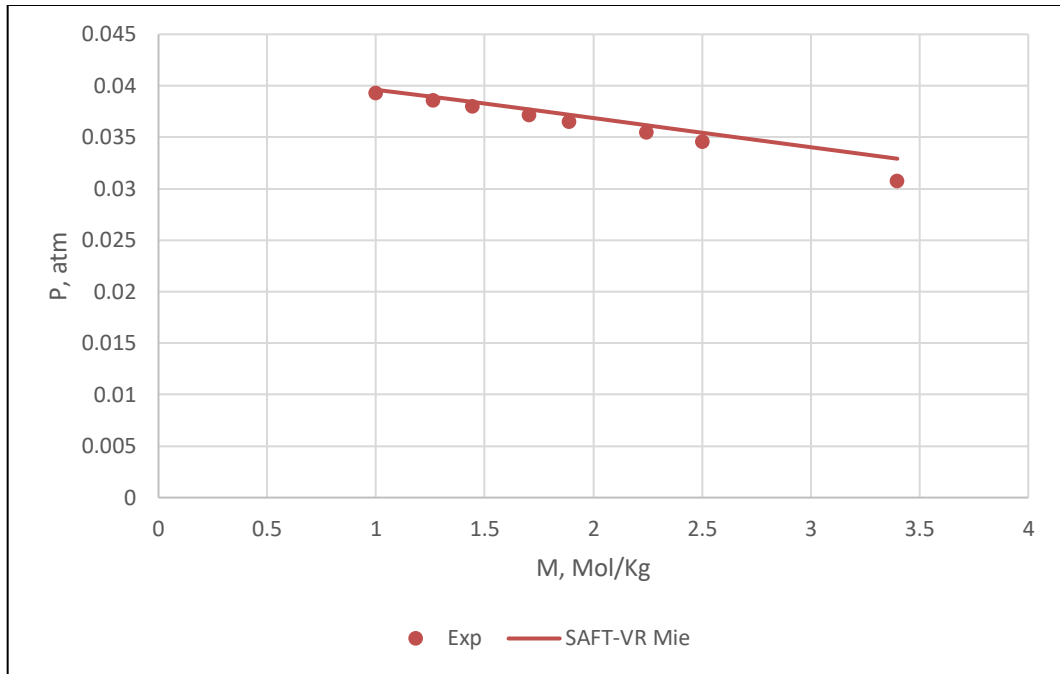


Figure 4-27: Comparison between the Experimental Results and SAFT-VR Mie EOS for the Vapor Pressure of Barium Bromide as function of Salt Concentration at T = 303 K

- Barium Chloride (BaCl₂)

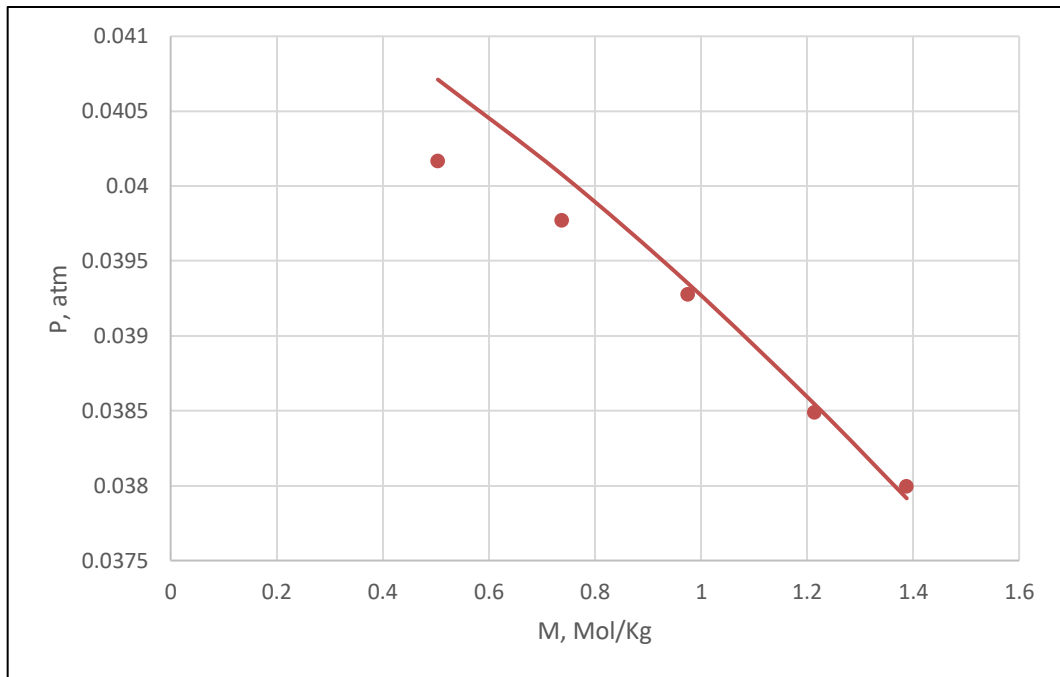


Figure 4-28: Comparison between the Experimental Results and SAFT-VR Mie EOS for the Vapor Pressure of Barium Chloride as function of Salt Concentration at T = 303 K

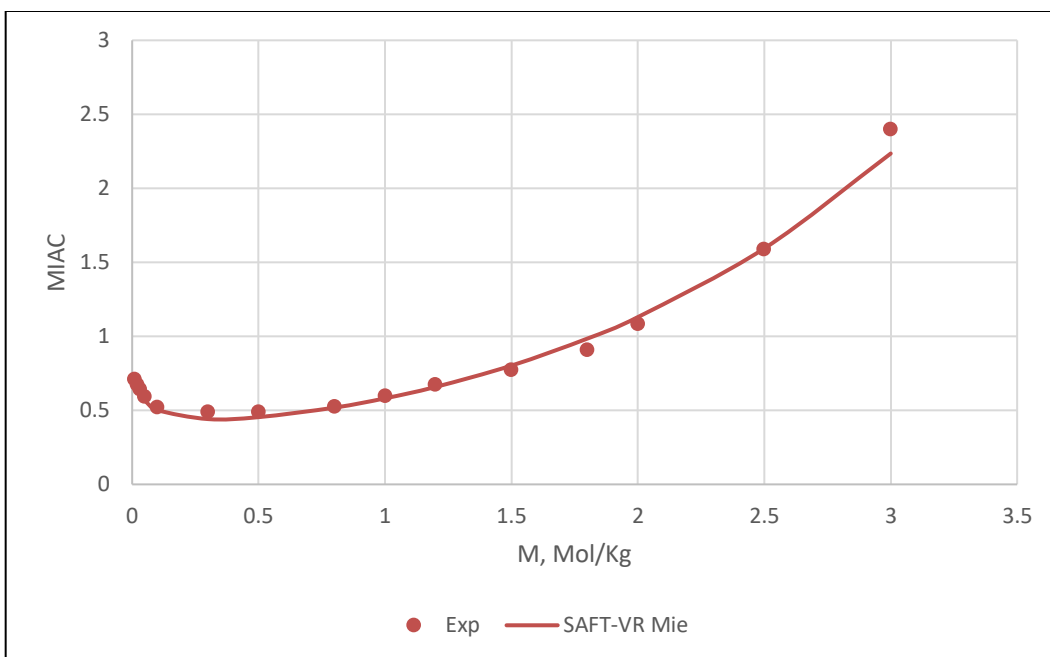


Figure 4-29: Comparison between the Experimental Results and SAFT-VR Mie EOS for the Mean Ionic Activity Coefficient (MIAC) of Lithium Chloride as function of Salt Concentration at T = 298 K

Table 4-3: Absolute Average Deviation Percentage for the Pressure, Mean Ionic Activity Coefficient, Osmotic Coefficient for different Electrolyte Solutions, Optimized parameters for each salt and Data used in the optimization process

Salt	%AAD			Optimized parameters (ϵ_{i-H_2O})		Data used for optimization			
	Pressure, MPa	MIAC	Osm. Coeff.	Cation	Anion	Range, Molality	T, K	Parameter Used	References
LiCl	11.22	9.49	5.47	300.807	390.024	0.1-6	298	MIAC	(Hamer, Walter and Wu 2009; Patil et al. 1990)
LiBr	20.05	10.73	2.71	1023.100	112.010	0.1-7	298	Osm. Coeff.	(Hamer, Walter and Wu 2009; Patil et al. 1990)
LiI	11.96	3.30	1.59	252.826	358.110	0.1-3	298	MIAC	(Hamer, Walter and Wu 2009; Patil et al. 1990)
NaF	---	1.03	0.61	292.469	299.236	0.001-1	298	MIAC	(Hamer, Walter and Wu 2009)
NaCl	3.98	2.23	3.15	244.334	285.059	0.5-3	298	MIAC	(Hamer, Walter and Wu 2009; Partanen and Covington 2009)
NaBr	6.82	7.24	1.16	241.764	293.505	0.1-7	298	MIAC	(Hamer, Walter and Wu 2009; Yamamoto et al. 1995)
NaI	5.87	2.64	2.76	539.680	142.660	0.001-3	298	Osm. Coeff.	(Hamer, Walter and Wu 2009; Patil, Olive, and Coronas 1994)
KF	---	1.70	3.08	422.461	27.851	0.05-7	298	MIAC	(Hamer, Walter and Wu 2009)

Table 4-4: Absolute Average Deviation Percentage for the Pressure, Mean Ionic Activity Coefficient, Osmotic Coefficient for different Electrolyte Solutions, Optimized parameters for each salt and Data used in the optimization process (continue)

Salt	%AAD			Optimized parameters (ϵ_{i-H_2O})		Data used for optimization			
	Pressure, MPa	MIAC	Osm. Coeff.	Cation	Anion	Range, Molality	T, K	Parameter Used	References
KCl	0.61	3.16	0.71	429.672	12.407	0.4-4.8	298	Osm. Coeff.	(Hamer, Walter and Wu 2009; Partanen and Covington 2009)
KBr	2.74	0.69	4.69	428.718	21.940	0.05-5.5	298	MIAC	(Hamer, Walter and Wu 2009; Patil et al. 1990)
KI	1.37	1.78	2.18	454.520	4.876	0.1-4.5	298	MIAC, Osm. Coeff.	(Hamer, Walter and Wu 2009; Patil et al. 1994)
CaBr ₂	6.48	6.68	---	348.097	404.963	0.05-7	298	MIAC	(Rodil and Vera 2001, 2003)
CaCl ₂	3.36	22.51	4.71	1988.470	24.822	0.05-7	298	MIAC	
BaBr ₂	2.27	3.08	---	293.404	329.551	0.01-2.3	298	MIAC	
BaCl ₂	0.72	4.13	---	1364.721	17.959	0.01-3	298	MIAC	

CHAPTER 5

GAS SOLUBILITY IN THE PRESENCE OF

ELECTROLYTE

5.1 Introduction

The solubility data of different gases is fundamental due to its wide application in different industries (e.g., geologic sequestration of CO₂ in underground formations). Therefore, it is essential to predict and understand the behavior of these gases. Also, the solubility considers as a part of the equilibrium calculation which is a part of the gas hydrate calculation for the gas-water system. Hence, the ability to predict the solubility of these gases in aqueous electrolyte water solutions accurately will play an essential role in the gas hydrate-electrolyte system calculation.

This chapter will focus on modeling the solubility of different gases in several aqueous electrolyte solutions and starting with the methodology section, which will highlight the model, optimization process and the parameterization. Finally, the results and discussion section will present the capability of the models by comparing the result of the model with the experimental data.

5.2 Methodology

Due to some convergence problem with MSA for the solubility and gas hydrate calculations, the modified DH used in this chapter. According to Maribo-Mogensen et al., (2012), the MSA and DH will have close results if the ion diameters used in the fitting process (Maribo-Mogensen, Kontogeorgis, and Thomsen 2012). They compared the two theories in terms of the numerical values of the screening length, residual Helmholtz free energy and the derivative properties. The results were almost similar for the two theories with different temperatures and compositions. Kontogeorgis et al., (2018) investigated this matter more deeply and provided some questions with some answers related to electrolyte modeling. They think that electrolyte modeling is difficult topics and that the Debye-Huckel model full version can work fines compared to the mean spherical approximation (Kontogeorgis, Maribo-Mogensen, and Thomsen 2018).

The activity coefficients for the non-electrolyte components were calculated from modified DH and they used as correction factor for the liquid phase in the gas solubility calculation following equation (2.1-8).**Error! Reference source not found.** The optimization of the gas solubility was performed first to determine the interaction coefficient between the non-electrolyte and the electrolyte (h_{iS}). The optimization of these coefficients was done manually with initial guess taken from the original work of the model (Aasberg-Petersen et al. 1991). The binary interaction parameters (k_{ij}) which describe the interaction between the non-electrolyte components in the system were taken from Waseem and Alsaifi work (Waseem & Alsaifi, 2018).

5.3 Results and Discussion

The model was able to predict the solubility of different gases in different electrolyte aqueous solution with excellent accuracy. Methane solubility was predicted in presence of different salts (NaCl, KCl and CaCl₂), at different temperatures and different concentrations. From Figure 5-1, the solubility of methane decreases with increasing of salt concentration. This can be attributed to the fact that the salt will dissociate into ions which will have an interaction with both components in the system (water and methane). Due to the nature of water molecule, ions will have stronger interactions with water compared to their interactions with methane which will make the methane implicitly less soluble in the solution. This phenomenon known as the salting out which can be defined the reduction in the solute solubility (methane in this case) at high concentration of salt while the reverse process called salting in (Kim et al. 2016). Back to the model, it was able to capture the effect of salting out of different salts and at different temperatures as shown from Figure 5-1 to Figure 5-3. The highest average absolute deviation percent for methane solubility in sodium chloride solution was 2.59% which is excellent for manual optimization. Also, the model has an excellent prediction of the effect of Potassium chloride on the methane solubility as shown from Figure 5-4 to Figure 5-6. The model was able to predict the behavior of the methane solubility with reasonable accuracy in potassium chloride solution as the maximum average absolute deviation percent was 3.14%. The deviation increases as the temperature increase due to the effect of temperature on the predictability of the model. The divalent salt (represented by calcium chloride) was also examined by the model. The model gave acceptable accuracy compared to the experimental data as shown in Figure 5-7 for different temperatures. There was an apparent

deviation in the highest temperature ($T = 398 \text{ K}$) was average absolute deviation percent of 4.63% which is acceptable compared to the literature with this number of fitting parameters. The carbon dioxide (CO_2) solubility was investigated by the model as well for sodium chloride solution and calcium chloride solutions. The carbon dioxide solubility in a solvent such as water is significant due to its many applications (Jiang et al. 2016; Najafloo et al. 2015). Therefore, the model was assessed by predicting its solubility in different electrolyte solutions. As shown in Figure 5-8, the model accurately predicts the solubility of the CO_2 with an average absolute deviation percent of 1.33% and 0.67%. Also, the solubility of CO_2 in the calcium chloride solution was predicted with a maximum average absolute deviation percent of 1.54% which is shown in Figure 5-9. The physical picture of the effect of the salt on the solubility of the CO_2 as salting out or salting in remain incomprehensible especially at the molecular level (Zhang et al. 2017). There are many factors such as temperature, the salt concentration and ion size could affect the CO_2 solubility (Docherty et al. 2007). The salting out effect of the sodium chloride and the calcium chloride can be explained as the following: the availability of the ions in the solution strength the hydrogen bond between the water molecules which will increase the non-polarity of the CO_2 in the solution compared to the pure water (Zhang et al. 2017).

Table 5-1 summarizes the optimized interaction parameters for each system, the average absolute deviation percent of the model compared to the experimental data and the reference of the experimental data used in the comparison.

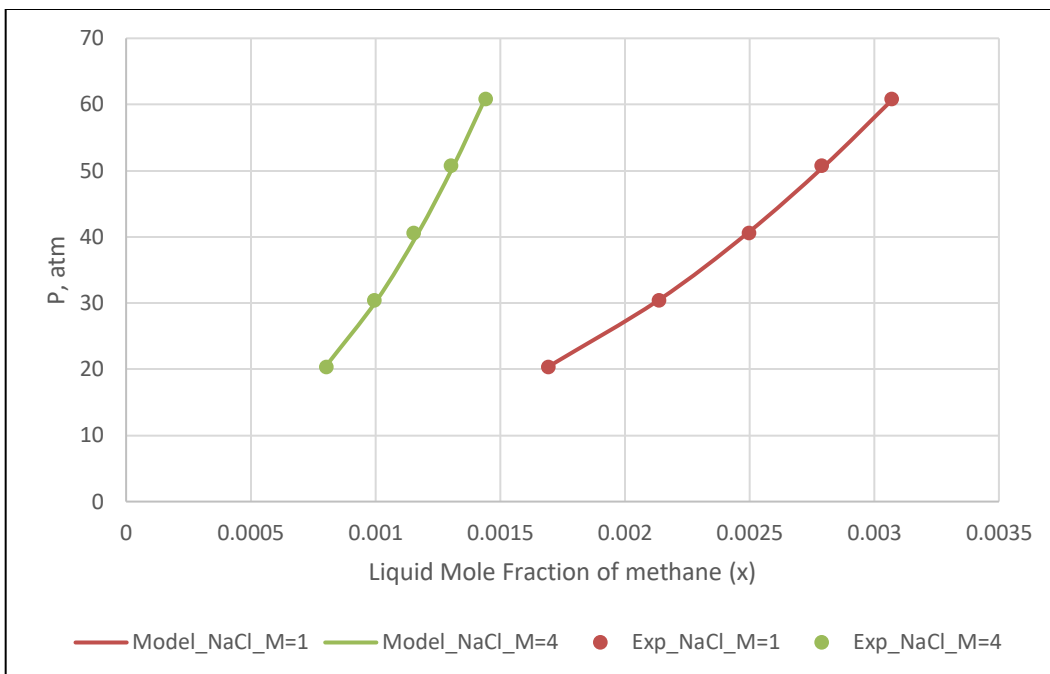


Figure 5-1: Comparison between the Experimental Results and SAFT-VR Mie EOS for the Solubility of Methane in NaCl Solution at concentrations of 1 M and 4 M @ 324.65 K

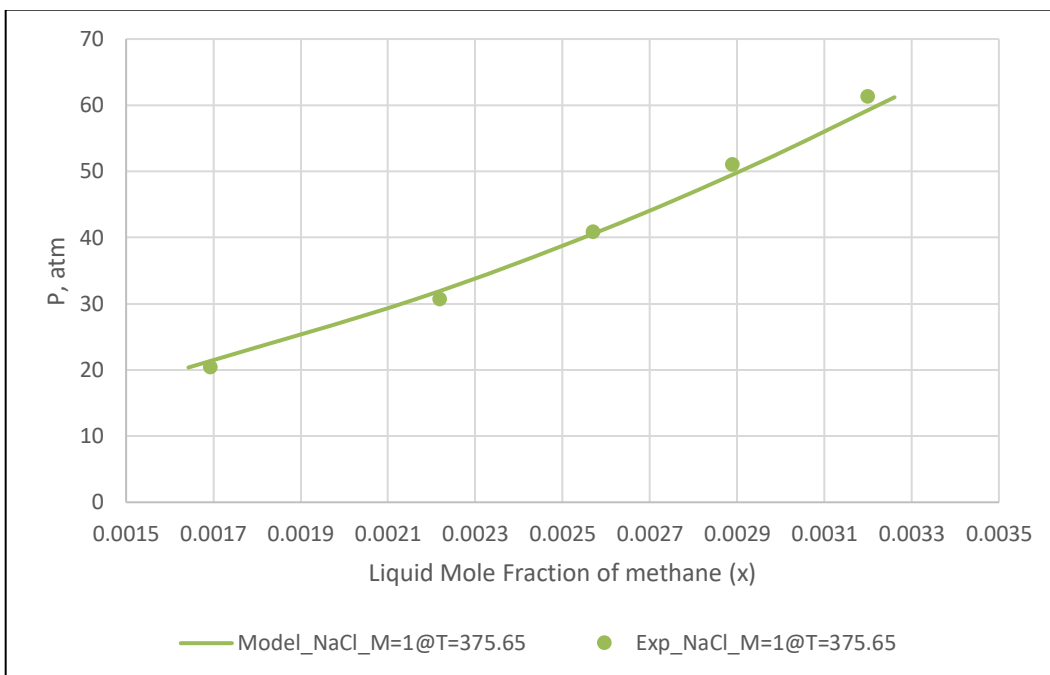


Figure 5-2: Comparison between the Experimental Results and SAFT-VR Mie EOS for Solubility of Methane in NaCl Solution at concentrations of 1 M @ 275.65 K

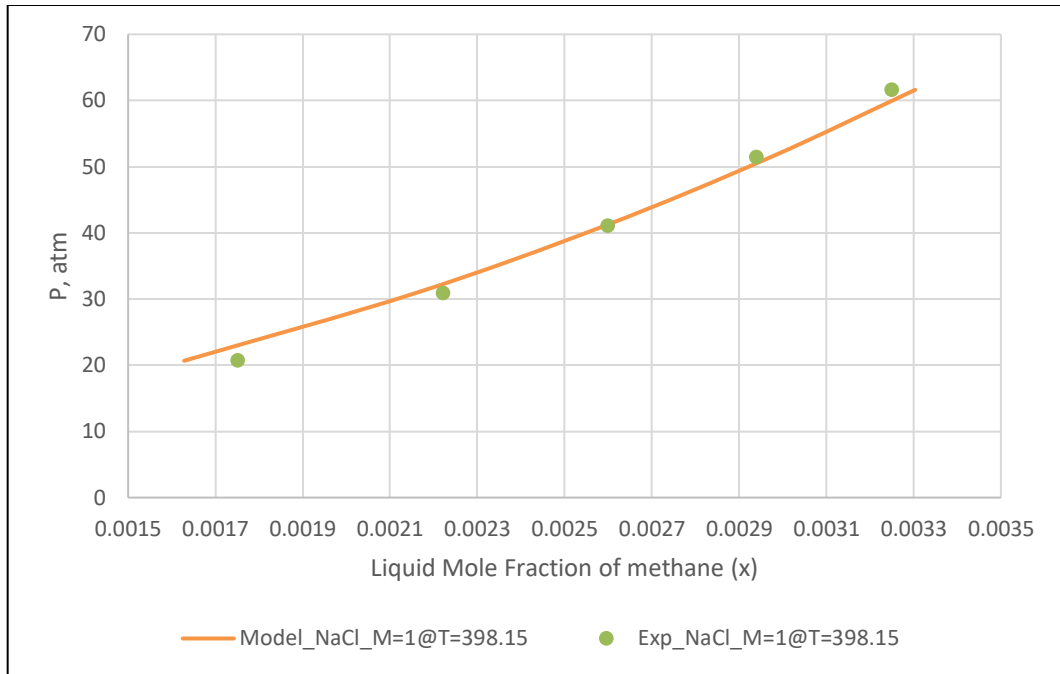


Figure 5-3: Comparison between the Experimental Results and SAFT-VR Mie EOS for the Solubility of Methane in NaCl Solution at concentrations of 1 M @ 398.15 K

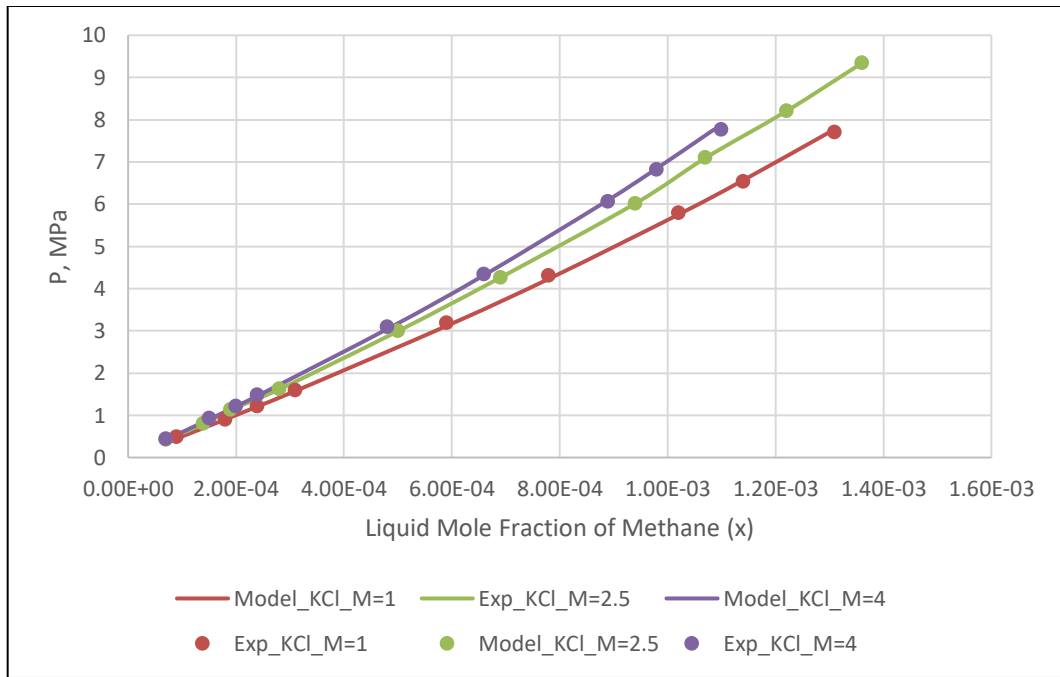


Figure 5-4: Comparison between the Experimental Results and SAFT-VR Mie EOS for Solubility of Methane in KCl Solution at concentrations of 1 M, 2.5 and 4 M @ 313.15

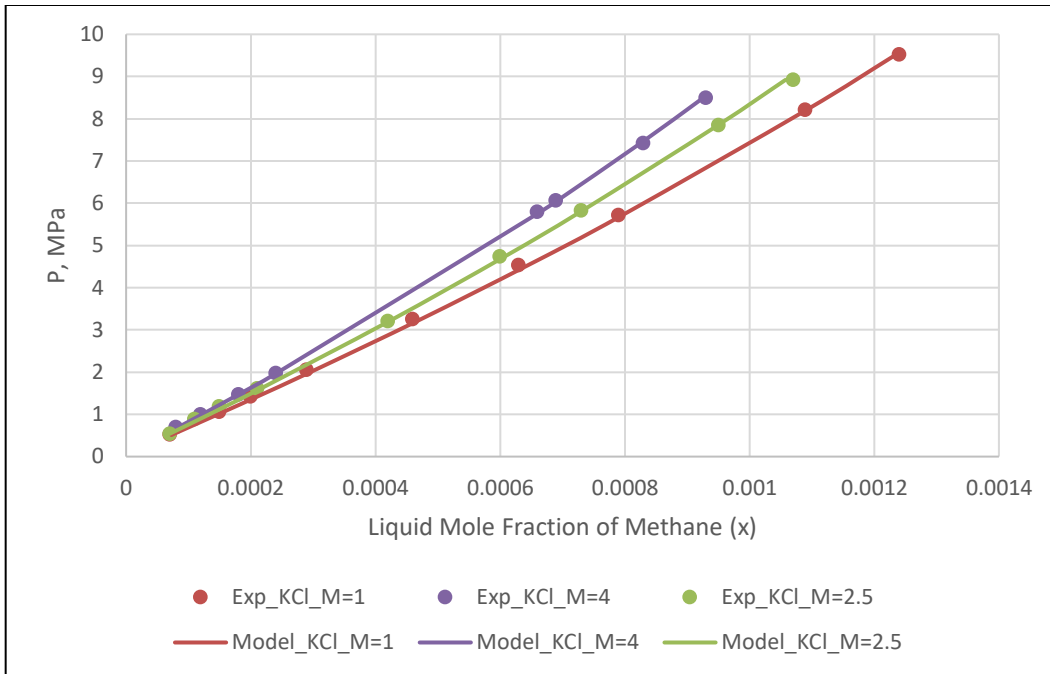


Figure 5-5: Comparison between the Experimental Results and SAFT-VR Mie EOS for Solubility of Methane in KCl Solution at concentrations of 1 M, 2.5 and 4 M @ 353.29

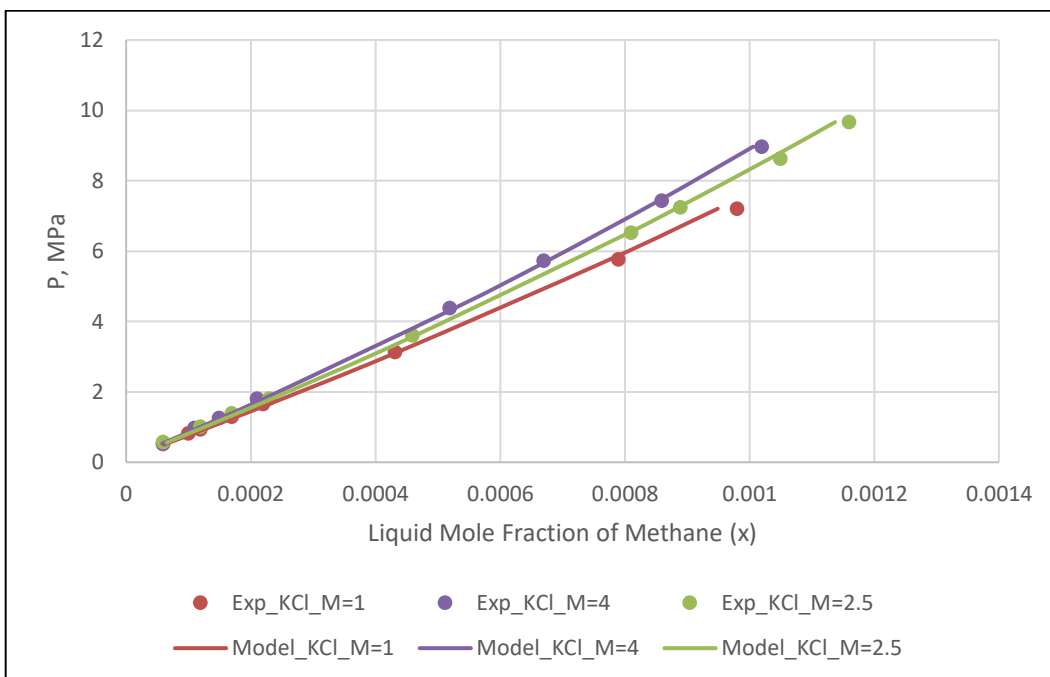


Figure 5-6: Comparison between the Experimental Results and SAFT-VR Mie EOS for the Solubility of Methane in KCl Solution at concentrations of 1 M, 2.5 and 4 M @ 373.17

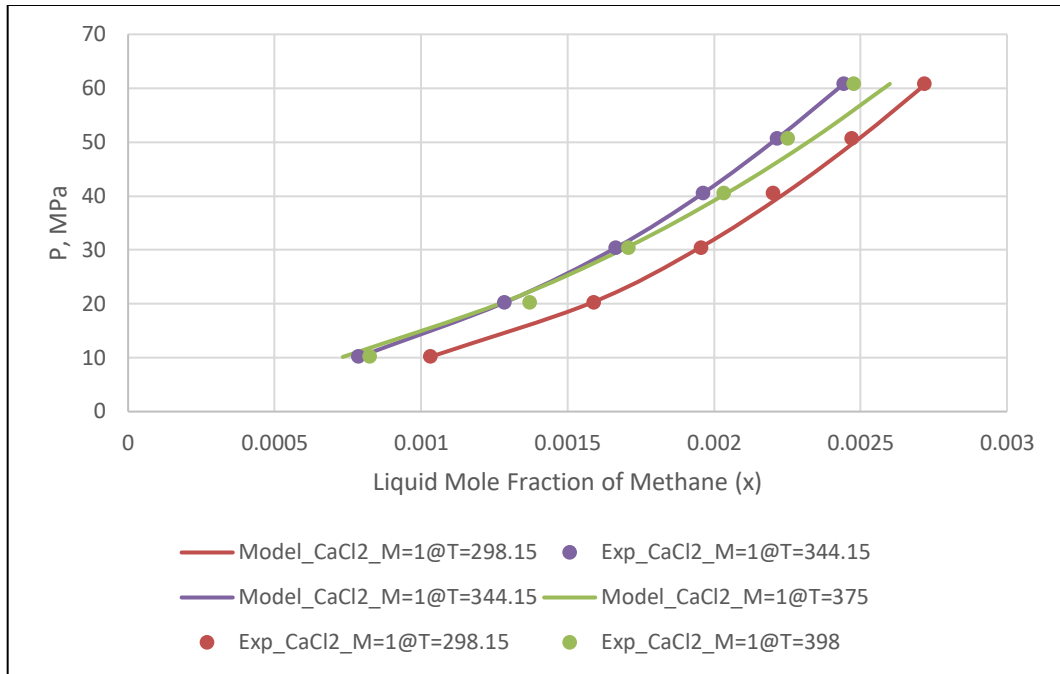


Figure 5-7: Comparison between the Experimental Results and SAFT-VR Mie EOS for the Solubility of Methane in CaCl₂ Solution at concentration of 1 M @ 298.15 K, 344.15 K and 398 K

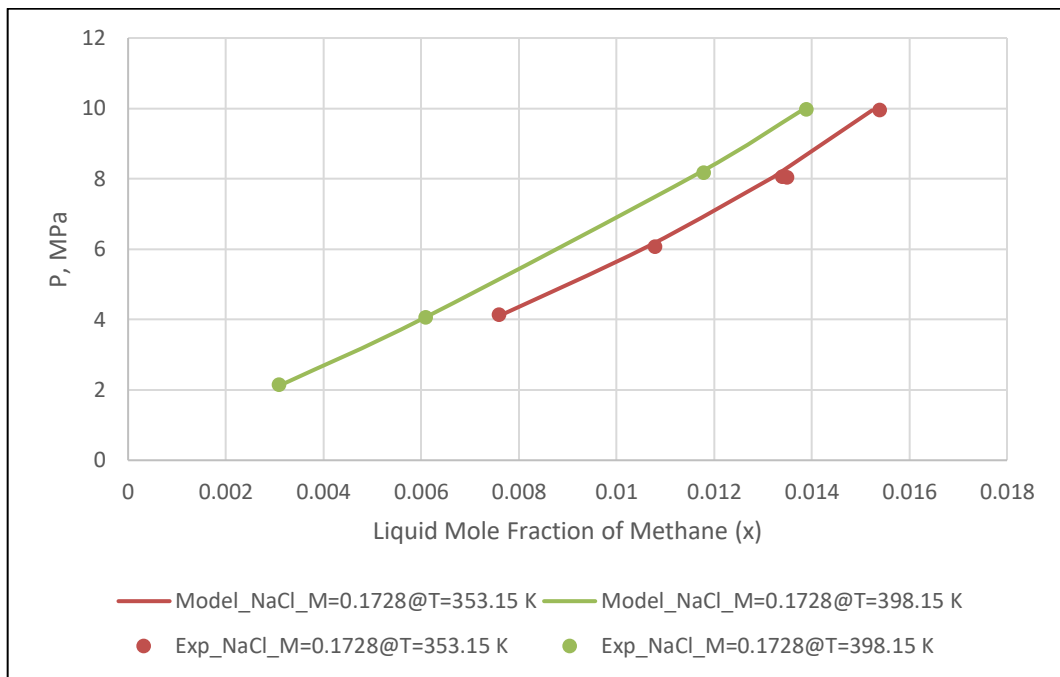


Figure 5-8: Comparison between the Experimental Results and SAFT-VR Mie EOS for the Solubility of Carbon Dioxide in NaCl Solution at concentration of 1 M @ 353.15 K and 398 K

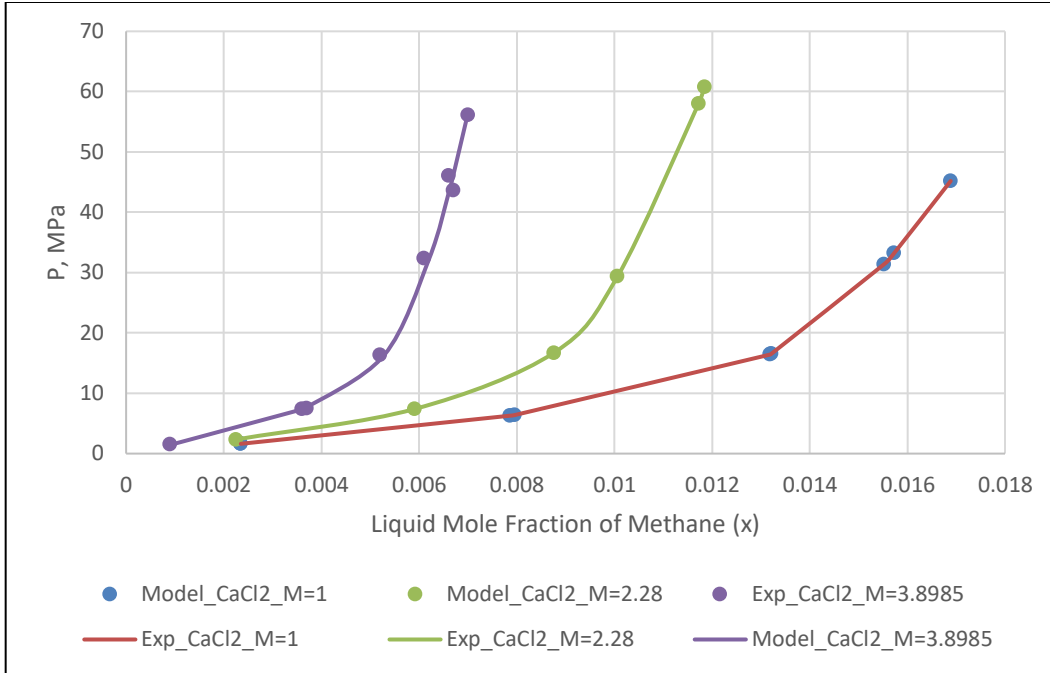


Figure 5-9: Comparison between the Experimental Results and SAFT-VR Mie EOS for the Solubility of Carbon Dioxide in CaCl₂ Solution at concentrations of 1 M, 2.28 M and 3.89 M @ 349 K

Table 5-1: The Component, Salt, Condition, Optimized Interaction Parameters used, the Average Absolute Deviation Percent of the Model and the Experimental Data used in the Optimization and Comparison Process

Component	Salt	Conditions		Optimized interaction coefficients				AAD %	Experimental data		
		T, K	Molality of the salt	k_{ij}^v	k_{ij}^l	h_{ws}	h_{gs}		Number of data point	Reference	
C ₁	NaCl	324.12	1	-0.078	-0.017	-7.85	182	0.289	5	(O'Sullivan and Smith 1970)	
			4				118.9	0.354	5		
		370.12	1				-7.85	370	1.926		5
		398.15	1				-7.85	438	2.595		5
C ₁	KCl	313.15	1	-0.078	-0.017	-7.85	110	1.616	10	(Kiepe et al. 2003)	
			2.5				57	2.041	10		
			4				42	1.421	10		
		353.29	1				227	2.504	9		
			2.5				103	2.050	9		
			4				74	1.140	8		
		373.17	1				270	3.141	8		
			2.5				117	2.738	9		
			4				80.5	2.254	8		
C ₁	CaCl ₂	298	1	-0.078	-0.017	-7.85	72	0.618	6	(Blanco C. and Smith 1978)	
		344					122.5	0.227	6		
		398					148	4.633	6		
CO ₂	NaCl	353.15	0.1728	-0.078	-0.017	-7.85	30	1.334	4	(Nighswander, Kalogerakis, and Mehrotra 1989)	
		398.15	0.1728	-0.078	-0.017	-7.85	55	0.671	4		
	CaCl ₂	349	1	-0.078	-0.017	-7.85	30	3.68	9		
			2.28				34	1.271	6		
			3.8985				37	1.542	8		

CHAPTER 6

GAS HYDRATE IN THE PRESENCE OF

ELECTROLYTE

6.1 Introduction

The electrolyte impact on gas hydrate incipient conditions cannot be ignored. These electrolyte compounds could inhibit the hydrate formation by shifting the pressure-temperature curve to higher pressure and lower temperature which is vital to identify. This chapter highlights the effect of electrolyte formation conditions of gas hydrate using the modified Debye-Huckel Model and the modifications needed to account for the salt in the hydrate system will be presented in the methodology section. The result and discussion section concludes this chapter by assessing the model ability in predicting the electrolyte effect on the formation conditions of different gases.

6.2 Methodology

As was mentioned in Chapter 5, the Modified DH is considered to be similar to the primitive MSA and it will be used to quantify the electrolyte effect on the formation condition of gas hydrate. These salts were accounted for by several modifications in the calculation methodology that was discussed in Chapter 5. The first modification is in calculating the chemical potential difference between water in the empty hydrate lattice and that in the liquid water as shown in equation (2.3-9) to include the effect of the salt as the following (Sun and Duan 2007):

$$\frac{\Delta\mu_w^L(T, P)}{RT} = \frac{\Delta\mu_w(T_0, P_0)}{RT_0} - \int_{T_0}^T \frac{\Delta h_w^L(T)}{RT^2} dT + \int_{P_0}^P \frac{\Delta v_w^L(T)}{RT} dP - \text{LN}(x_w \gamma_w) \quad (6.2-1)$$

Where all the terms defined previously in Chapter 2.3. The last term accounts for the solubility of a gas in the liquid phase which can be significant when the pressure exceeds 10 MPa (Waseem & Alsaifi, 2018). Also, the activity coefficients for the system components were calculated from modified DH then used as a correction factor for the liquid phase in equation (2.3-13) to become the following:

$$f_i^V = \gamma_i f_i^L = f_i^H \quad (6.2-2)$$

The binary interaction parameters (k_{ij}) were taken from the gas solubility chapter for each system (Chapter 5) and used in the calculation of gas hydrate for the same system. For the

salt interaction coefficient with system component, they were optimized by using the values that were obtained in the gas solubility chapter as initial guess using the following objective function:

$$\text{MIN } F_{obj} = \sum_o \left(\frac{\omega_o}{n_{p,o}} \sum_j^{n_{p,o}} \left[\frac{P_{o,j}^{exp} - P_{o,j}^{calc}}{P_{o,j}^{exp}} \right]^2 \right) \quad (6.2-3)$$

where F_{obj} , ω_o , $n_{p,o}$, $P_{o,j}^{exp}$ and $P_{o,j}^{calc}$ are the objective output, the weight given for each property o , the number of data points, the experiment value of the formation pressure and the calculated value of the formation pressure.

While the absolute average deviation percent (%AAD) was calculated to evaluate the model accuracy as the following:

$$\%AAD = \frac{100}{n_{p,o}} \sum_o \left| \frac{P_{o,j}^{exp} - P_{o,j}^{calc}}{P_{o,j}^{exp}} \right| \quad (6.2-4)$$

6.3 Results and Discussion

For methane gas hydrate, the model was able to capture the pure methane and the inhibition of different salts with different concentrations as shown from Figure 6-1 to Figure 6-3.

Sodium Chloride effect on the formation conditions of methane hydrate was predicted with excellent accuracy as shown in Figure 6-1. The increase of the salt concentration effect was captured which can be identified by more inhibition. For potassium chloride, its inhibition effect was predicted with satisfactory results compared to the experimental data. As shown in Figure 6.3-5, there is a slight deviation in the prediction which can be attributed to the fact that the binary interaction coefficient (k_{ij}) that was used from the gas solubility for temperature ($T_{ave} = 346$ k) out from the gas hydrate calculation range (271-285). In addition, the calcium chloride is the divalent salt which was modeled with reasonable accuracy compared to the experimental data as shown in Figure 6-3. The calcium chloride inhibition effect was captured with percent absolute deviation of 2.9% which is acceptable compared to other models in literature where an excess number of fitting parameters were used.

The ethane hydrate formation conditions were captured as well with excellent accuracy compared to the experimental data as shown from Figure 6-4 to Figure 6-6. The inhibition effect of the sodium chloride, the potassium chloride and the calcium chloride were all captured with good accuracy. The highest average absolute deviation percent of the ethane was 3.04% for the calcium chloride with a concentration of 0.474 M

Carbon dioxide hydrate was modeled with satisfactory accuracy even though carbon dioxide has very high solubility which makes it more difficult compared to the other gases. The formation conditions of carbon dioxide hydrate in pure water were modeled with an average absolute deviation percent of 1.849% as shown in Figure 6-7. Also, the effect of sodium chloride was predicted well by the model as shown in Figure 6-7. As the concentration of the salt increases, the deviation increases which seems one of the limitations of the model. For the potassium chloride case, the model took the change of adding the salt

by shifting the curve as expected. The average absolute deviation percent was 1.78%. The same can be said for the calcium chloride inhibition effect as the model predicted effect with excellent accuracy.

For propane gas which forms structure II, the model was able to predict the gas hydrate formation conditions with good accuracy as shown in Figure 6-10. The inhibition effect, also, was captured for the different salts with reasonable accuracy as shown from Figure 6-10 to Figure 6-12.

An explicit limitation of the model is the ability to capture the effect of high concentration of the salt on the hydrate formation accurately which could be due to the ion pairing (ion association) in the system. Fitting more parameters would solve this issue but this will make the model lose its physical representation. The ions effect can be attributed to different points; the ions decrease the solubility of the gas inside the liquid phase (as shown in Chapter 6) which will reduce the amount of solid formed. Also, the ion adoration to the solid hydrate formed will affect the formation and dissociation process.

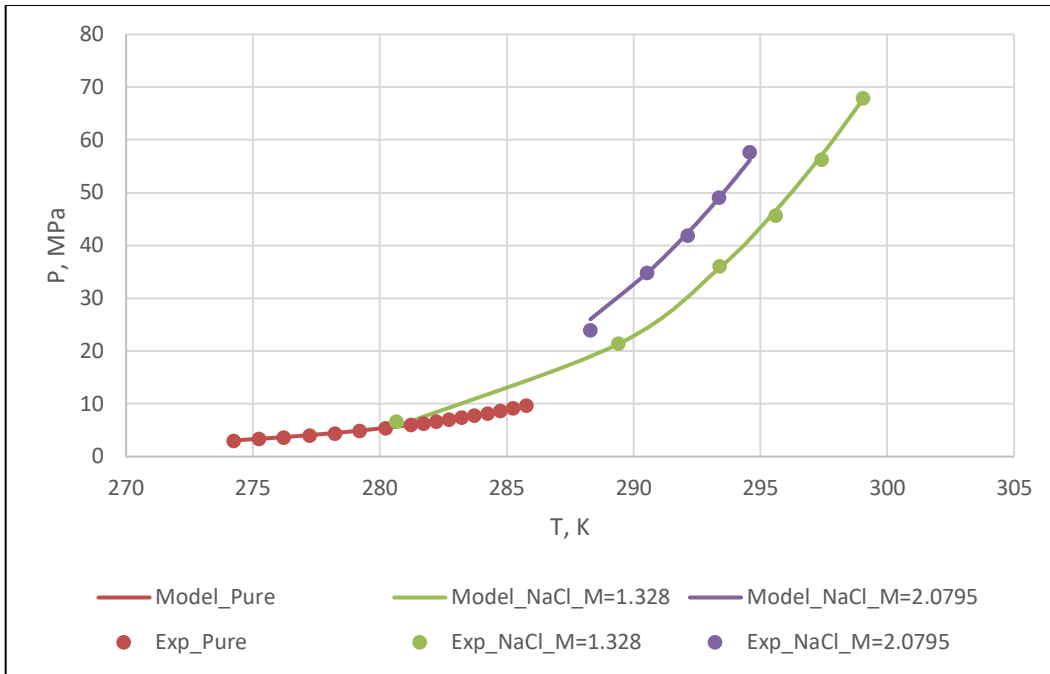


Figure 6-1: Comparison between the Experimental Results and SAFT-VR Mie EOS with MDH Model for the Methane Gas Hydrate in Pure Water and NaCl Solution at concentration of 1.328 M and 2.0795

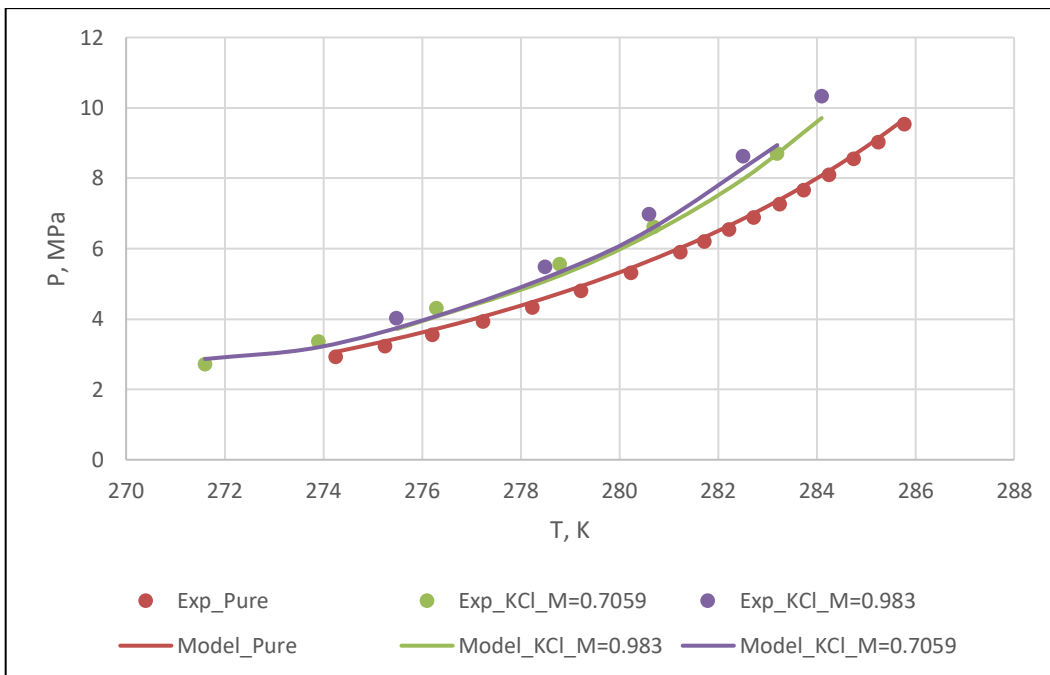


Figure 6-2: Comparison between the Experimental Results and SAFT-VR Mie EOS with MDH Model for the Methane Gas Hydrate in Pure Water and NaCl Solution at concentration of 1.328 M and 2.0795

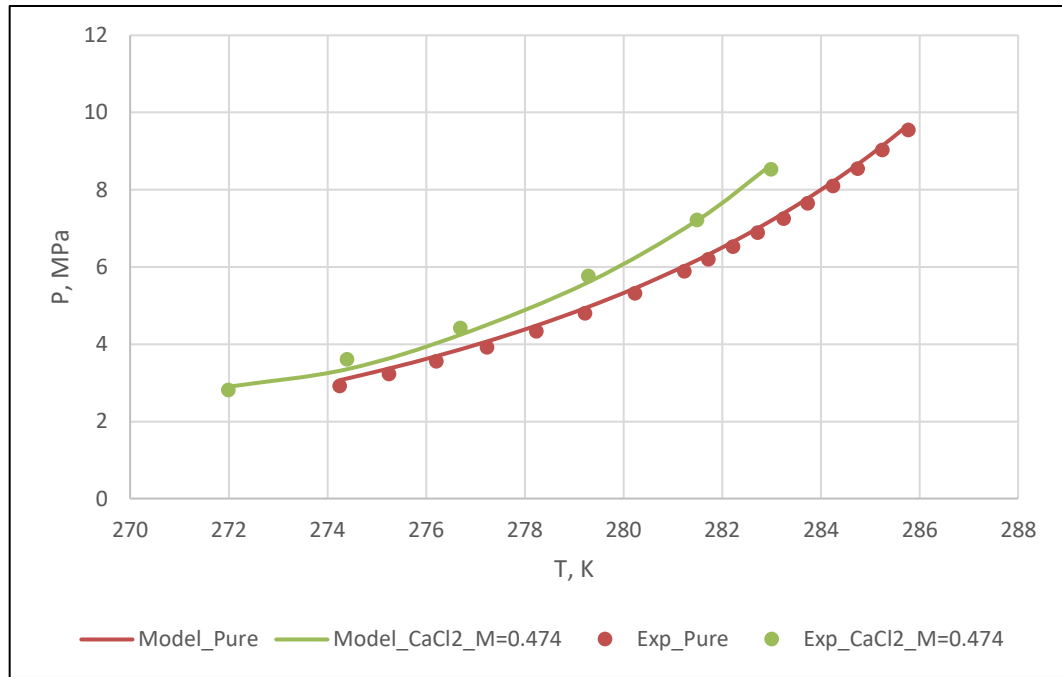


Figure 6-3: Comparison between the Experimental Results and SAFT-VR Mie EOS with MDH Model for the Methane Gas Hydrate in Pure Water and CaCl₂ Solution at concentration of 0.474 M

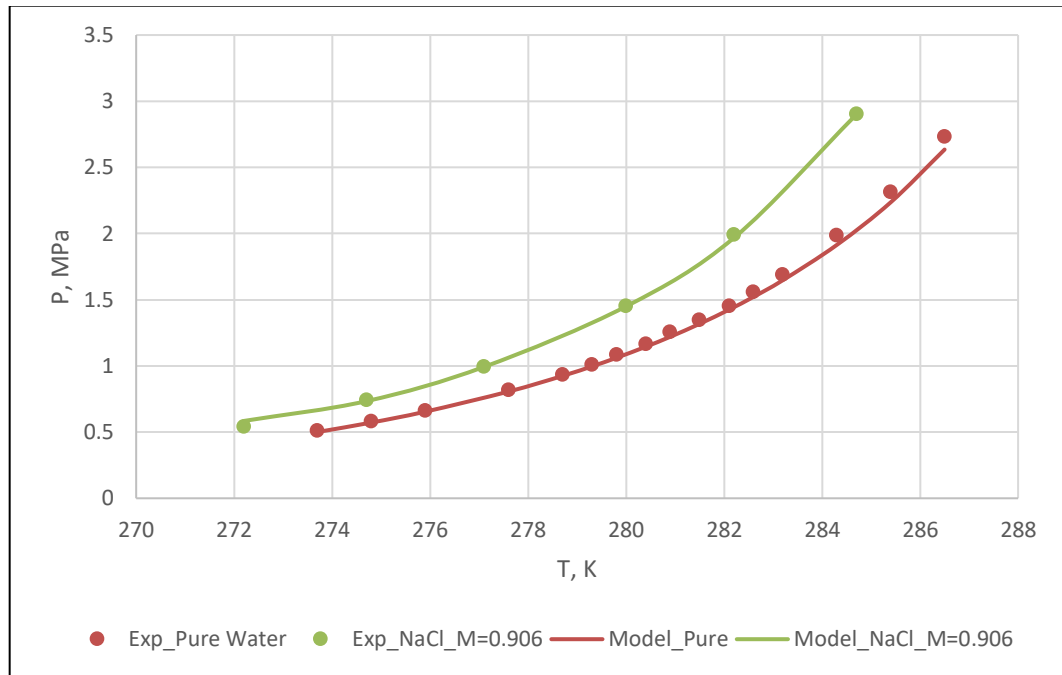


Figure 6-4: Comparison between the Experimental Results and SAFT-VR Mie EOS with MDH Model for the Ethane Gas Hydrate in Pure Water and NaCl Solution at concentration of 0.906 M

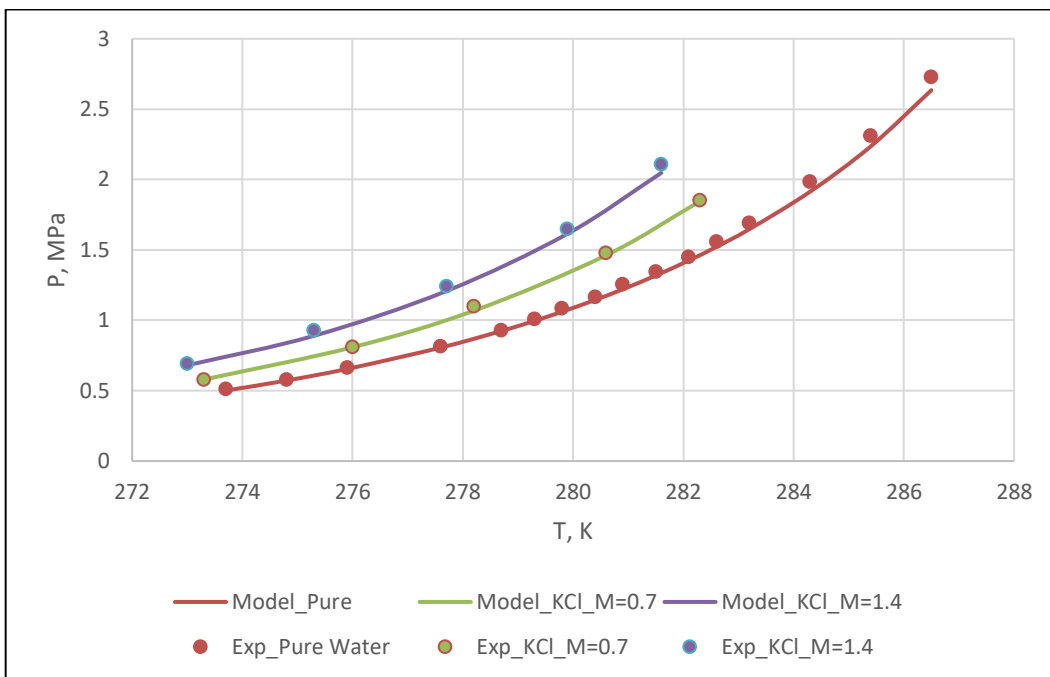


Figure 6-5: Comparison between the Experimental Results and SAFT-VR Mie EOS with MDH Model for the Ethane Gas Hydrate in Pure Water and KCl Solution at concentration of 0.7 M and 1.4 M

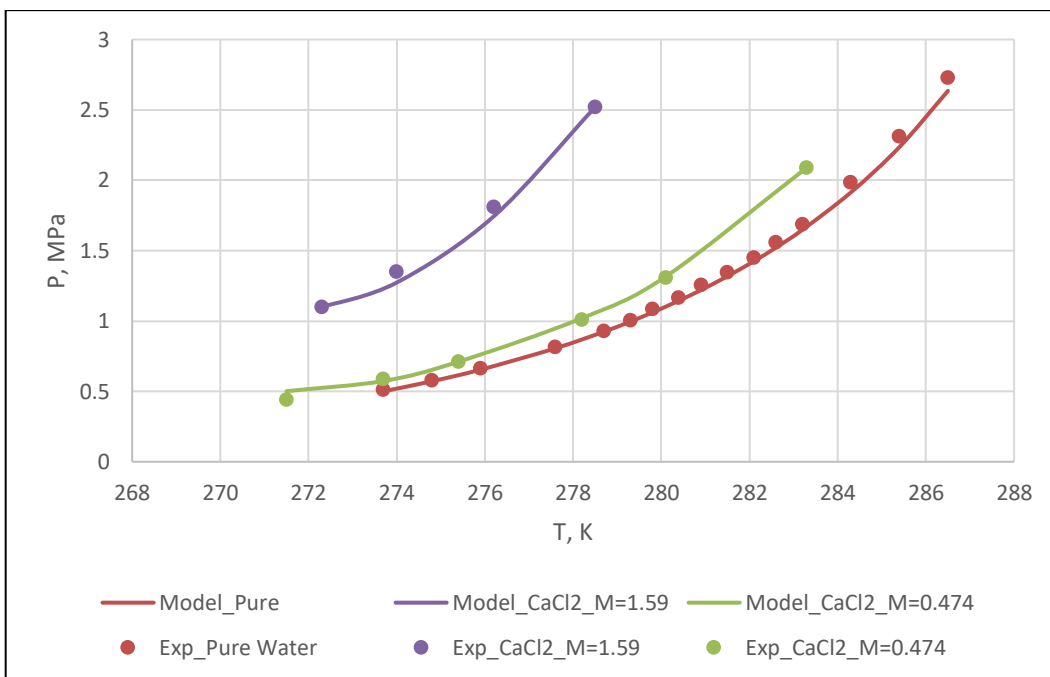


Figure 6-6: Comparison between the Experimental Results and SAFT-VR Mie EOS with MDH Model for the Ethane Gas Hydrate in Pure Water and CaCl₂ Solution at concentration of 0.474 M and 1.59 M

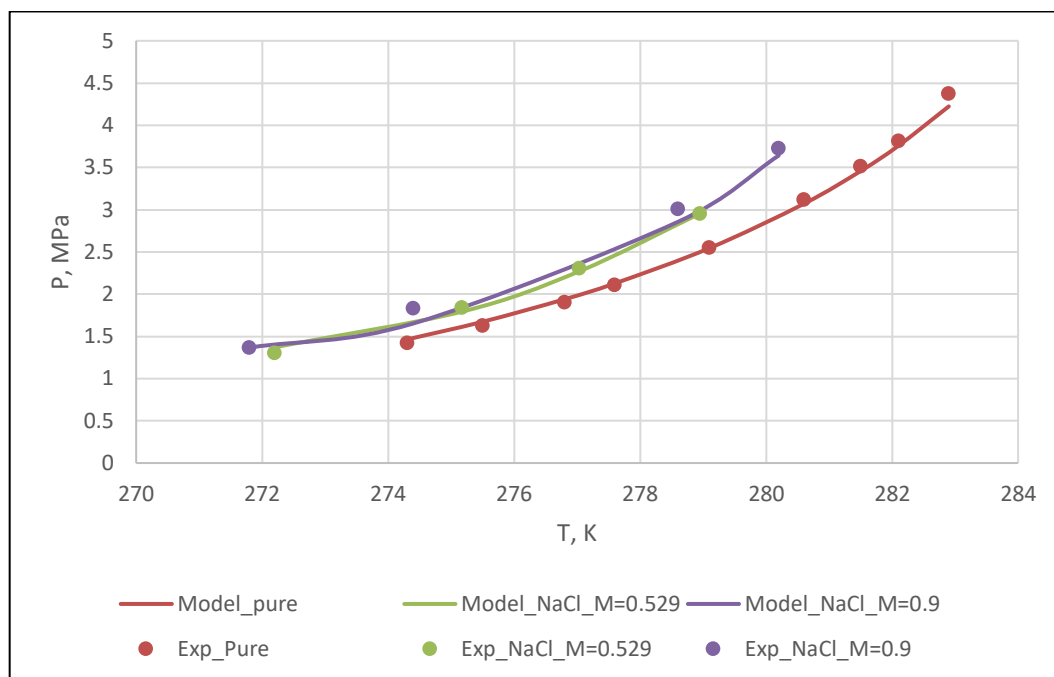


Figure 6-7: Comparison between the Experimental Results and SAFT-VR Mie EOS with MDH Model for the Carbon Dioxide Gas Hydrate in Pure Water and NaCl Solution at concentration of 0.529 M and 0.9 M

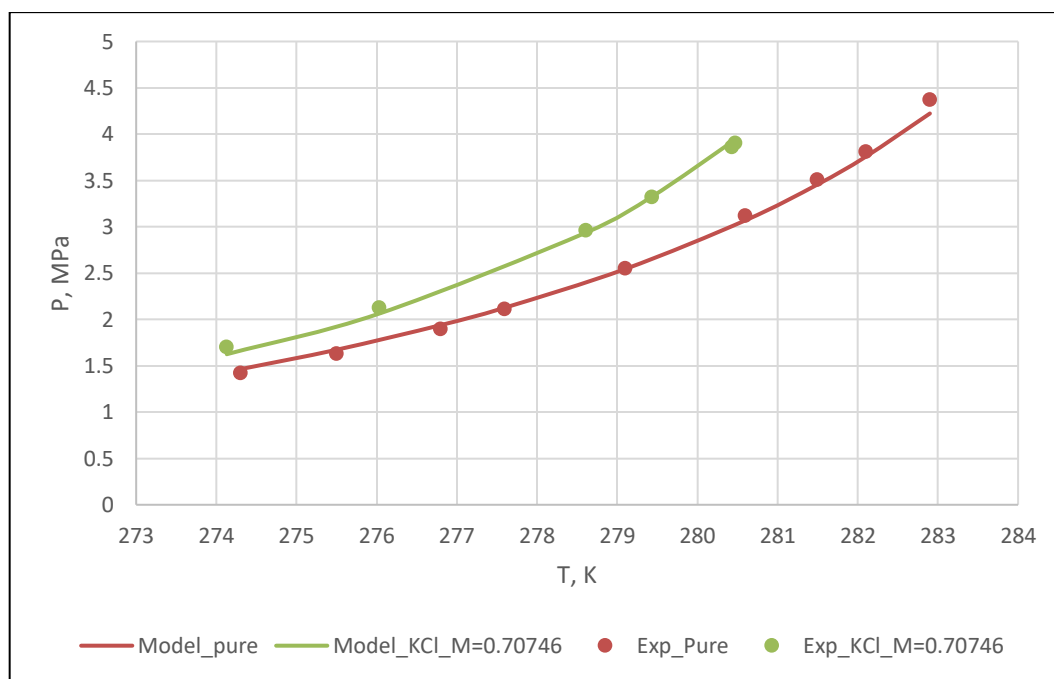


Figure 6-8: Comparison between the Experimental Results and SAFT-VR Mie EOS with MDH Model for the Carbon Dioxide Gas Hydrate in Pure Water and KCl Solution at concentration of 0.70746 M

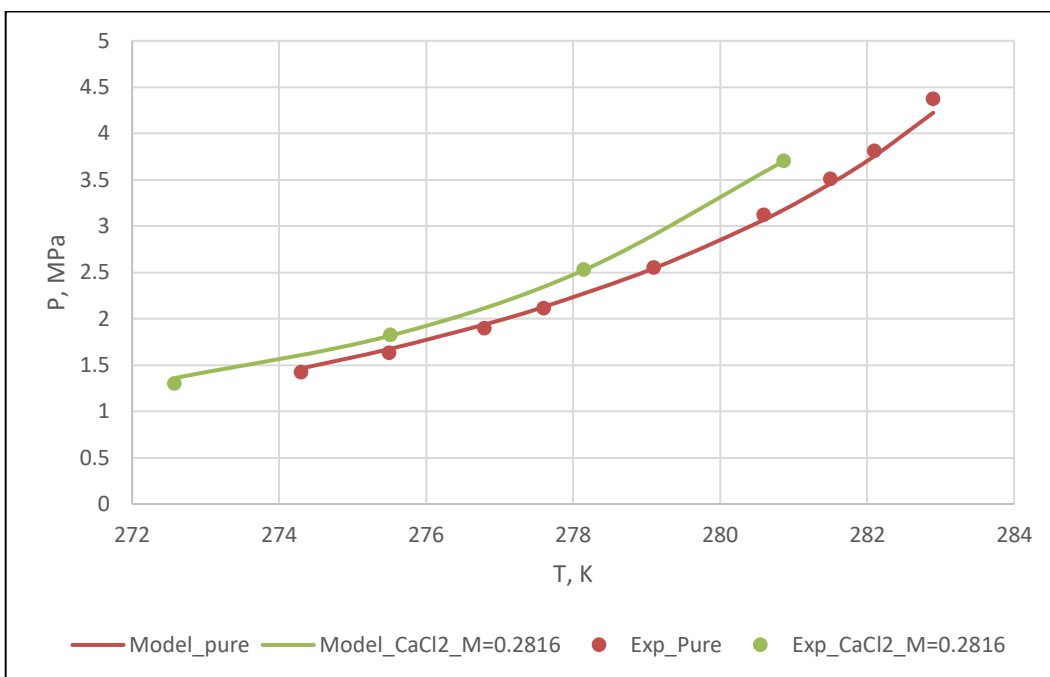


Figure 6-9: Comparison between the Experimental Results and SAFT-VR Mie EOS with MDH Model for the Carbon Dioxide Gas Hydrate in Pure Water and CaCl₂ Solution at concentration of 0.2816 M

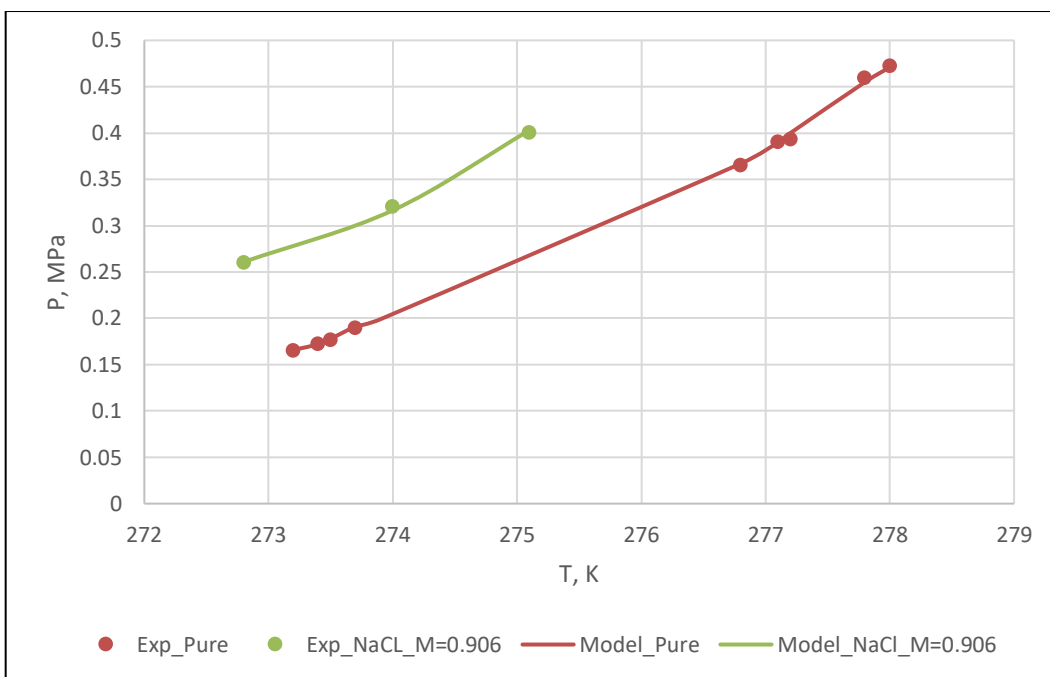


Figure 6-10: Comparison between the Experimental Results and SAFT-VR Mie EOS with MDH Model for the Propane Gas Hydrate in Pure Water and NaCl Solution at concentration of 0.906 M

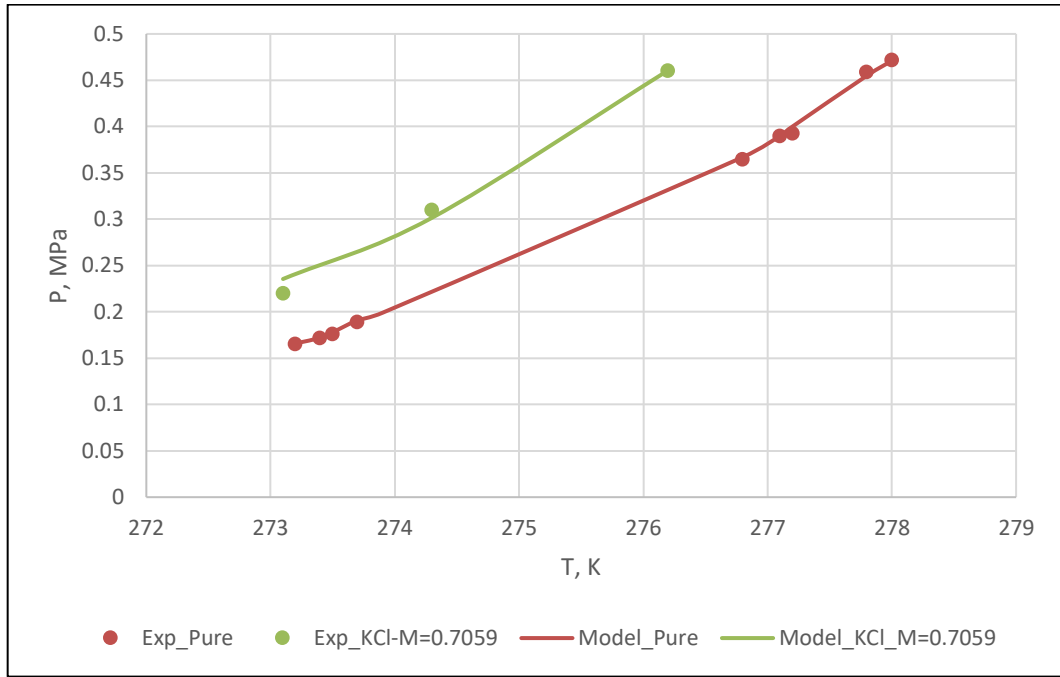


Figure 6-11: Comparison between the Experimental Results and SAFT-VR Mie EOS with MDH Model for the Propane Gas Hydrate in Pure Water and KCl Solution at concentration of 0.7059 M

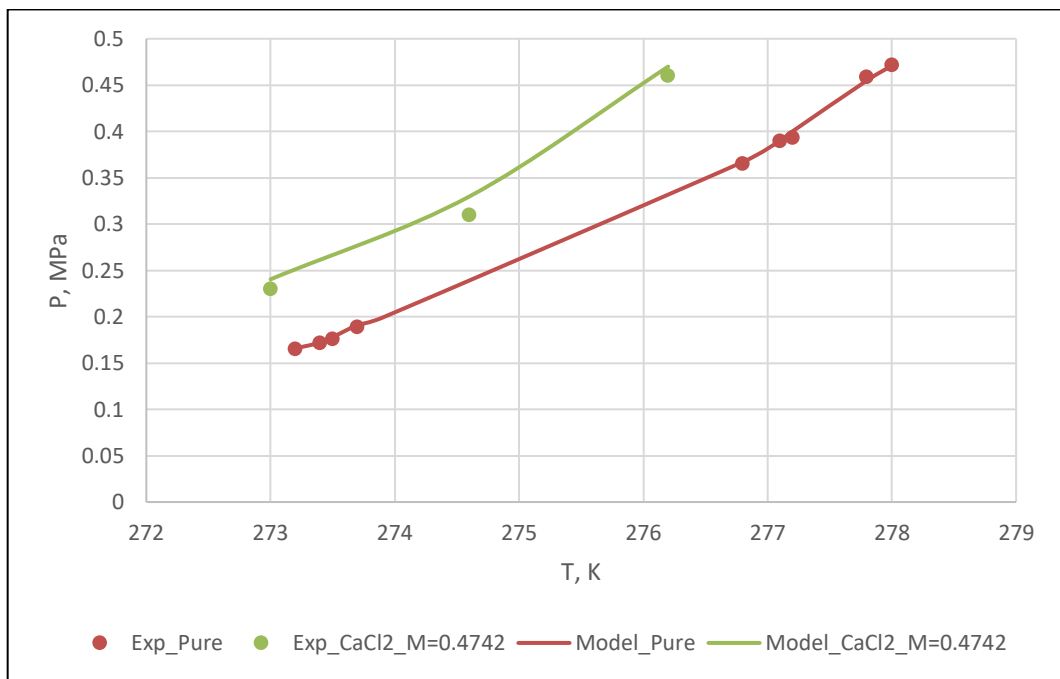


Figure 6-12: Comparison between the Experimental Results and SAFT-VR Mie EOS with MDH Model for the Propane Gas Hydrate in Pure Water and CaCl₂ Solution at concentration of 0.7059 M

Table 6-1: The Gas Hydrate Former, Salt, Condition, Optimized Interaction Parameters used, the Average Absolute Deviation Percent of the Model and the Experimental Data used in the Optimization and Comparison Process

Gas Hydrate Former	Salt	Conditions		Optimized Interactions Coefficients		AAD%	Experimental data	
		Temperature Range, K	Molality of the salt	h_{ws}	h_{gs}		Number of data point	References
C ₁	---	274.25-285.78	---	---	---	2.7101	17	(Nakamura et al. 2003)
	NaCl	280.66-299.06	1.328	-6.350	0.699	3.023	6	(Jager and Sloan 2001)
		288.3-294.58	2.0795	-8.004	-9.343	2.694	5	
	KCl	273.9-283.2	0.7059	-1849.6	-231.9	3.2848	5	(Mohammadi, Afzal, and Richon 2008a)
		275.49-282.51	0.983	-2168.5	-139.6		4	(Cha, Hu, and Sum 2016)
CaCl ₂	274.4-283	0.474	-1088.2	-101.3	2.9486	5	(Mohammadi, Afzal, and Richon 2008b)	
C ₂	---	273.7-286.5	---	---	---	2.011	16	(Deaton and Frost 1946)
	NaCl	272.2-284.7	0.906	-7.8625	-349.463	1.7467	6	(Mohammadi et al. 2008b)
	KCl	273.3-282.3	0.7	-7.7652	-419.148	0.945	5	
		273-281.6	1.4	-7.6174	-126.855	2.6718	5	
	CaCl ₂	271.5-283.3	0.474	-2.1155	-352.339	3.0405	6	
270-278.5		1.59	-5.3177	-105.351	2.3408	4		
C ₃	---	273.2-278	---	---	---	0.960	9	(Sloan and Koh 2008)
	NaCl	272.5-275.1	0.906	-7.00	4973.6	0.7205	3	(Mohammadi et al. 2008b)
	KCl	272-276.2	0.7059	-6.7139	-198.935	3.295	3	
	CaCl ₂	273-276.2	0.4742	-3.5521	75.9201	4.4214	3	
CO ₂	---	274.3-282.9	---	---	---	1.8490	9	(Adisasmito, Frank, and Sloan 1991)
	NaCl	272.2-278.9	0.529	-140.1	-16.97	2.3383	4	(Dholabhai, Kalogerakis, and Bishnoi 1993)
		271.8-280.2	0.9	-400.2	219.0	4.3356	4	(Mohammadi et al. 2008b)
	KCl	274.13-280.47	0.70746	-817.098	405.8072	1.7836	6	(Dholabhai et al. 1993)
	CaCl ₂	272.58-280.87	0.2816	-535.15	343.039	1.2394	4	

CHAPTER 7

CONCLUSION & RECOMMENDATIONS

7.1 Conclusion

In this thesis work, the effect of electrolyte on gas hydrate formation conditions was assessed using Statistical Associating Fluid Theory – Variable Range using Mie potential (SAFT-VR Mie) coupled with Van der Waals Platuew (VdwP) model and Modified Debye-Huckle (M-DH). The first part of this work focus on the theoretical background for electrolyte and hydrate modeling. Then, an extensive literature review is made for electrolyte modeling and modeling the electrolyte with a gas hydrate system. The electrolyte properties including the mean ionic activity coefficient, osmotic coefficient, and the vapor pressure for different electrolyte systems were predicted using the SAFT-VR Mie coupled with primitive MSA. The formation conditions of different gas hydrate formers were predicted with reasonable accuracy with and without electrolyte in the system.

The SAFT-VR Mie coupled with Primitive MSA gave very good result for different monovalent and divalent electrolyte systems including Lithium Chloride, Lithium Bromide, Lithium Iodide, Sodium Chloride, Sodium Bromide, Sodium Iodide, Potassium Fluoride, Potassium Chloride, Potassium Bromide, Potassium Iodide, Calcium Bromide, Calcium Chloride, Calcium Iodide, Barium Bromide, Barium Chloride. The vapor pressure, the mean ionic activity coefficient (MIAC) and the osmotic coefficient (Φ) were predicted with an excellent match with the experimental data. Only one property either the

MIAC or Φ used in the optimization process for two reasons: to maintain the physical base of the model by avoiding the excess fitting parameters and to have a benchmark property in evaluating the model predictivity capability. The highest absolute average deviation percentage (AAD%) for MIAC is 22.51, 5.47 for the osmotic coefficient and 20.05 for the vapor pressure.

The effect of different electrolytes on gas solubility was also investigated in this thesis work. It was modeled using a modified version of Debye-Huckel which to some extent equivalent to the primitive mean spherical approximation as well with excellent accuracy. The model gave a reasonable prediction for methane and carbon dioxide solubility in different electrolyte solutions including sodium chloride, potassium chloride and calcium chloride at different conditions. The highest average absolute deviation percent was 4.63%

The inhibition of the different salts of the gas hydrate conditions was predicted with excellent accuracy for structure I and structure II gases. These salts were monovalent and divalent salts (sodium chloride, potassium chloride and calcium chloride) with different concentrations. The model was able to capture the inhibition of all the mention salts with a maximum average absolute deviation percent of 4.33%.

7.2 Recommendations and Future Work

There are many versions of SAFT and electrolyte models existing in the literature. Therefore, it will be recommended to investigate more versions and models in modeling electrolyte systems. Also, the effect of ion association at high salt concentration should be considered to improve the model. In addition, comparing the different versions of MSA

(Primitive, semi-primitive, non-primitive) and their impact on the accuracy of the results.

Coupling the result of the molecular dynamics with the different models can enhance the prediction capability of the models.

For the gas hydrate, the modeling of the different inhibitors is an area that needs more investigation. These inhibitors include thermodynamics, kinetic and anti-agglomerate inhibitors. Developing a thermodynamics model that can predict the impact of these inhibitors will have a great value in the gas hydrate researches. In addition, industrial gases which are recognized as non-hydrate former could be examined to see their impact on the gas formers gases in the presence of an electrolyte.

References

- Aasberg-Petersen, Kim, Erling Stenby, and Aage Fredenslund. 1991. "Prediction of High-Pressure Gas Solubilities in Aqueous Mixtures of Electrolytes." *Industrial and Engineering Chemistry Research* 30(9):2180–85.
- Abdoul, W., E. Rauzy, and A. Péneloux. 1991. "Group-Contribution Equation of State for Correlating and Predicting Thermodynamic Properties of Weakly Polar and Non-Associating Mixtures: Binary and Multicomponent Systems." *Fluid Phase Equilibria* 68:47–102.
- Abolala, Mostafa, Maryam Karamoddin, and Farshad Varaminian. 2014. "Thermodynamic Modeling of Phase Equilibrium for Gas Hydrate in Single and Mixed Refrigerants by Using SPC-SAFT Equation of State." *Fluid Phase Equilibria* 370:69–74.
- Adidharma, Hertanto and Maciej Radosz. 1998. "Prototype of an Engineering Equation of State for Heterosegmented." *Industrial & Engineering Chemistry Research* 37(11):4453–62.
- Adisasmito, Sanggono, Robert J. Frank, and E. Dendy Sloan. 1991. "Hydrates of Carbon Dioxide and Methane Mixtures." *Journal of Chemical and Engineering Data* 36(1):68–71.
- Ahmed, Saifuddin. 2015. "The Role of Electrostatic Interactions in the Prediction of Phase Equilibrium of Dme Mixtures Using Saft Eos." King Fahd University of Petroleum & Minerals.
- Ahmed, Saifuddin, Nicolas Ferrando, Jean-Charles De Hemptinne, Jean-Pierre Simonin, Olivier Bernard, and Olivier Baudouin. 2017. "Modeling of Mixed-Solvent Electrolyte Systems." *Fluid Phase Equilibria* (December).
- Ahmed, T. 2007. *Equations of State and PVT Analysis: Applications for Improved Reservoir Modeling*. Elsevier.
- Al-eisa, Rashed M., Mohamed S. Elanany, Khalid A. Al-majnouni, and Ali A. Al-jabran. 2015. "Kinetic Hydrate Inhibitors for Natural Gas Fields : Rational Design and Experimental Development." *SAUDI ARAMCO JOURNAL OF TECHNOLOGY*.
- Al-Joboury, M. I. and D. W. Turner. 1967. "Molecular Photoelectron Spectroscopy. Part VI. Water, Methanol, Methane, and Ethane." *Journal of the Chemical Society B: Physical Organic* 0(0):373.
- Ameripour, S. and M. Barrufet. 2009. "Improved Correlations Predict Hydrate Formation Pressures or Temperatures for Systems with or Without Inhibitors." *Journal of Canadian Petroleum Technology* 48(5):45–50.

- Anderson, B. J., J. W. Tester, G. P. Borghi, and B. L. Trout. 2005. "Properties of Inhibitors of Methane Hydrate Formation via Molecular Dynamics Simulations." *Journal of the American Chemical Society* 127(50):17852–62.
- Anderson, F. E. and J. M. Prausnitz. 1986. "Inhibition of Gas Hydrates by Methanol." *AIChE Journal* 32(8):1321–33.
- Anvari, Monir Hosseini, Gholamreza Pazuki, Saeed Seyfi Kakhki, and Babak Bonakdarpour. 2013. "Application of the SAFT-VR Equation of State in Estimation of Physiochemical Properties of Amino Acid Solutions." *Journal of Molecular Liquids* 184:24–32.
- Atik, Zadjia, Christoph Windmeier, and Lothar R. Oellrich. 2010. "Experimental and Theoretical Study on Gas Hydrate Phase Equilibria in Seawater." *Journal of Chemical & Engineering Data* 55(2):804–7.
- Avlonitis, Dimitrios. 1994. "The Determination of Kihara Potential Parameters from Gas Hydrate Data." *Chemical Engineering Science* 49(8):1161–73.
- B. Klauda, Jeffery and Stanley I. Sandler. 2003. "Phase Behavior of Clathrate Hydrates: A Model for Single and Multiple Gas Component Hydrates." *Chemical Engineering Science* 58(1):27–41.
- Bahadori, A. 2008. "Correlation Accurately Predicts Hydrate Forming Pressure of Pure Components." *Journal of Canadian Petroleum Technology* 47(02).
- Bahadori, A., H. B. Vuthaluru, M. O. Tade, and S. Mokhatab. 2009. "Novel Correlations for Determining Appropriate Mono-Ethylene Glycol Injection Rate to Avoid Gas Hydrate Formation." *Canadian International Petroleum Conference* 1–15.
- Bahadori, Alireza. 2011. "A Simple Mathematical Predictive Tool for Estimation of a Hydrate Inhibitor Injection Rate." *Nafta* 62(7–8):213–23.
- Bahadori, Alireza, S. Mokhatab, and B. Towler. 2008. "Predict Hydrate Formation Conditions for Light Alkanes and Sweet Natural Gases." *Chemical Engineering* 87:65–68.
- Bahadori, Alireza and Hari B. Vuthaluru. 2009. "A Novel Correlation for Estimation of Hydrate Forming Condition of Natural Gases." *Journal of Natural Gas Chemistry* 18(4):453–57.
- Bakker, R. J. 1998. "Improvements in Clathrate Modelling II: The H₂O-CO₂-CH₄-N₂-C₂H₆ Fluid System." *Geological Society, London, Special Publications* 137(1):75–105.
- Ballard, A. L. 2002. "A NON-IDEAL HYDRATE SOLID SOLUTION MODEL FOR A MULTI-PHASE EQUILIBRIA PROGRAM." Colorado School of Mines.
- Ballard, A. L. and E. D. Sloan. 2002. "The Next Generation of Hydrate Prediction: An Overview." *Journal of Supramolecular Chemistry* 2(4–5):385–92.

- Barker, J. A. and D. Henderson. 1967a. "Perturbation Theory and Equation of State for Fluids: The Square-Well Potential." *The Journal of Chemical Physics* 47(8):2856–61.
- Barker, J. A. and D. Henderson. 1967b. "Perturbation Theory and Equation of State for Fluids. II. A Successful Theory of Liquids." *The Journal of Chemical Physics* 47(11):4714–21.
- Berge, B. K. 1986. "Hydrate Predictions on a Microcomputer." in *Petroleum Industry Application of Microcomputers*. Sliver Creek: Society of Petroleum Engineers.
- Blanco C., Luis H. and Norman O. Smith. 1978. "The High Pressure Solubility of Methane in Aqueous Calcium Chloride and Aqueous Tetraethylammonium Bromide. Partial Molar Properties of Dissolved Methane and Nitrogen in Relation to Water Structure." *The Journal of Physical Chemistry* 82(2):186–91.
- Blum, L. 1975. "Mean Spherical Model for Asymmetric Electrolyte 1. Method of Solution." *Molecular Physics* 30(5):1529–35.
- Blum, L. and D. Q. Wei. 1987. "Analytical Solution of the Mean Spherical Approximation for an Arbitrary Mixture of Ions in a Dipolar Solvent." *J. Chem. Phys.* 87(1):555–65.
- van Bochove, G. H. 2003. "Two- and Three-Liquid Phase Equilibria in Industrial Mixed-Solvent Electrolyte Solutions." Technische Universiteit Delft.
- Born, M. 1920. "Volumes and Heats of Hydration of Ions." *Z. Phys.*
- Boublik, Tomas. 1986. "Background Correlation Functions in the Hard Sphere Systems." *Molecular Physics* 59(4):775–93.
- Boublík, Tomáš. 1970. "Hard Sphere Equation of State." 471:6–8.
- Branscomb, Lewis M. 1966. "Photodetachment Cross Section, Electron Affinity, and Structure of the Negative Hydroxyl Ion." *Physical Review* 148(1):11–18.
- Cameretti, Luca F., Gabriele Sadowski, and Jørgen Mollerup. 2005. "Modeling of Aqueous Electrolyte Solutions with Perturbed-Chain Statistical Associated Fluid Theory." *Industrial & Engineering Chemistry Research* 44(9):3355–62.
- Carnahan, Norman F. and Kenneth E. Starling. 1972. "Intermolecular Repulsions and the Equation of State for Fluids." *AIChE Journal* 18(6):1184–89.
- Carroll, John. 2003. *Natural Gas Hydrates*. Gulf Professional Publishing.
- Carson, Don B. and D. L. Katz. 1941. "Natural Gas Hydrates." *Transactions of the AIME* 146:150–58.
- Carvalho, Pedro J., Luís M. C. Pereira, Neusa P. F. Gonçalves, António J. Queimada, and João A. P. Coutinho. 2015. "Carbon Dioxide Solubility in Aqueous Solutions of NaCl: Measurements and Modeling with Electrolyte Equations of State." *Fluid*

Phase Equilibria 388:100–106.

- Cha, Minjun, Yue Hu, and Amadeu K. Sum. 2016. “Methane Hydrate Phase Equilibria for Systems Containing NaCl, KCl, and NH₄Cl.” *Fluid Phase Equilibria* 413:2–9.
- Chapman, Walter G., Keith E. Gubbins, George Jackson, and Maciej Radosz. 1990. “New Reference Equation of State for Associating Liquids.” 1709–21.
- Chapman, Walter G., Keith E. Gubbins, George Jackson, and M. Radosz. 1989. “SAFT: Equation-of-State Solution Model for Associating Fluids.” *Fluid Phase Equilibria* 52.
- Chapman, Walter G., George Jackson, and Keith E. Gubbins. 1988. “Phase Equilibria of Associating Fluids Chain Molecules with Multiple Bonding Sites.” *Molecular Physics* 65(5):1057–79.
- Chapoy, Antonin. 2004. “Phase Behaviour in Water / Hydrocarbon Mixtures Involved in Gas Production Systems.” Paris School of Mines.
- Chen, Chau??Chyun ??C and L. B. Evans. 1982. “A Local Composition Model for the Excess Gibbs Energy of Aqueous Electrolyte Systems.” *AIChE Journal* 28(4):588–96.
- Chong, Zheng Rong, She Hern Bryan Yang, Ponnivalavan Babu, Praveen Linga, and Xiao Sen Li. 2016. “Review of Natural Gas Hydrates as an Energy Resource: Prospects and Challenges.” *Applied Energy* 162:1633–52.
- Chouai, A., S. Laugier, and D. Richon. 2002. “Modeling of Thermodynamic Properties Using Neural Networks.” *Fluid Phase Equilibria* 199(1–2):53–62.
- Clarke, Matthew A. and P. R. Bishnoi. 2004. “Development of a New Equation of State for Mixed Salt and Mixed Solvent Systems, and Application to Vapour-Liquid and Solid (Hydrate)-Vapour-Liquid Equilibrium Calculations.” *Fluid Phase Equilibria* 220(1):21–35.
- Claussen, W. F. 1951. “A Second Water Structure for Inert Gas Hydrates.” *The Journal of Chemical Physics* 19(11):1425.
- Copeman, Thomas W. and Fred P. Stein. 1986. “AN EXPLICIT NON-EQUAL DIAMETER MSA MODEL FOR ELECTROLYTES.” 30:237–45.
- Copeman, Thomas W. and Fred P. Stein. 1987. “A Perturbed Hard-Sphere Equation of State for Solutions Containing an Electrolyte.” *Fluid Phase Equilibria* 35(1–3):165–87.
- Corbett, P. W. ... 2000. *PVT and Phase Behaviour of Petroleum Reservoir Fluids*. Vol. 17.
- Corti HR, Fernandez and Blum L. Prini R. 1987. “An Analytical Approximation to the Hypernetted Chain (HNC) Pair Correlation Functions: The Case of 2:2

- Electrolytes.” *Journal of Chemical Physics* 87(5):302.
- Cotterman, R. L., B. J. Schwarz, and J. M. Prausnitz. 1986. “Molecular Thermodynamics for Fluids at Low and High Densities. Part I: Pure Fluids Containing Small or Large Molecules.” *AIChE Journal* 32(11):1787–98.
- Courtial, Xavier, Nicolas Ferrando, Jean Charles de Hemptinne, and Pascal Mougin. 2014. “Electrolyte CPA Equation of State for Very High Temperature and Pressure Reservoir and Basin Applications.” *Geochimica et Cosmochimica Acta* 142:1–14.
- Das, Gaurav, Stepan Hlushak, and Clare McCabe. 2015. “A SAFT-VR+DE Equation of State Based Approach for the Study of Mixed Dipolar Solvent Electrolytes.” *Fluid Phase Equilibria* 416:72–82.
- Das, Gaurav, Stepan Hlushak, M. Carolina Dos Ramos, and Clare McCabe. 2015. “Predicting the Thermodynamic Properties and Dielectric Behavior of Electrolyte Solutions Using the SAFT-VR+DE Equation of State.” *AIChE Journal* 61(504):3–194.
- Das, Gaurav, M. Carolina dos Ramos, and Clare McCabe. 2018. “Predicting the Thermodynamic Properties of Experimental Mixed-Solvent Electrolyte Systems Using the SAFT-VR+DE Equation of State.” *Fluid Phase Equilibria* 460:105–18.
- Davidson, D. W., S. R. Gough, J. A. Ripmeester, and I. Haruo Nakayama. 1981. “The Effect of Methanol on the Stability of Clathrate Hydrates I.” *Canadian Journal of Chemistry* 59(2):2587–90.
- Deaton, W. M. and E. M. J. Frost. 1946. “Gas Hydrates and Their Relation to the Operation of Natural-Gas Natural-Gas Pipe Lines,.” *U.S. Bur. Mines Monogr* 8:101.
- Debye, P. and E. Hückel. 1923. “Zur Theorie Der Elektrolyte.” *Physik Z.* 24:185–206.
- Dharmawardhana, P. B., W. R. Parrish, and E. D. Sloan. 1980. “Experimental Thermodynamic Parameters for the Prediction of Natural Gas Hydrate Dissociation Conditions.” *Industrial & Engineering Chemistry Fundamentals* (1976):410–14.
- Dholabhai, Pankaj D., Nicolas Kalogerakis, and P. Raj Bishnoi. 1993. “Equilibrium Conditions for Carbon Dioxide Hydrate Formation in Aqueous Electrolyte Solutions.” *Journal of Chemical & Engineering Data* 38(4):650–54.
- Docherty, H., A. Galindo, E. Sanz, and C. Vega. 2007. “Investigation of the Salting out of Methane from Aqueous Electrolyte Solutions Using Computer Simulations.” *Journal of Physical Chemistry B* 111(30):8993–9000.
- Doozandeh, Sara Ghayour, Gholamreza Pazuki, and Ali Asghar. 2012. “Study of Protein Partitioning in Polymer-Salt Aqueous Two-Phase Systems Using Electrolyte-SAFT (E-SAFT) Equation of State.” *Journal of Dispersion Science and Technology* 33(5):756–62.
- DR Lide. 2005. *Magnetic Susceptibility of the Elements and Inorganic Compounds*.

- Drive, Corporate and J. Carroll. 2009. *Natural Gas Hydrates: A Guide for Engineers*.
- Dufal, Simon, Thomas Lafitte, Andrew J. Haslam, Amparo Galindo, Gary N. I. Clark, Carlos Vega, and George Jackson. 2015. "The A in SAFT: Developing the Contribution of Association to the Helmholtz Free Energy within a Wertheim TPT1 Treatment of Generic Mie Fluids." *Molecular Physics* 113(9–10):948–84.
- Elgibaly, Ahmed A. and Ali M. Elkamel. 1998. "A New Correlation for Predicting Hydrate Formation Conditions for Various Gas Mixtures and Inhibitors." *Fluid Phase Equilibria* 152(1):23–42.
- Englezos, P. 1992. "Computation of the Incipient Equilibrium Carbon-Dioxide Hydrate Formation Conditions in Aqueous-Electrolyte Solutions." *Industrial & Engineering Chemistry Research* 31(9):2232–37.
- Englezos, P. 1993. "Clathrate Hydrates." *Ind. Eng. Chem.* 32(7):1251–74.
- Englezos, P., Z. Huang, and P. R. Bishnoi. 1991. "Prediction Of Natural Gas Hydrate Formation Conditions In The Presence Of Methanol Using The Trebble-Bishnoi Equation Of State." *Journal of Canadian Petroleum Technology* 30(02).
- Eriksen, Daniel K., Georgia Lazarou, Amparo Galindo, George Jackson, Claire S. Adjiman, and Andrew J. Haslam. 2016. "Development of Intermolecular Potential Models for Electrolyte Solutions Using an Electrolyte SAFT-VR Mie Equation of State." *Molecular Physics* 114(18):2724–49.
- Friedman, Harold L. 1981. "Electrolyte Solutions at Equilibrium." *Physical Chemistry* 32(1992):179–204.
- Fürst, W. and H. Renon. 1993. "Representation of Excess Properties of Electrolyte Solutions Using a New Equation of State." *AIChE Journal* 39(2):335–43.
- Galindo, Amparo, Alejandro Gil-Villegas, George Jackson, and Andrew N. Burgess. 1999. "SAFT-VRE: Phase Behavior of Electrolyte Solutions with the Statistical Associating Fluid Theory for Potentials of Variable Range." *J. Phys. Chem. B* 103(46):10272–81.
- Galindo, Amparo, Paul J. Whitehead, George Jackson, and Andrew N. Burgess. 1996. "Predicting the High-Pressure Phase Equilibria of Water + n -Alkanes Using a Simplified SAFT Theory with Transferable Intermolecular Interaction Parameters." *J. Phys. Chem.* 100:6781–92.
- Ghiasi, Mohammad Mahdi. 2012. "Initial Estimation of Hydrate Formation Temperature of Sweet Natural Gases Based on New Empirical Correlation." *Journal of Natural Gas Chemistry* 21(5):508–12.
- Gil-villegas, Alejandro, Amparo Galindo, Paul J. Whitehead, Stuart J. Mills, George Jackson, Alejandro Gil-villegas, Amparo Galindo, Paul J. Whitehead, Stuart J. Mills, and Andrew N. Burgess. 1997. "Statistical Associating Fluid Theory for Chain Molecules with Attractive Potentials of Variable Range Statistical

- Associating Fluid Theory for Chain Molecules with Attractive Potentials of Variable Range.” 4168.
- Gross, Joachim and Gabriele Sadowski. 2001. “Perturbed-Chain SAFT: An Equation of State Based on a Perturbation Theory for Chain Molecules.” *Industrial and Engineering Chemistry Research* 40(4):1244–60.
- Gross, Joachim and Gabriele Sadowski. 2002. “Application of the Perturbed-Chain SAFT Equation of State to Associating Systems.” *Ind. Eng. Chem. Res.* 41:5510–15.
- Guo, Jian Lian and Tian-Min. 1999. “Prediction of Gas Hydrate Formation Conditions in Aqueous Solutions Containing Electrolytes and (Electrolytes + Methanol).” *Industrial & Engineering Chemistry* 38(5):1700–1705.
- Haghighi, Hooman. 2009. “Phase Equilibria Modelling of Petroleum Reservoir Fluids Containing Water, Hydrate Inhibitors and Electrolyte Solutions.” Heriot-Watt University Institute.
- Haghtalab, Ali, Abolfazl Shojaeian, and Seyed Hossein Mazloumi. 2011. “Nonelectrolyte NRTL-NRF Model to Study Thermodynamics of Strong and Weak Electrolyte Solutions.” *Journal of Chemical Thermodynamics* 43(3):354–63.
- Hamer, Walter and Wu, Yung-Chi. 2009. “Osmotic Coefficients and Mean Activity Coefficients of Uni-Univalent Electrolytes in Water at 25C.” *Journal Physical and Chemical Reference* 1(4):1–54.
- Handa, Y. Paul and John S. Tse. 1986. “Thermodynamic Properties of Empty Lattices of Structure I and Structure II Clathrate Hydrates.” *J. Phys. Chem.* (26156):5917–21.
- Harvey, Allan H., Thomas W. Copeman, and John M. Prausnitz. 1988. “Explicit Approximations to the Mean Spherical Approximation for Electrolyte Systems with Unequal Ion Sizes.” *Journal of Physical Chemistry* 92(22):6432–36.
- Harvey, Allan H. and John M. Prausnitz. 1989. “Thermodynamics of High-pressure Aqueous Systems Containing Gases and Salts.” *AIChE Journal* 35(4):635–44.
- Hejrati Lahijani, Mir Arsalan and Chongwei Xiao. 2017. “SAFT Modeling of Multiphase Equilibria of Methane-CO₂-Water-Hydrate.” *Fuel* 188:636–44.
- Held, Christoph, Luca F. Cameretti, and Gabriele Sadowski. 2008. “Modeling Aqueous Electrolyte Solutions. Part 1. Fully Dissociated Electrolytes.” *Fluid Phase Equilibria* 270(1–2):87–96.
- Held, Christoph, Axel Prinz, Viktoria Wallmeyer, and Gabriele Sadowski. 2012. “Measuring and Modeling Alcohol/Salt Systems.” *Chemical Engineering Science* 68(1):328–39.
- Held, Christoph, Thomas Reschke, Sultan Mohammad, Armando Luza, and Gabriele Sadowski. 2014. “EPC-SAFT Revised.” *Chemical Engineering Research and Design* 92(12):1884–97.

- Held, Christoph and Gabriele Sadowski. 2009. "Modeling Aqueous Electrolyte Solutions. Part 2. Weak Electrolytes." *Fluid Phase Equilibria* 279(2):141–48.
- Henderson, D., L. Blum, and Alessandro Tani. 1986. "EQUATION OF STATE OF IONIC FLUIDS." 300:281–96.
- Henderson, D. and L. Blum. 1980. "Perturbation Theory for Charged Hard Spheres." *Molecular Physics* 1509:1980.
- Henderson, DOUGLAS. 1983. "Perturbation Theory, Ionic Fluids, and the Electric Double Layer." Pp. 47–71 in.
- Herzog, Stefanie, Joachim Gross, and Wolfgang Arlt. 2010. "Equation of State for Aqueous Electrolyte Systems Based on the Semirestricted Non-Primitive Mean Spherical Approximation." *Fluid Phase Equilibria* 297(1):23–33.
- Holder, G. D., G. Corbin, and K. D. Papadopoulos. 1980. "Thermodynamic and Molecular Properties of Gas Hydrates from Mixtures Containing Methane, Argon, and Krypton." *Industrial & Engineering Chemistry Fundamentals* 19(3):282–86.
- Holder, G. D., S. T. Malekar, and E. Dendy Sloan. 1984. "Determination of Hydrate Thermodynamic Reference Properties from Experimental Hydrate Composition Data." *Industrial & Engineering Chemistry Fundamentals* 123–26.
- Holder, G. D., S. P. Zetts, and N. Pradhan. 1988. "Phase Behavior in Systems Containing Clathrate Hydrates: A Review." *Reviews in Chemical Engineering* 5(1–4):1–70.
- Huang, SH and M. Radosz. 1991. "Equation of State for Small, Large, Polydisperse, and Associating Molecules: Extension to Fluid Mixtures." *Industrial & Engineering Chemistry Research* 30:1994–2005.
- Huang, Stanley H. and Maciej Radosz. 1990. "Equation of State for Small, Large, Polydisperse and Associating Molecules." *Ind. Eng. Chem. Res.* 29:2284–94.
- Inchekel, Radia, Jean Charles de Hemptinne, and Walter Fürst. 2008. "The Simultaneous Representation of Dielectric Constant, Volume and Activity Coefficients Using an Electrolyte Equation of State." *Fluid Phase Equilibria* 271(1–2):19–27.
- Ingram, Thomas, Thomas Gerlach, Tanja Mehling, and Irina Smirnova. 2012. "Extension of COSMO-RS for Monoatomic Electrolytes: Modeling of Liquid-Liquid Equilibria in Presence of Salts." *Fluid Phase Equilibria* 314:29–37.
- Jackson, G., W. G. Chapman, and K. E. Gubbins. 1988. "Phase Equilibria of Associating Fluids of Spherical and Chain Molecules." 9(5):769–79.
- Jäger, Andreas, Václav Vinš, Johannes Gernert, Roland Span, and Jan Hrubý. 2013. "Phase Equilibria with Hydrate Formation in H₂O+CO₂ mixtures Modeled with Reference Equations of State." *Fluid Phase Equilibria* 338:100–113.
- Jager, M. .. and E. .. Sloan. 2001. "The Effect of Pressure on Methane Hydration in Pure

- Water and Sodium Chloride Solutions.” *Fluid Phase Equilibria* 185(1–2):89–99.
- Javanmardi, Jafar, Mahmood Moshfeghian, and Robert N. Maddox. 1998. “Simple Method for Predicting Gas-Hydrate-Forming Conditions in Aqueous Mixed-Electrolyte Solutions.” *Energy* 28(8):219–22.
- Javanmardi, Jafar, Mahmood Moshfeghian, and Robert N. Maddox. 2001. “An Accurate Model for Prediction of Gas Hydrate Electrolyte Solutions and Alcohol.” *The Canadian Journal of Chemical Engineering* 79.
- Jeffery B. Klauda and Stanley I. Sandler. 2000. “A Fugacity Model for Gas Hydrate Phase Equilibria.” *Ind. Eng. Chem* 39(9):3377–86.
- Jeffrey, G. A. and R. K. McMullen. 1967. “The Clathrate Hydrates.” *Prog. Inorg. Chem.* 8(97):43–108.
- Ji, Xiaoyan and Hertanto Adidharma. 2008. “Ion-Based SAFT2 to Represent Aqueous Multiple-Salt Solutions at Ambient and Elevated Temperatures and Pressures.” *Chemical Engineering Science* 63:131–40.
- Ji, Xiaoyan, Hertanto Adidharma, and Petroleum Engineering. 2006. “Ion-Based SAFT2 to Represent Aqueous Single- and Multiple-Salt Solutions.” *Ind. Eng. Chem. Res.* 45:7719–28.
- Ji, Xiaoyan, Sugata P. Tan, Hertanto Adidharma, and Maciej Radosz. 2005. “Statistical Associating Fluid Theory Coupled with Restricted Primitive Model to Represent Aqueous Strong Electrolytes : Multiple-Salt Solutions.” *Ind. Eng. Chem. Res.* 44(4):7584–90.
- Ji, Xiaoyan, Sugata P. Tan, Hertanto Adidharma, and Maciej Radosz. 2006. “Statistical Associating Fluid Theory Coupled with Restrictive Primitive Model Extended to Bivalent Ions. SAFT2: 2. Brine/Seawater Properties Predicted.” *The Journal of Physical Chemistry B* 110(33):16700–706.
- Jiang, H and H. Adidharma. 2012a. “Modeling of Hydrate Dissociation Conditions for Alkanes in the Presence of Single and Mixed Electrolyte Solutions Using Ion-Based Statistical Associating Fluid Theory.” *Industrial & Engineering Chemistry Research* 51:5818–25.
- Jiang, H and H. Adidharma. 2012b. “Prediction of Hydrate Dissociation Conditions for Alkanes in the Presence of Alcohol and Electrolyte Solutions Using Ion-Based Statistical Associating Fluid Theory.” *Chemical Engineering Science* 82:14–21.
- Jiang, Hao and Hertanto Adidharma. 2015. “Molecular Simulation Study of Thermodynamic Properties of Symmetric and Asymmetric Electrolyte Systems in Mixture with Neutral Components: Monte Carlo Simulation Results and Integral Equation Predictions Study of Thermodynamic Properties of Symmetric And.” *Molecular Simulation* 41(9):727–34.
- Jiang, Hao, Athanassios Z. Panagiotopoulos, and Ioannis G. Economou. 2016. “Modeling

- of CO₂ Solubility in Single and Mixed Electrolyte Solutions Using Statistical Associating Fluid Theory.” *Geochimica et Cosmochimica Acta* 176:185–97.
- Jin, Gang and Marc D. Donohue. 1988a. “An Equation of State for Electrolyte Solutions. 1. Aqueous Systems Containing Strong Electrolytes.” *Industrial & Engineering Chemistry Research* 27(6):1073–84.
- Jin, Gang and Marc D. Donohue. 1988b. “An Equation of State for Electrolyte Solutions. 2. Single Volatile Weak Electrolytes in Water.” *Industrial and Engineering Chemistry Research* 27(9):1737–43.
- Jin, Gang and Marc D. Donohue. 1991. “An Equation of State for Electrolyte Solutions. 3. Aqueous Solutions Containing Multiple Salts.” *Industrial & Engineering Chemistry Research* 30:240–48.
- John, V. T., K. D. Papadopoulos, and G. D. Holder. 1985. “A Generalized Model for Predicting Equilibrium Conditions for Gas Hydrates.” 31(2):252–59.
- Kadyshevich, E. A., Kyoo Y. Song, and E. Dendy Sloan. 1987. “Phase Behavior of Water/Hydrocarbon Systems (1987 PEH Chapter 25).” *Petroleum Engineering Handbook*.
- Katz, Donald L. 1945. “Prediction of Conditions for Hydrate Formation in Natural Gases.” *Transactions of the AIME* 160(1):140–49.
- Kelland, Malcolm a. 2006. “History of the Development of Low Dosage Hydrate Inhibitors.” *Energy Fuels* 20(3):825–47.
- Khan, M. Naveed, Pramod Warriar, Cor J. Peters, and Carolyn A. Koh. 2018. “Fluid Phase Equilibria Advancements in Hydrate Phase Equilibria and Modeling of Gas Hydrates Systems.” *Fluid Phase Equilibria* 463:48–61.
- Kiepe, Jörn, Sven Horstmann, Kai Fischer, and Jürgen Gmehling. 2003. “Experimental Determination and Prediction of Gas Solubility Data for Methane + Water Solutions Containing Different Monovalent Electrolytes.” *Industrial and Engineering Chemistry Research* 42(21):5392–98.
- Kihara, T. 1953. “Virial Coefficients and Models of Molecules in Gases.” *Reviews of Modern Physics* 25(4):1–8.
- Kim, Kwangmin, Kyeongjun Seo, Jaewon Lee, Myung Gil Kim, Kyoung Su Ha, and Choongik Kim. 2016. “Investigation and Prediction of the Salting-out Effect of Methane in Various Aqueous Electrolyte Solutions.” *Journal of Industrial and Engineering Chemistry* 34:117–21.
- Kjellander, Roland. 2005. “Modified Debye-Hueckel Approximation with Effective Charges: An Application of Dressed Ion Theory for Electrolyte Solutions.” *The Journal of Physical Chemistry* 99(25):10392–407.
- Klamt, Andreas, Frank Eckert, and Wolfgang Arlt. 2010. “COSMO-RS: An Alternative

- to Simulation for Calculating Thermodynamic Properties of Liquid Mixtures.” *Annual Review of Chemical and Biomolecular Engineering* 1(1):101–22.
- Klauda, Jeffery B. and Stanley I. Sandler. 2003. “Phase Behavior of Clathrate Hydrates: A Model for Single and Multiple Gas Component Hydrates.” *Chemical Engineering Science* 58(1):27–41.
- Klein, Stéphane, Elise Kochanski, and Alain Strich. 1996. “Electric Properties of the Oxonium Ion in Its Ground and Two Lowest Excited States.” *Chemical Physics Letters* 260(1–2):34–42.
- Kontogeorgis, Georgios M. and Georgios K. Folas. 2009. “Thermodynamic Models for Industrial Applications: From Classical and Advanced Mixing Rules to Association Theories.”
- Kontogeorgis, Georgios M., Bjørn Maribo-Mogensen, and Kaj Thomsen. 2018. “The Debye-Hückel Theory and Its Importance in Modeling Electrolyte Solutions.” *Fluid Phase Equilibria* 462:130–52.
- Kontogeorgis, Georgios M., Michael L. Michelsen, Georgios K. Folas, Samer Derawi, Nicolas Von Solms, and Erling H. Stenby. 2006a. “Ten Years with the CPA (Cubic-Plus-Association) Equation of State. Part 1. Pure Compounds and Self-Associating Systems.” *Industrial and Engineering Chemistry Research* 45(14):4855–68.
- Kontogeorgis, Georgios M., Michael L. Michelsen, Georgios K. Folas, Samer Derawi, Nicolas Von Solms, and Erling H. Stenby. 2006b. “Ten Years with the CPA (Cubic-Plus-Association) Equation of State. Part 2. Cross-Associating and Multicomponent Systems.” *Industrial and Engineering Chemistry Research* 45(14):4869–78.
- Kwaterski, Matthias and Jean Michel Herri. 2014. “Modelling of Gas Clathrate Hydrate Equilibria Using the Electrolyte Non-Random Two-Liquid (ENRTL) Model.” *Fluid Phase Equilibria* 371:22–40.
- Lafitte, Thomas, Anastasia Apostolakou, Carlos Avendaño, Amparo Galindo, Claire S. Adjiman, Erich A. Müller, and George Jackson. 2013. “Accurate Statistical Associating Fluid Theory for Chain Molecules Formed from Mie Segments.” *Journal of Chemical Physics* 139(15).
- Lafitte, Thomas, David Bessieres, Manuel M. Piñeiro, and Jean-luc Daridon. 2007. “Simultaneous Estimation of Phase Behavior and Second-Derivative Properties Using the Statistical Associating Fluid Theory with Variable Range Approach Simultaneous Estimation of Phase Behavior and Second-Derivative Properties Using the Statistical Associa.” 024509(May 2014).
- Lebowitz, J. L. and J. K. Percus. 1966. “Mean Spherical Model for Lattice Gases with Extended Hard Cores and Continuum Fluids.” *Physical Review* 144(1):251–58.
- Lederhos, J. P., J. P. Long, a. Sum, R. L. Christiansen, and E. D. Sloan. 1996. “Effective Kinetic Inhibitors for Natural Gas Hydrates.” *Chemical Engineering Science*

51(8):1221–29.

- Lee, Bong-seop and Ki-chang Kim. 2009. “Modeling of Aqueous Electrolyte Solutions Based on Perturbed-Chain Statistical Associating Fluid Theory Incorporated with Primitive Mean Spherical Approximation.” *Journal of Chemical Engineering* 26(6):1733–47.
- Lee, Bong Seop and Ki Chang Kim. 2015. “Liquid-Liquid Equilibrium of Associating Fluid Mixtures Using Perturbed-Hard-Sphere-Chain Equation of State Combined with the Association Model.” *Industrial and Engineering Chemistry Research* 54(1):540–49.
- Lee, Lloyd L. 1988. *MOLECULAR THERMODYNAMICS OF NONIDEAL FLUIDS*. Butterworth.
- Lee, Lloyd L. 2008. *Molecular Thermodynamics of Electrolyte Solutions*.
- Lennard-Jones, J. E. and A. F. Devonshire. 1937. “Critical Phenomena in Gases. I.” *Proceedings of the Royal Society A: Mathematical, Physical and Engineering Sciences* 163(912):53–70.
- Lennard-Jones, J. E. and A. F. Devonshire. 1938. “Critical Phenomena in Gases. II. Vapour Pressures and Boiling Points.” *Proceedings of the Royal Society of London. Series A, Mathematical and Physical Sciences* 165:1–11.
- Levenberg, Kenneth and Frankford Arsenal. 1943. “A Method for the Solution of Certain Non-Linear Problems in Least Squares.” *Quarterly of Applied Mathematics* 1(278):536–38.
- Lewis, Gilbert. N. and Merle Randall. 1923. *Thermodynamics and the Free Energy of Chemical Substances*. First Edit. MCGRAW-HILL BOOK COPANY, Inc.
- Lewis, H. W. and G. H. Wannier. 1952. “The Spherical Model of a Ferromagnet.” *Physical Review* 86(6):821–35.
- Li, Xiao-Sen, Chun-Gang Xu, Yu Zhang, Xu-Ke Ruan, Gang Li, and Yi Wang. 2016. “Investigation into Gas Production from Natural Gas Hydrate: A Review.” *Applied Energy* 172:286–322.
- Lin, Y. and Kaj Thomsen. 2007. “Development of an Equation of State for Solutions Containing Electrolytes.” Technical University of Denmark.
- Lin, Yi, Kaj Thomsen, and Jean-Charles de Hemptinne. 2007. “Multicomponent Equations of State for Electrolytes.” *AIChE Journal* 53(4):989–1105.
- Liu, Wen-Bin, Yi-Gui Li, and Jiu-Fang Lu. 1998. “Nonprimitive Model of Mean Spherical Approximation Applied to Aqueous Electrolyte Solutions.” *Ind. Eng. Chem. Res.* 5885(37):4183–89.
- Liu, Wen-Bin, Yi-Gui Li, and Jiu-Fang Lu. 1999. “A New Equation of State for Real

- Aqueous Ionic Fluids Based on Electrolyte Perturbation Theory, Mean Spherical Approximation and Statistical Associating Fluid Theory.” *Fluid Phase Equilibria* 158–160:595–606.
- Liu, Zhiping, Wenchuan Wang, and Yigui Li. 2005. “An Equation of State for Electrolyte Solutions by a Combination of Low-Density Expansion of Non-Primitive Mean Spherical Approximation and Statistical Associating Fluid Theory.” 227:147–56.
- Loeche, Joseph R. and Marc D. Donohue. 1997. “Recent Advances in Modeling Thermodynamic Properties of Aqueous Strong Electrolyte Systems.” *AIChE Journal* 43(1):180–95.
- Loh, M. R. N. and E. J. H. James. 1983. “NEW HYDRATE-FORMATION DATA REVEAL DIFFERENCES.” *Oil Gas J* 81:96–98.
- Loveday, J. S., R. J. Nelmes, M. Guthrie, D. D. Klug, and J. S. Tse. 2001. “Transition from Cage Clathrate to Filled Ice: The Structure of Methane Hydrate III.” *Physical Review Letters* 87(21):215501.
- Luongo-ortiz, Juan F. and Kenneth E. Starling. 1997. “A New Combining Rule for Mixture Equations of State: Higher Order Composition Dependencies Reduce to Quadratic Composition Dependence Juan.” *Fluid Phase Equilibria* 132(96):159–67.
- Makogon, Yuri F. 1981. “Hydrates of Natural Gases.” 12–13.
- Malanowski, By S. and A. Anderko. 1992. *Modelling Phase Equilibria: Thermodynamic Background and Practical Tools*. Wiley.
- Mann, Susan L. 1988. *Vapor-Solid Equilibrium Ratios for Structure I and II Natural Gas Hydrates*. Gas Processors Association.
- Mann, Susan L., M. T. McClure, F. Poettmann, and E. D. Sloan. 1989. “Vapor-Solid Equilibrium Ratios for Structure II Natural Gas Hydrate.” in *68th Gas Processors Association Conference*. San Antonio.
- Mansoori, G. A., N. F. Carnahan, K. E. Starling, and T. W. Leland. 1971. “Equilibrium Thermodynamic Properties of the Mixture of Hard Spheres.” *The Journal of Chemical Physics* 54(4):1523–25.
- Maribo-Mogensen, Bjorn, Georgios M. Kontogeorgis, and Kaj Thomsen. 2012. “Comparison of the Debye-Huckel and the Mean Spherical Approximation Theories for Electrolyte Solutions.” *Industrial and Engineering Chemistry Research* 51(14):5353–63.
- Maribo-mogensen, Bjørn, Georgios M. Kontogeorgis, and Kaj Thomsen. 2013. “Modeling of Dielectric Properties of Aqueous Salt Solutions with an Equation of State.” *The Journal of Physical Chemistry B* 117:10523–33.
- Maribo-mogensen, Bjørn, Georgios Kontogeorgis, and Kaj Thomsen. 2014. “Development of an Electrolyte CPA Equation of State for Applications in the

- Petroleum and Chemical Industries.” Technical University of Denmark.
- Maribo-mogensen, Bjørn, Kaj Thomsen, and Georgios M. Kontogeorgis. 2015. “An Electrolyte CPA Equation of State for Mixed Solvent Electrolytes.” *AIChE Journal* 61(9):2933–50.
- Marion, Giles M., David C. Catling, and Jeffrey S. Kargel. 2006. “Modeling Gas Hydrate Equilibria in Electrolyte Solutions.” *Calphad* 30(3):248–59.
- Marion, Giles M. and Steven A. Grant. 1994. “FREZCHEM : A Chemical-Thermodynamic Model for Aqueous Solutions at Subzero Temperatures.” *Cold Regions Research and Engineering Lab Hanover* 36.
- Marquardt, D. W. 1963. “AN ALGORITHM FOR LEAST-SQUARES ESTIMATION OF NONLINEAR PARAMETERS.” *J. Soc. Indst. Appi. MATH* 11(2).
- Martin, Angel and C. J. Peters. 2009a. “Hydrogen Storage in SH Clathrate Hydrates : Thermodynamic Model.” *J. Phys. Chem. B* 113:7558–63.
- Martin, Angel and C. J. Peters. 2009b. “New Thermodynamic Model of Equilibrium States of Gas Hydrates Considering Lattice Distortion.” *J. Phys. Chem.* 113:422–30.
- Martin, Angel and C. J. Peters. 2009c. “Thermodynamic Modeling of Promoted Structure II Clathrate Hydrates of Hydrogen.” *J. Phys. Chem. B* 7548–57.
- McKoy, V. and O. Sinanoğlu. 1963. “Theory of Dissociation Pressures of Some Gas Hydrates.” *The Journal of Chemical Physics* 38(12):2946–56.
- McMillan, William G. and Joseph E. Mayer. 1945. “The Statistical Thermodynamics of Multicomponent Systems.” *The Journal of Chemical Physics* 13(7):276–305.
- McQuarrie, D. A. and J. L. Katz. 1966. “High-Temperature Equation of State.” *J. Chem. Phys.* 2393(44).
- McQuarrie, Donald A. 1976. *Statistical Mechanics*. Harper & Row.
- Mei, Dong-Hai, Jian Liao, Ji-Tao Yang, and Tian-Min Guo. 1996. “Experimental and Modeling Studies on the Hydrate Formation of a Methane + Nitrogen Gas Mixture in the Presence of Aqueous Electrolyte Solutions.” *Industrial & Engineering Chemistry Research* 35(11):4342–47.
- El Meragawi, Sally, Nikolaos I. Diamantonis, Ioannis N. Tsimpanogiannis, and Ioannis G. Economou. 2016. “Hydrate - Fluid Phase Equilibria Modeling Using PC-SAFT and Peng-Robinson Equations of State.” *Fluid Phase Equilibria* 413:209–19.
- Michelsen, Michael L. and Eric M. Hendriks. 2001. “Physical Properties from Association Models.” *Fluid Phase Equilibria* 180(1–2):165–74.
- Mohammad, S., G. Grundl, Rainer Müller, W. Kunz, G. Sadowski, and C. Held. 2016. “Influence of Electrolytes on Liquid-Liquid Equilibria of Water/1-Butanol and on the Partitioning of 5-Hydroxymethylfurfural in Water/1-Butanol.” *Fluid Phase*

Equilibria 428:102–11.

- Mohammad, S., C. Held, E. Altuntepe, T. Köse, T. Gerlach, I. Smirnova, and G. Sadowski. 2015. “Salt Influence on MIBK/Water Liquid-Liquid Equilibrium: Measuring and Modeling with EPC-SAFT and COSMO-RS.” *Fluid Phase Equilibria* 416:83–93.
- Mohammadi, Abolfazl, Mehrdad Manteghian, Amir H. Mohammadi, and Arash Kamran-Pirzaman. 2014. “Thermodynamic Modeling of the Dissociation Conditions of Hydrogen Sulfide Clathrate Hydrate in the Presence of Aqueous Solution of Inhibitor (Alcohol, Salt or Ethylene Glycol).” *Chemical Engineering Research and Design* 92(11):2283–93.
- Mohammadi, Amir H., Waheed Afzal, and Dominique Richon. 2008a. “Gas Hydrates of Methane, Ethane, Propane, and Carbon Dioxide in the Presence of Single NaCl, KCl, and CaCl₂ Aqueous Solutions: Experimental Measurements and Predictions of Dissociation Conditions.” *Journal of Chemical Thermodynamics* 40(12):1693–97.
- Mohammadi, Amir H., Waheed Afzal, and Dominique Richon. 2008b. “Gas Hydrates of Methane, Ethane, Propane, and Carbon Dioxide in the Presence of Single NaCl, KCl, and CaCl₂ Aqueous Solutions: Experimental Measurements and Predictions of Dissociation Conditions.” *Journal of Chemical Thermodynamics* 40(12):1693–97.
- Mohammadi, Amir H., Veronica Belandria, and Dominique Richon. 2010. “Use of an Artificial Neural Network Algorithm to Predict Hydrate Dissociation Conditions for Hydrogen+water and Hydrogen+tetra-n-Butyl Ammonium Bromide+water Systems.” *Chemical Engineering Science* 65(14):4302–5.
- Mohammadi, Amir H. and Dominique Richon. 2007. “Thermodynamic Modeling of Salt Precipitation and Gas Hydrate Inhibition Effect of Salt Aqueous Solution.” *Industrial and Engineering Chemistry Research* 46(14):5074–79.
- Mohammadi, Amir H. and Dominique Richon. 2010. “Hydrate Phase Equilibria for Hydrogen+water and Hydrogen+tetrahydrofuran+water Systems: Predictions of Dissociation Conditions Using an Artificial Neural Network Algorithm.” *Chemical Engineering Science* 65(10):3352–55.
- Moradi, Gholamreza and Ehsan Khosravani. 2012. “Application of PRSV2 Equation of State to Predict Hydrate Formation Temperature in the Presence of Inhibitors.” *Fluid Phase Equilibria* 333:18–26.
- Moradi, Gholamreza and Ehsan Khosravani. 2013. “Modeling of Hydrate Formation Conditions for CH₄, C₂H₆, C₃H₈, N₂, CO₂ and Their Mixtures Using the PRSV2 Equation of State and Obtaining the Kihara Potential Parameters for These Components.” *Fluid Phase Equilibria* 338:179–87.
- Moradi, M. R., K. Nazari, S. Alavi, and M. Mohaddesi. 2013. “Prediction of Equilibrium Conditions for Hydrate Formation in Binary Gaseous Systems Using Artificial Neural Networks.” *Energy Technology* 1(2–3):171–76.

- Muert, Erich and Keith E. Gubbins. 1995. "An Equation of State for Water from a Simplified Intermolecular Potential." *Ind. Eng. Chem* 34:3662–73.
- Munck, Jan, Steen Skjold-Jørgensen, and Peter Rasmussen. 1988. "Computations of the Formation of Gas Hydrates." *Chemical Engineering Science* 43(10):2661–72.
- Myers, Jason a., Stanley I. Sandler, and Robert H. Wood. 2002. "An Equation of State for Electrolyte Solutions Covering Wide Ranges of Temperature, Pressure, and Composition." *Industrial & Engineering Chemistry Research* 41(13):3282–97.
- Najafloo, Azam, Farzaneh Feyzi, and Ali T. Zoghi. 2015. "Modeling Solubility of CO₂ in Aqueous MDEA Solution Using Electrolyte SAFT-HR EoS." *Journal of the Taiwan Institute of Chemical Engineers* 58:381–90.
- Najafloo, Azam, Farzaneh Feyzi, and Ali Taghi Zoghi. 2014. "Development of Electrolyte SAFT-HR Equation of State for Single Electrolyte Solutions." *Korean Journal of Chemical Engineering* 31(12):2251–60.
- Nakamura, Toshiyuki, Takashi Makino, Takeshi Sugahara, and Kazunari Ohgaki. 2003. "Stability Boundaries of Gas Hydrates Helped by Methane - Structure-H Hydrates of Methylcyclohexane and Cis-1,2-Dimethylcyclohexane." *Chemical Engineering Science* 58(2):269–73.
- Nasrifar, Khashayar and Mahmood Moshfeghian. 2001. "A Model for Prediction of Gas Hydrate Formation Conditions in Aqueous Solutions Containing Electrolytes and/or Alcohol." *Journal of Chemical Thermodynamics* 33(9):999–1014.
- NG, Heng-Joo and Donald B. Robinson. 1985. "Hydrate Formation in Systems Containing Methane, Ethane, Propane, Carbon Dioxide or Hydrogen Sulfide in the Presence of Methanol." *Fluid Phase Equilibria* 21:145–55.
- NguyenHuynh, D., J. P. Passarello, P. Tobaly, and J. C. de Hemptinne. 2008. "Application of GC-SAFT EOS to Polar Systems Using a Segment Approach." *Fluid Phase Equilibria* 264(1–2):62–75.
- Nighswander, John A., Nicolas Kalogerakis, and Anil K. Mehrotra. 1989. "Solubilities of Carbon Dioxide in Water and 1 Wt. % Sodium Chloride Solution at Pressures up to 10 MPa and Temperatures from 80 to 200.Degree.C." *Journal of Chemical & Engineering Data* 34(3):355–60.
- Nixon, M. F. and J. L. H. Grozic. 2007. "Submarine Slope Failure Due to Gas Hydrate Dissociation: A Preliminary Quantification." *Canadian Geotechnical* 2007.
- Nordholm, Sture. 1983. "Corrected Debye–Hückel Theory of Electrolyte Solutions." *The Journal of Chemical Physics* 78(9):5759–63.
- O’Sullivan, Thomas D. and Norman Obed Smith. 1970. "Solubility and Partial Molar Volume of Nitrogen and Methane in Water and in Aqueous Sodium Chloride from 50 to 125.Deg. and 100 to 600 Atm." *The Journal of Physical Chemistry* 74(7):1460–66.

- Osfouri, Shahriar, Reza Azin, Reza Gholami, and Amir Abbas Izadpanah. 2015. "Modeling Hydrate Formation Conditions in the Presence of Electrolytes and Polar Inhibitor Solutions." *Journal of Chemical Thermodynamics* 89:251–63.
- Outhwaite, C. W. 1969. "Extension of the Debye–Hückel Theory of Electrolyte Solutions." *The Journal of Chemical Physics* 50(6):2277–88.
- Parent, J. ... and P. R. Bishnoi. 1996. "Investigation in to the Nucleation Behavior of Methane Gas Hydrates." *Chemical Engineering Communications* 1996.
- Parrish, W. R. and J. M. Prausnitz. 1972. "Dissociation Pressures of Gas Hydrates Formed by Gas Mixtures." *Industrial & Engineering Chemistry Process Design and Development* 11(1):26–35.
- Partanen, Jaakko I. and Arthur K. Covington. 2009. "Re-Evaluation of the Thermodynamic Activity Quantities in Aqueous Sodium and Potassium Chloride Solutions at 25 ° C †." *J. Chem. Eng. Data* 54:208–19.
- Patel, B. H., P. Paricaud, A. Galindo, and G. C. Maitland. 2003. "Prediction of the Salting-Out Effect of Strong Electrolytes on Water + Alkane Solutions." *Ind. Eng. Chem. Res.* 42:3809–23.
- Patel, Navin C. and Aryn S. Teja. 1982. "A New Cubic Equation of State for Fluids and Fluid Mixtures." *Chemical Engineering Science* 37(3):463–73.
- Patil, Kashinath K., Ffc RRAN Olive, and Alberto Coronas. 1994. "Experimental Measurements of Vapor Pressures of Electrolyte Solutions by Differential Static Method." *Journal of Chemical Engineering of Japan* 27(5):680–81.
- Patil, Kashinath R., Atri D. Tripathi, Gopal Pathak, and Sushilendra S. Katti. 1990. "Thermodynamic Properties of Aqueous Electrolyte Solutions.1 1. Vapor Pressure of Aqueous Solutions of LiCl, LiBr, and Li I." *J. Chem. Eng. Data* 35:166–68.
- Pauling, L. and R. E. Marsh. 1952. "The Structure of Chlorine Hydrate." *Proceedings of the National Academy of Sciences of the United States of America* 38(2):112–18.
- Pedersen, Karen and Peter Christensen. 2007. *Phase Behavior of Petroleum Fluids*. CRC Press.
- Peng, Ding Yu and Donald B. Robinson. 1976. "A New Two-Constant Equation of State." *Industrial and Engineering Chemistry Fundamentals* 15(1):59–64.
- Perez, Alfonso Gonzalez, Alain Valtz, Christophe Coquelet, Patrice Paricaud, and Antonin Chapoy. 2016. "Experimental and Modelling Study of the Densities of the Hydrogen Sulphide + Methane Mixtures at 253, 273 and 293 K and Pressures up to 30 MPa." *Fluid Phase Equilibria* 427:371–83.
- Pitzer, Kenneth S. 1973. "Thermodynamics of Electrolytes. I. Theoretical Basis and General Equations." *Journal of Physical Chemistry* 77(2):268–77.

- Pitzer, Kenneth S. 1980. "Electrolytes. From Dilute Solutions to Fused Salts Kenneth." *Journal of American Chemical Society* 2902–6.
- Pitzer, Kenneth S. n.d. *Activity Coefficients in Electrolyte Solutions*. Second Edi. CRC Press.
- Pitzer, Kenneth S. and Guillermo Mayorga. 1973. "Thermodynamics of Electrolytes. II. Activity and Osmotic Coefficients for Strong Electrolytes with One or Both Ions Univalent." *Journal of Physical Chemistry* 77(19):2300–2308.
- Planche, Henri and Henri Renon. 1981. "Mean Spherical Approximation Applied to a Simple but Nonprimitive Model of Interaction for Electrolyte Solutions and Polar Substances." *Journal of Physical Chemistry* 85(25):3924–29.
- Poling, Bruce E., John M. Prausnitz, and John O'Connell. 1988. *The Properties of Gases & Liquids*. Vol. 1. 5th ed. McGRAW-HILL BOOK COPANY, Inc.
- Pyper, N. C., C. G. Pike, and P. P. Edwards. 1992. "The Polarizabilities of Species Present in Ionic Solutions." *Molecular Physics* 76(2):353–72.
- Quarati, P. and A. M. Scarfone. 2007. "Modified Debye-Huckel Electron Shielding and Penetration Factor." *The Astrophysical Journal* 666(2):1303–10.
- Raabe, Gabriele. 2016. *Molecular Simulation Studies on Thermophysical Properties With Application to Working Fluids*. Springer.
- Rashidabad, Vahid Nikkhah, Ali Hatami, and Amin Ebrahimi. 2013. "The Thermodynamics Effect of Sodium Chloride and Sodium Sulfate on the Prevention of Methane Hydrate Formation and Offering Its Thermodynamics Model by Using Neural Networks." *Journal of American Science* 9:116–24.
- Rashin, Alexander A. and Barry Honig. 1985. "Reevaluation of the Born Model of Ion Hydration." *J. Phys. Chem.* 89:5588–93.
- Redlich, Otto and J. N. S. Kwong. 1948. "On The Thermodynamics Of Solution. V Equation Of State. Fugacities Of Gaseous SSolutions." 233–44.
- Renault-Crispo, Jean Sébastien, Francis Lang, and Phillip Servio. 2014. "The Importance of Liquid Phase Compositions in Gas Hydrate Modeling: Carbon Dioxide-Methane-Water Case Study." *Journal of Chemical Thermodynamics* 68:153–60.
- Renon, H. and J. M. Pruasnitz. 1968. "Local Compositions in Thermodynamics Excess Functions for Liquids Mixtures." *AIChE J.* 14(1):116–28.
- Robinson, R. A. and R. H. Stokes. 1960. *Electrolyte Solutions*. Vol. 72. Dover Publications, Inc.
- Rodil, Eva and J. H. Vera. 2001. "Individual Activity Coefficients of Chloride Ions in Aqueous Solutions of MgCl₂, CaCl₂ and BaCl₂ at 298.2 K Eva." *Fluid Phase Equilibria* 188:15–27.

- Rodil, Eva and J. H. Vera. 2003. "The Activity of Ions: Analysis of the Theory and Data for Aqueous Solutions of MgBr₂, CaBr₂ and BaBr₂ at 298.2 K." *Fluid Phase Equilibria* 205(1):115–32.
- RONALD FAWCETT, W. 2004. *Liquids, Solutions, and Interfaces*. Oxford University Press.
- Rowland, Darren and Peter M. May. 2015. "Comparison of the Pitzer and Hückel Equation Frameworks for Activity Coefficients, Osmotic Coefficients, and Apparent Molar Relative Enthalpies, Heat Capacities, and Volumes of Binary Aqueous Strong Electrolyte Solutions at 25 °c." *Journal of Chemical and Engineering Data* 60(7):2090–97.
- Rozmus, J., J. C. de Hemptinne, and P. Mougin. 2011. "Application of GC-PPC-SAFT EoS to Amine Mixtures with a Predictive Approach." *Fluid Phase Equilibria* 303(1):15–30.
- Rozmus, Justyna, Jean Charles De Hemptinne, Nicolas Ferrando, and Pascal Mougin. 2012. "Long Chain Multifunctional Molecules with GC-PPC-SAFT: Limits of Data and Model." *Fluid Phase Equilibria* 329:78–85.
- Rozmus, Justyna, Jean Charles De Hemptinne, Amparo Galindo, Simon Dufal, and Pascal Mougin. 2013. "Modeling of Strong Electrolytes with EPPC-SAFT up to High Temperatures." *Industrial and Engineering Chemistry Research* 52(29):9979–94.
- Saito, Shozaburo, Donald R. Marshall, and Riki Kobayashi. 1964. "Hydrates at High Pressures: Part II. Application of Statistical Mechanics to the Study of the Hydrates of Methane, Argon, and Nitrogen." *AIChE Journal* 10(5):734–40.
- Sanchez-Castro, C. and L. Blum. 1989. "Explicit Approximation for the Unrestricted Mean Spherical Approximation for Ionic Solutions." *Journal of Physical Chemistry* 93(21):7478–82.
- Sander, Bo, Aage Fredenslund, and Peter Rasmussen. 1986. "Calculation of Vapour-Liquid Equilibria in Mixed Solvent/Salt Systems Using an Extended UNIQUAC Equation." *Chemical Engineering Science* 41(5):1171–83.
- Schlaikjer, Anders, Kaj Thomsen, and Georgios M. Kontogeorgis. 2017. "Simultaneous Description of Activity Coefficients and Solubility with ECPA." *Industrial and Engineering Chemistry Research* 56(4):1074–89.
- Schmidt, G. and H. Wenzel. 1980. "A Modified van Der Waals Type Equation of State." *Chemical Engineering Science* 35(7):1503–12.
- Schmitz, Jones E., Roger J. Zemp, and Mário J. Mendes. 2006. "Artificial Neural Networks for the Solution of the Phase Stability Problem." *Fluid Phase Equilibria* 245(1):83–87.
- Schreckenber, Jens M. A., Simon Dufal, Andrew J. Haslam, Claire S. Adjiman, and

- Amparo Galindo. 2014. "Modelling of the Thermodynamic and Solvation Properties of Electrolyte Solutions with the Statistical Associating Fluid Theory for Potentials of Variable Range." *Molecular Physics* 112(17):2339–64.
- Shadloo, Azam, Mostafa Abolala, and Kiana Peyvandi. 2016. "Application of Ion-Based EPC-SAFT in Prediction of Density of Aqueous Electrolyte Solutions." *Journal of Molecular Liquids* 221:904–13.
- Shadloo, Azam and Kiana Peyvandi. 2017. "The Implementation of Ion-Based EPC-SAFT EOS for Calculation of the Mean Activity Coefficient of Single and Mixed Electrolyte Solutions." *Fluid Phase Equilibria* 433:226–42.
- Shadravanan, R., M. Schaffie, and M. Ranjbar. 2014. "The Prediction of Hydrate Formation Rate in the Presence of Inhibitors." *Energy Sources, Part A: Recovery, Utilization and Environmental Effects* 36(6):661–72.
- Shahnazar, Sheida and Nurul Hasan. 2014. "Gas Hydrate Formation Condition: Review on Experimental and Modeling Approaches." *Fluid Phase Equilibria* 379:72–85.
- Shannon, R. D. 1976. "Revised Effective Ionic Radii and Systematic Studies of Interatomic Distances in Halides and Chalcogenides." *Acta Cryst* 751–67.
- Simon, Hans-Günter, Hans Kistenmacher, John M. Prausnitz, and Dieter Vortmeyer. 1991. "An Equation of State for Systems Containing Electrolytes and Nonelectrolytes." *Chemical Engineering and Processing: Process Intensification* 29(3):139–46.
- Sirino, Thales H., Moises A. Marcelino Neto, Dalton Bertoldi, Rigoberto E. M. Morales, and Amadeu K. Sum. 2018. "Multiphase Equilibrium Flash Calculations for Systems Containing Gas Hydrates." *Fluid Phase Equilibria* 53(C):97–104.
- Sloan, D., C. Koh, A. Sum, A. Ballard, J. Creek, M. Eaton, J. Larchance, N. McMullen, T. Palermo, G. Shoup, and L. Talley. 2010. *Natural Gas Hydrates in Flow Assurance*. Elsevier Ltd.
- Sloan, E. Dendy. and Carolyn A. Koh. 2008. *Clathrate Hydrates of Natural Gases*. Third Edit. CRC Press.
- Sloan, E. Dendy. 2004. "Introductory Overview: Hydrate Knowledge Development." *American Mineralogist* 89(8–9):1155–61.
- Smith, E. B. and B. J. Alder. 1959. "Perturbation Calculations in Equilibrium Statistical Mechanics. I. Hard Sphere Basis Potential." *J. Chem. Phys.* 1190(30).
- Soave, Giorgio. 1972. "Equilibrium Constants from a Modified Redlich-Kwong Equation of State." *Chemical Engineering Science* 27(6):1197–1203.
- Stell, G. and J. L. Lebowitz. 1968. "Equilibrium Properties of a System of Charged Particles." *J. Chem. Phys.* 48(8):3706.

- Stokes, R. H. 1972. "Debye Model and the Primitive Model for Electrolyte Solutions." *The Journal of Chemical Physics* 56(7):3382–83.
- Sultan, Abdullah. 2017. *Electrolyte , and Polymer Solutions*.
- Sun, Rui and Zhenhao Duan. 2007. "An Accurate Model to Predict the Thermodynamic Stability of Methane Hydrate and Methane Solubility in Marine Environments." *Chemical Geology* 244(1–2):248–62.
- Sutherland, William. 1887. "On the Law of Molecular Force." 24(146).
- Tabatabaei, Ali R., Bahman Tohidi, and Adrian C. Todd. n.d. "VAPOUR-SOLID EQUILIBRIUM RATIO CHARTS FOR STRUCTURE-H HEAVY HYDRATE HYDROCARBON COMPOUNDS." (1954).
- Takaoki, T., T. Iwasaki, T. Katoh, A. Takashi, and H. Kiyoshi. 2002. "Use of Hydrate Pellets for Natural Gas Transportation." P. 2002 in *Inter. Conf. on Gas Hydrates*. Yokohama, Japan.
- Tamouza, Sofiane, J. Philippe Passarello, Pascal Tobaly, and J. Charles De Hemptinne. 2004. "Group Contribution Method with SAFT EOS Applied to Vapor Liquid Equilibria of Various Hydrocarbon Series." *Fluid Phase Equilibria* 222–223:67–76.
- Tamouza, Sofiane, J. Philippe Passarello, Pascal Tobaly, and J. Charles De Hemptinne. 2005. "Application to Binary Mixtures of a Group Contribution SAFT EOS (GC-SAFT)." *Fluid Phase Equilibria* 228–229:409–19.
- Tan, Sugata P., Hertanto Adidharma, and Maciej Radosz. 2005. "Statistical Associating Fluid Theory Coupled with Restricted Primitive Model to Represent Aqueous Strong Electrolytes." *Ind. Eng. Chem. Res.* 44(12):4442–52.
- Tan, Sugata P., Xiaoyan Ji, Hertanto Adidharma, and Maciej Radosz. 2006. "Statistical Associating Fluid Theory Coupled with Restrictive Primitive Model Extended to Bivalent Ions. SAFT2: 1. Single Salt + Water Solutions." *Journal of Physical Chemistry B* 110(33):16694–99.
- Tobergte, David R. and Shirley Curtis. 2013. *Computational Material Science-An Introduction*. Vol. 53.
- Tohidi, Bahman, Ross Anderson, Houra Mozaffar, and Foroogh Tohidi. 2015. "The Return of Kinetic Hydrate Inhibitors." *Energy and Fuels* 29(12):8254–60.
- Torrecilla, José S., César Tortuero, John C. Cancilla, and Pablo Díaz-Rodríguez. 2013a. "Estimation with Neural Networks of the Water Content in Imidazolium-Based Ionic Liquids Using Their Experimental Density and Viscosity Values." *Talanta* 113:93–98.
- Torrecilla, José S., César Tortuero, John C. Cancilla, and Pablo Díaz-Rodríguez. 2013b. "Neural Networks to Estimate the Water Content of Imidazolium-Based Ionic Liquids Using Their Refractive Indices." *Talanta* 116:122–26.

- Trebble, M. A. and P. R. Bishnoi. 1987. "Development of a New Four-Parameter Cubic Equation of State." *Fluid Phase Equilibria* 35(1-3):1-18.
- Trebble, M. A. and P. R. Bishnoi. 1988a. "Extension of the Trebble-Bishnoi Equation of State to Fluid Mixtures." *Fluid Phase Equilibria* 40(1-2):1-21.
- Trebble, M. A. and P. R. Bishnoi. 1988b. "Extension of the Trebble-Bishnoi Equation of State to Fluid Mixtures." *Fluid Phase Equilibria* 40(1-2):1-21.
- Tumba, Kaniki, Hamed Hashemi, Paramespri Naidoo, Amir H. Mohammadi, and Deresh Ramjugernath. 2013. "Dissociation Data and Thermodynamic Modeling of Clathrate Hydrates of Ethene, Ethyne, and Propene." *Journal of Chemical & Engineering Data* 58(11):3259-64.
- Udachin, K. a and J. a Ripmeester. 1999. "A Complex Clathrate Hydrate Structure Showing Bimodal Guest Hydration." *Nature* 397(February):420-23.
- Uematsu, M. and E. U. Frank. 1980. "Static Dielectric Constant of Water and Steam." *Journal of Physical and Chemical Reference Data* 9(4):1291-1306.
- Valavi, Masood and Mohammad Reza Dehghani. 2012. "Application of PHSC Equation of State in Prediction of Gas Hydrate Formation Condition." *Fluid Phase Equilibria* 333:27-37.
- Veluswamy, Hari Prakash, Sharad Kumar, Rajnish Kumar, Pramoch Rangsunvigit, and Praveen Linga. 2016. "Enhanced Clathrate Hydrate Formation Kinetics at near Ambient Temperatures and Moderate Pressures: Application to Natural Gas Storage." *Fuel* 182:907-19.
- Vimalchand, P., Marc D. Donohue, and Ilga Celmins. 1986. "Thermodynamics of Multipolar Molecules: The Perturbed-Anisotropic-Chain Theory." Pp. 297-313 in *Equations of State: Theories and Applications*.
- Vimalchand, Pannalal and Marc D. Donohue. 1985. "Thermodynamics of Quadrupolar Molecules: The Perturbed-Anisotropic-Chain Theory." *Industrial & Engineering Chemistry Fundamentals* 24(2):246-57.
- Vu, Vinh Quang, Pierre Duchet Suchaux, and Walter Fürst. 2002. "Use of a Predictive Electrolyte Equation of State for the Calculation of the Gas Hydrate Formation Temperature in the Case of Systems with Methanol and Salts." *Fluid Phase Equilibria* 194-197:361-70.
- W., Zwanzig. R. 1954. "High-Temperature Equation of State by a Perturbation Method. I. Nonpolar Gases." *J. Chem. Phys.* 1420.
- Van der Waals, J. D. 1873. "On the Continuity of the Liquid and Gaseous State." Leiden University.
- Waals, J. H. van der and J. C. Platteuw. 1959. "Clathrate Solutions." *Advances in Chemical Physics* 1-57.

- Waisman, Eduardo. 1972. "Mean Spherical Model Integral Equation for Charged Hard Spheres I. Method of Solution." *The Journal of Chemical Physics* 56(6):3086.
- Waisman, Eduardo and J. L. Lebowitz. 1970. "Exact Solution of an Integral Equation for the Structure of a Primitive Model of Electrolytes." *The Journal of Chemical Physics* 52(8):4307–9.
- Waisman, Eduardo and J. L. Lebowitz. 1972. "Mean Spherical Model Integral Equation for Charged Hard Spheres. II. Results." *The Journal of Chemical Physics* 56(6):3093.
- Waseem, Muhammad S. and Nayef M. Alsaifi. 2018. "Prediction of Vapor-Liquid-Hydrate Equilibrium Conditions for Single and Mixed Guest Hydrates with the SAFT-VR Mie EOS." *Journal of Chemical Thermodynamics* 117:223–35.
- Waseem, Muhammad Saad. 2017. "Thermodynamics Modeling of the Inceipient Conditions for Single and Mixed Gas Hydrate System." King Fahad University of Petroleum and Mineral.
- Wei, Dongqing and Lesser Blum. 1987. "The Mean Spherical Approximation for an Arbitrary Mixture of Ions in a Dipolar Solvent : Approximate Solution , Pair Correlation Functions , and Thermodynamics." *The Journal of Chemical Physics* 87(87).
- Wertheim, M. S. 1964. "Analytic Solution of the Percus-Yevick Equation." *Journal of Mathematical Physics* 5(5):643–51.
- Wertheim, M. S. 1984a. "Fluids with Highly Directional Attractive Forces. I. Statistical Thermodynamics." *Journal of Statistical Physics* 35(1–2):19–34.
- Wertheim, M. S. 1984b. "Fluids with Highly Directional Attractive Forces. II. Thermodynamic Perturbation Theory and Integral Equations." *Journal of Statistical Physics* 35(1–2):35–47.
- Wertheim, M. S. 1986a. "Fluids with Highly Directional Attractive Forces. IV. Equilibrium Polymerization." *Journal of Statistical Physics* 42(3–4):477–92.
- Wertheim, M. S. 1986b. "Fluids with Highly Directional Attractive Forces . III . Multiple Attraction Sites." *Journal of Statistical Physics* 42:459–76.
- Willcox, Willard, Don B. Carson, and D. L. Katz. 1941. "Natural Gas Hydrates." *Industrial & Engineering Chemistry* 33(5):662–65.
- Wright, Margaret Robson. 2007. *An Introduction to Aqueous Electrolyte Solutions*. John Wiley & Sons.
- Wu, Jianzhong and John M. Prausnitz. 1998. "Phase Equilibria for Systems Containing Hydrocarbons, Water, and Salt: An Extended Peng–Robinson Equation of State." *Industrial & Engineering Chemistry Research* 37(97):1634–43.

- Xiao, Tiejun and Xueyu Song. 2017. "A Molecular Debye-Hückel Theory and Its Applications to Electrolyte Solutions: The Size Asymmetric Case." *Journal of Chemical Physics* 146(12):124118.
- Yamamoto, Hideki, Tamotsu Terano, Masahiko Yanagisawa, and Junji Tokunaga. 1995. "Salt Effect of CaCl₂, NH₄I and NaI on Vapor-Liquid Equilibrium of Ethanol + Water System at 298.15 K." *The Canadian Journal of Chemical Engineering* 73:779–83.
- Zarenezhad, Bahman. 2014. "Accurate Prediction of the Interfacial Tension of Surfactant/Fluid Mixtures during Gas Hydrate Nucleation: The Case of SDS Surfactant-Based Systems near Ethylene Hydrate Formation Region." *Journal of Molecular Liquids* 191:161–65.
- Zele, S. R., S. Y. Lee, and G. D. Holder. 1999. "A Theory of Lattice Distortion in Gas Hydrates." *J. Phys. Chem.* 103(46):10250–57.
- Zhang, Xia, Lu Zhang, Tan Jin, Zhi Jun Pan, Zhe Ning Chen, Qiang Zhang, and Wei Zhuang. 2017. "Salting-in/Salting-out Mechanism of Carbon Dioxide in Aqueous Electrolyte Solutions." *Chinese Journal of Chemical Physics* 30(6):811–16.
- Zhao, Honggang, M. Carolina Dos Ramos, and Clare McCabe. 2007. "Development of an Equation of State for Electrolyte Solutions by Combining the Statistical Associating Fluid Theory and the Mean Spherical Approximation for the Nonprimitive Model." *Journal of Chemical Physics* 126(24).
- Zuo, YOU-XIANG and Tian-Min Guo. 1991. "Extension of the Patel-Teja Equation of State to the Prediction of the Solubility of Natural Gas in Formation Water." *Chemical Engineering Science* 46(12):3251–58.
- Zuo, You Xiang and Tian Min Guo. 1991. "Extension of the Patel-Teja Equation of State to the Prediction of the Solubility of Natural Gas in Formation Water." *Chemical Engineering Science* 46(12):3251–58.

Vitae

Name : Gaber Bark Al Jaberi

Nationality : Yemeni

Date of Birth : 9/24/1992

Email : jaber.aljaberi@outlook.com

Address : KSA – Al Khober

Academic Background : M.S. Petroleum Engineering
KFUPM, Saudi Arabia – April 2019
B. S. Petroleum Engineering
KFUPM, Saudi Arabia

Research Interests : Flow assurance, Statistical thermodynamics and
Molecular dynamics.